

ALK1 SIGNALING IN VASCULAR DEVELOPMENT

by

Derek William Laux

B.A. Biology, Case Western Reserve University, 2007

Submitted to the Graduate Faculty of the Kenneth P.

Dietrich School of Arts and Sciences in partial fulfillment

of the requirements for the degree of Doctor of Philosophy

University of Pittsburgh

2013

UNIVERSITY OF PITTSBURGH

KENNETH P. DIETRICH SCHOOL OF ARTS AND SCIENCES

This dissertation was presented

by

Derek William Laux

It was defended on

May 20, 2013

and approved by

Gerard Campbell, Ph.D., Associate Professor, Biological Sciences

Deborah Chapman, Ph.D., Associate Professor, Biological Sciences

Jeffrey Hildebrand, Ph.D., Associate Professor, Biological Sciences

Michael Tsang, Ph.D., Associate Professor, Microbiology and Molecular Genetics

Dissertation Advisor: Beth Roman, Ph.D., Assistant Professor, Biological Sciences

ALK1 SIGNALING IN VASCULAR DEVELOPMENT

Derek W. Laux, Ph.D.

University of Pittsburgh, 2013

Heterozygous loss of the endothelial-specific transforming growth factor-beta (TGF- β) Type 1 receptor, activin receptor-like kinase 1 (*ALK1*), results in the autosomal dominant disorder, hereditary hemorrhagic telangiectasia type 2 (HHT2), which is characterized by mucocutaneous telangiectasias as well as arteriovenous malformations (AVMs) in the brain, lungs, liver, gastrointestinal tract, and spinal cord. As a result, patients suffer from a range of clinical symptoms including epistaxis, hemorrhage, and stroke. Using zebrafish, our laboratory has demonstrated that AVMs form via a two-step mechanism involving an initial increase in endothelial cell number caused by lack of *alk1*, and then an adaptive response to increased blood flow in downstream vessels. This adaptive response involves increased arterial caliber and maintenance of normally transient connections between arteries and veins, thereby forming high-flow AVMs. Furthermore, we have demonstrated that *alk1* expression is dependent on blood flow, and that lack of flow mimics loss of *alk1*, suggesting that Alk1 might act downstream of blood flow to stabilize arterial caliber. To date, the in vivo ligand and intracellular mediators required for flow-dependent, Alk1-mediated endothelial quiescence and AVM prevention remain unknown. In this work, I demonstrate that bone morphogenetic protein 10 (Bmp10) is the

physiologically relevant Alk1 ligand during zebrafish embryonic development. Bmp10 paralogs are expressed exclusively in the heart, and loss of blood flow affects arterial pSmad1/5/9, *cxcr4a*, and *edn1* expression similarly to loss of *alk1*, even when *alk1* expression is restored via a flow-independent transgene. Together, these data suggest that flow is required not only for *alk1* expression but also to deliver cardiac-derived Bmp10 ligand to arterial endothelial cell Alk1 to promote endothelial cell quiescence. Downstream of Bmp10/Alk1, Alk1 kinase activity is required to prevent AVMs. However characterization of a pSmad1/5-responsive transgenic reporter, *Tg(BRE:EGFP)*, suggests that although phosphorylation of Smad1/5/9 in arterial endothelium is clearly dependent on Alk1, pSmad1/5/9 may not activate transcription via a canonical mechanism within these cells. In sum, the work presented in this thesis constructs a novel blood flow-responsive signaling pathway, suggests novel mechanisms by which Alk1 may control gene expression, and finally, describes a new tool for studying Alk1 and BMP signaling in vivo.

TABLE OF CONTENTS

PREFACE.....	xvi
1.0 INTRODUCTION.....	1
1.1 VASCULAR DEVELOPMENT.....	1
1.1.1 Overview of vascular architecture.....	1
1.1.2 Developmental model systems in vascular biology.....	2
1.1.3 Vasculogenesis.....	4
1.1.3.1 Angioblast specification.....	5
1.1.3.2 Development of vasculogenic cords.....	6
1.1.3.3 Lumen formation in vasculogenic vessels.....	6
1.1.4 Angiogenesis.....	7
1.1.4.1 Tip cell selection.....	7
1.1.4.2 Guidance of angiogenic sprouts.....	8
1.1.4.3 Lumen formation in angiogenic vessels.....	9
1.1.4.4 Angiogenic resolution.....	10
1.1.5 The role of blood flow in vessel development.....	11

1.1.5.1 Endocrine factors in vascular development and homeostasis.....	12
1.1.5.2 Hemodynamic forces in vascular development and homeostasis.....	12
1.1.5.2.1 Effects of laminar shear on vessel development.....	13
1.1.5.2.2 Mechanosensation of shear stress in endothelial cells.....	14
1.1.5.2.3 Mechanotransduction pathways in endothelial cells.....	15
1.2 ARTERIOVENOUS MALFORMATIONS.....	19
1.2.1 Arterial-venous specification and AVM development.....	19
1.2.1.1 Arterial-venous specification.....	20
1.2.1.2 Loss of arterial-venous identity can promote development of AVMs.....	21
1.2.2 Genetic causes of AVMs.....	22
1.3 HEREDITARY HEMORRHAGIC TELANGIECTASIA.....	24
1.3.1 Overview of TGF- β signaling.....	25
1.3.1.1 BMP ligands.....	25
1.3.1.2 BMP receptors.....	27

1.3.1.3 BMP-related Smad proteins.....	28
1.3.2 Genetics of HHT.....	30
1.3.3 ALK1 signaling in endothelial cells.....	31
1.3.3.1 ALK1 ligands.....	32
1.3.3.2 Signaling pathways downstream of ALK1.....	32
1.3.3.3 Genes regulated downstream of ALK1.....	33
1.3.4 Animal models of HHT.....	34
1.3.4.1 Mouse HHT models.....	34
1.3.4.2 Zebrafish HHT2 model.....	34
1.3.4.3 <i>alk1</i> -positive arteries in zebrafish.....	35
1.4 DISSERTATION AIMS.....	36
2.0 CIRCULATING BMP10 ACTS THROUGH ENDOTHELIAL ALK1 TO MEDIATE FLOW-DEPENDENT ARTERIAL QUIESCENCE.....	37
2.1 INTRODUCTION.....	38
2.2 RESULTS.....	41
2.2.1 Blood flow is required not only for <i>alk1</i> expression but also for <i>Alk1</i> activity.....	41

2.2.2 <i>bmp10</i> knockdown phenocopies <i>alk1</i> mutants.....	47
2.2.3 <i>bmp10</i> paralogs are expressed exclusively in the heart.....	52
2.2.4 Circulating Bmp10 acts via Alk1 to limit endothelial cell number in nascent arteries.....	56
2.3 DISCUSSION.....	59
3.0 PHOSPHORYLATED SMADS1/5/9 ARE PRESENT AND ACTIVE DOWNSTREAM OF ALK1 IN THE ZEBRAFISH ENDOTHELIUM.....	64
3.1 INTRODUCTION.....	64
3.2 RESULTS.....	67
3.2.1 Detection of pSmads1/5/9 is dependent on <i>alk1</i>	67
3.2.2 Detection of pSmads1/5/9 is dependent on Alk1 activity.....	69
3.2.3 Individual <i>smad</i> transcripts are undetectable in <i>alk1</i> -positive arteries.....	72
3.2.4 pSmads1/5/9 mediated <i>Tg(bre:egfp)</i> expression is undetectable in <i>alk1</i> -positive arteries.....	74
3.2.5 Inhibition of pSmads1/5/9 partially phenocopies <i>alk1</i> mutants.....	78
3.3 DISCUSSION.....	83

4.0 DYNAMIC ANALYSIS OF BMP-RESPONSIVE SMAD ACTIVITY	
IN LIVE ZEBRAFISH EMBRYOS.....	87
4.1 INTRODUCTION.....	87
4.2 RESULTS.....	91
4.2.1 Generation of transgenic zebrafish lines expressing EGFP	
under the control of a BRE.....	91
4.2.2 <i>bre:egfp</i> expression correlates with many established domains	
of BMP activity.....	92
4.2.3 Temporal correlation between pSmads1/5/9 expression	
and <i>bre</i> -driven EGFP fluorescence.....	97
4.2.4 <i>bre:egfp</i> transgene expression is responsive to changes	
in Smad1/5/9 phosphorylation.....	100
4.2.5 <i>bre:egfp</i> transgene expression is decreased by knockdown	
of <i>smad1</i> or <i>smad5</i>	104
4.3 DISCUSSION.....	108
5.0 CONCLUSIONS AND FUTURE DIRECTIONS.....	112

5.1 BMP10 COORDINATES WITH ALK1 TO MEDIATE FLOW DEPENDENT QUIESCENCE.....	114
5.2 ALK1 INITIATION AND MAINTENANCE.....	116
5.3 THE ROLE OF SMADS IN ALK1 SIGNALING.....	117
5.4 ALK1 AND CANCER.....	121
5.5 SUMMARY.....	122
6.0 MATERIALS AND METHODS.....	123
6.1 ZEBRAFISH LINES AND MAINTENANCE.....	123
6.2 MORPHOLINO KNOCKDOWN.....	124
6.3 MORPHOLINO VALIDATION.....	124
6.4 IN SITU HYBRIDIZATION.....	125
6.5 IMMUNOHISTOCHEMISTRY AND IMMUNOSTAINING.....	125
6.6 MICROINJECTION OF RHBMP9 AND RHBMP10.....	126
6.7 LIVE CONFOCAL IMAGING.....	127
6.8 C2C12 TRANSFECTIONS AND LUCIFERASE ASSAYS.....	127
6.9 GENERATION OF TG(BRE:EGFP).....	128
6.10 MRNA SYNTHESIS.....	129

6.11 DRUG EXPOSURES.....	129
BIBLIOGRAPHY.....	130

LIST OF TABLES

Table 1: Sensitivity of <i>bre:egfp</i> Expression to Manipulation of Smad1/5 Activity and Expression.....	106
Table 2: Morpholino sequences.....	124

LIST OF FIGURES

Figure 1: Steps of Angiogenesis.....	11
Figure 2: Differences in shear are present at vascular bifurcations.....	18
Figure 3: Artery-Vein differentiation and the formation of Arteriovenous Malformations.....	23
Figure 4: Processing of BMP ligands.....	26
Figure 5: BMP signaling pathway.....	28
Figure 6: Domain structure of Smad proteins.....	29
Figure 7: Restoration of <i>alk1</i> expression does not rescue <i>cxcr4a</i> and <i>edn1</i> expression in the absence of blood flow.....	43
Figure 8: <i>Tg(flia:alk1-myc)</i> drives <i>alk1</i> in all endothelial cells independently of flow.....	44
Figure 9: Alk1 activity is dependent on blood flow.....	46
Figure 10: <i>bmp9</i> , <i>bmp10</i> , and <i>bmp10-like</i> knockdown their respective targets in vivo.....	47
Figure 11: <i>bmp9</i> knockdown does not phenocopy <i>alk1</i> ^{-/-} mutants.....	48
Figure 12: Knockdown of <i>bmp10</i> phenocopies zebrafish <i>alk1</i> mutants.....	51
Figure 13: <i>bmp10</i> and <i>bmp10-like</i> expression is independent of flow.....	53
Figure 14: <i>bmp10</i> and <i>bmp10-like</i> are expressed in the heart.....	55
Figure 15: Bmp10/Alk1 lies downstream of blood flow in regulation of pSmad1/5/9, <i>cxcr4a</i> , and <i>edn1</i>	58
Figure 16: pSmad1/5/9 expression in <i>alk1</i> -Positive Endothelial Cells Depends on <i>alk1</i>	68
Figure 17: dpERK expression is not dependent on <i>alk1</i> expression.....	69

Figure 18: pSmad1/5/9 expression is dependent on Alk1 activity.....	71
Figure 19: dpERK expression is not dependent on Alk1 activity.....	72
Figure 20: <i>smad1</i> , <i>smad5</i> , and <i>smad9</i> are undetectable in <i>alk1</i> -positive arteries.....	73
Figure 21: <i>smad1</i> and <i>smad5</i> are undetectable by FISH in <i>alk1</i> -positive arteries.....	74
Figure 22: <i>Tg(bre:egfp)</i> expression is absent in <i>alk1</i> -positive arteries.....	75
Figure 23: <i>Tg(bre:egfp)</i> expression is not detectable in <i>alk1</i> -positive arteries at later time points or by in situ hybridization or immunofluorescence.....	77
Figure 24: rhBMP9 and rhBMP10 do not induce <i>Tg(bre:egfp)</i> expression.....	78
Figure 25: <i>smad1/smad5/smad9</i> knockdown does not phenocopy <i>alk1</i> mutants.....	80
Figure 26: Inhibition of Alk1 kinase activity phenocopies <i>alk1</i> mutant.....	82
Figure 27: <i>smad5</i> misexpression does not rescue <i>alk1</i> ^{-/-} embryos	82
Figure 28: Developmental profile of pSmad1/5/9-mediated transcriptional activity in <i>Tg(bre:egfp)</i> ^{pt510} embryos.....	96
Figure 29: Temporal relationship between pSmad1/5/9 activity and EGFP fluorescence in <i>Tg(bre:egfp)</i> embryos.....	99
Figure 30: Expression of the <i>bre:egfp</i> transgene is responsive to changes in BMP type I receptor signaling.....	101
Figure 31: Expression of the <i>bre:egfp</i> transgene is globally downregulated by small molecule inhibition of BMP type I receptor-mediated Smad phosphorylation.....	103
Figure 32: <i>smad5</i> knockdown down-regulates <i>bre:egfp</i> transgene expression primarily in somites.....	104
Figure 33: <i>smad1</i> knockdown downregulates <i>bre:egfp</i> transgene expression in <i>smad1</i> -expressing domains.....	107

Figure 34: Proposed pathway for Bmp10 and Alk1.....113

PREFACE

I was once told that in the life of a scientist, your relationship with graduate advisor would be the second most important relationship you ever formed. It is with this that I would like to extend my sincerest gratitude to my advisor, Dr. Beth Roman. I have been blessed to have many wonderful teachers throughout the years, but none have compared in either quality or impact, to Beth. Over my graduate career, Beth has remained a constant source of support, ideas, and enthusiasm. It was because of Beth, that I came to the University of Pittsburgh, and it is because of Beth, that I now leave a far better person and scientist than when I came in.

I have had the opportunity to work with a wonderful group of individuals in the Roman lab over the past several years. My lab mate, Elizabeth Rochon, has been wonderful support both in and out of the lab. Shane Wright and Zak Kupchinsky besides being excellent friends outside of the laboratory have provided excellent care to our fish facility, making all of this work possible. My friend, Sarah Young, provided countless technical and intellectual contributions to this project. We have had many wonderful undergraduates who have made the lab an enjoyable place to work. Special thanks to Jim Donovan for his help with characterizing *bmp10-like*, and Jenny Febbo and Ashley Miller for their help with the generation and validation of *Tg(bre:egfp)*.

I would like to thank each of my committee members, Dr. Nathan Bahary, Dr. Gerard Campbell, Dr. Debbie Chapman, Dr. Jeff Hildebrand, Dr. Beth Stronach, and Dr. Michael Tsang. Each of them has been instrumental to my growth as a scientist, and the aid that they have provided my research has made this work possible. Most importantly, the kindness they have shown towards me will never be forgotten.

A special thanks belongs to Dr. Wendy Mars and the Angiopathy Training Program at the University of Pittsburgh for funding. In addition, the program has given me a unique opportunity to explore and discuss topics outside the breadth of my own research.

To my friends, Tolstoy wrote, “In life, there are only two truths, love and happiness. All else is folly.” I would like to thank each one of them for providing me with nothing but love and happiness over the past several years.

My final and most heartfelt thanks belongs to my family. Everything I have ever done, all that I am, and anything I will ever become, I owe to the love and support of my family. The road is long and the journey, tiresome. In my most trying times however, I need only to remember... The road leads home.

1.0 INTRODUCTION

The complexities of the vasculature are dictated by a myriad of factors. In addition to paracrine factors from surrounding tissue, the closed circuitry of the vascular network aids in distributing endocrine factors that affect endothelial cell behavior. The mechanical forces imparted by blood flow also govern gene expression profiles and endothelial cell actions. All of these factors must work coordinately to ensure that blood vessels are meeting the body's ever-changing requirements for oxygen and nutrients.

The work presented in this thesis will focus on a novel pathway in which circulating blood provides a heart-derived endocrine factor that binds to a receptor expressed on arterial endothelial cells, initiating a signal transduction cascade that mediates flow-dependent vascular quiescence and ultimately helps to shape the vascular tree.

1.1 VASCULAR DEVELOPMENT

1.1.1 Overview of vascular architecture

Proper formation of the vascular network is critical for supplying oxygen and nutrients to tissues to maintain normal physiological function. The basic framework of the vascular tree is universally known. Arteries carry oxygenated blood away from the heart, progressively decreasing in diameter and leading into highly branched capillaries that provide a large surface

area for gas and nutrient exchange with surrounding tissues. Deoxygenated blood is returned to the heart via venules and then veins. The lumen of these vessels is lined with endothelial cells, which, beyond serving a barrier function by preventing leakage of protein and fluid into surrounding tissue, also contribute to hemostasis, vasoconstriction/vasodilation, hormone trafficking and other processes. Vascular smooth muscle cells (vSMCs) or pericytes surround the endothelial tubes and function in part to control vascular caliber primarily through adrenergic receptors. Because the magnitudes of hemodynamic forces imparted by blood flow are inextricably linked to heartbeat, arteries must possess a thicker layer of vSMCs (*tunica media*) than veins. Capillaries are minimally covered with support cells known as pericytes, which encourage vessel quiescence and regulate endothelial permeability, thereby enabling efficient transfer of oxygen and nutrients [for review, see [1]]. This complex network develops during embryogenesis through two fundamental processes: vasculogenesis, the de novo formation of blood vessels from endothelial cell precursors, and angiogenesis, which involves remodeling as well as sprouting of new vessels from existing vessels. Most of our understanding of these two processes comes from the study of three important vertebrate model organisms: chick, mouse, and zebrafish.

1.1.2 Developmental model systems in vascular biology

Historically, avian embryos were the primary developmental model for studying vertebrate vascular development because development *in ovo* provided a distinct advantage over mammalian models in terms of accessibility for manipulation and live observation. For example, intravascular ink injections can be used to highlight the patent vasculature; chicken-quail chimeras can be generated in which quail cells can be unequivocally identified and tracked to determine the origin and fate of endothelial cells; and vessel ligations can be performed to assess

the effects of hemodynamic forces or hypoxia on vessel development and arterial-venous differentiation [2]. These types of experiments led to many of the first descriptions of the migration and coalescence of angioblasts during vasculogenesis [3]. More modern developments in dynamic image analysis and quantitative assessments have kept avian models an important tool in studying vascular development [4]. The chick chorioallantoic membrane also serves as an important in vivo model for angiogenesis [5].

Mice have served as a valuable mammalian model for studying vertebrate vascular development. Whole organism and endothelial specific genetic knockouts have elucidated many of the known players in vascular biology, and have served as genetic models for human pathologies [6, 7]. In addition, application of histological analysis, immunostaining, and in situ hybridization to these models has proven useful in fleshing out the molecular pathways that guide the development of different vascular beds [8]. 3-D architecture of the vascular network has been exposed with angiography, scanning electron microscopy, and light microscopy of vascular casts [9]. Furthermore, time lapse confocal microscopy, Pulsed Doppler, and hetastarch injections to increase blood viscosity have all been utilized to dynamically examine blood velocities and the effects of hemodynamics [10, 11]. Work with mouse retinal explants provides a means to study in vivo vascular development in real time [12]. In addition, multiphoton imaging is used with cranial windows to study vascular development in adult mice [13]. However, many techniques still rely on sacrificing the embryo and hence can only provide a still image of vascular development.

Zebrafish offer many advantages over mouse and chick in studying vascular development. Their size and fecundity make them ideal as a developmental model system. Their external fertilization and optical clarity have made possible dynamic in vivo analysis of vascular

development from the earliest stages of angioblast differentiation through methods such as confocal microscopy and microangiography [14]. External fertilization also provides a means to manipulate gene expression from the earliest stage of development through mRNA and DNA injections. DNA incorporation into the germ line allows for the creation of transgenic lines providing yet another means to monitor changes in the zebrafish vascular tree. Morpholino-modified antisense oligonucleotides allow for knockdown of translation of specific mRNA transcripts [15] and genetic knockouts by homologous recombination are now available with Transcription activator-like effector nucleases (TALENs) [16]. In addition, their small size allows oxygen to freely diffuse into the embryo allowing them to develop with impaired or abrogated circulation for up to 5 days post fertilization [17]. These attributes have allowed for large-scale forward genetic screens that have identified key players in vascular development [14, 18]. Finally, the zebrafish vascular anatomy is so well characterized that vascular mutants are readily identified [19].

1.1.3 Vasculogenesis

The specification of the earliest endothelial precursors, angioblasts, and their formation into a primitive vascular network is termed vasculogenesis, or the de novo synthesis of blood vessels [20]. In the zebrafish embryo proper, angioblasts are specified in the lateral plate mesoderm by paracrine signals from the underlying endoderm [21]. In the trunk, these angioblasts migrate medially and will coalesce to form the first intraembryonic blood vessels, the dorsal aorta and cardinal vein. In the mammalian head, mesodermal angioblasts coalesce to form the perineural vascular plexus. On the mammalian yolk sac, endothelial cells differentiate within the perimeter of mesodermal blood islands, surrounding primitive erythrocytes, and these blood islands connect to form a primitive vascular plexus. Both the perineural and yolk sac vascular plexuses,

originally comprised of a honeycomb-like network of similarly sized vessels, will be remodeled into a hierarchical pattern of arteries, capillaries, and veins [for review, see [20]].

1.1.3.1 Angioblast specification.

The specification, maturation, and maintenance of endothelial cells require complex interplay between many different transcription factors. The Ets family of winged helix-turn-helix transcription factors is critical for the earliest stages of endothelial cell specification. Most endothelial cell enhancers and promoters contain several conserved Ets binding sites [22, 23] and within the human genome, Ets sites are strongly associated with endothelial genes [24]. Mice harboring mutations in the Ets family gene *Etv2*^{-/-} die with no discernible embryonic blood vessels or blood islands within the yolk sac, and knockdown of *Etsrp* in zebrafish leads to early defects in vascular development [25-28]. In addition, mRNA injection of constitutively active *fli1* (an Ets transcription factor) can induce expression of several endothelial-specific markers including *Vascular Endothelial Growth Factor Receptor 2* (*vegfr2*) in zebrafish [29]. However, no Ets factor is exclusive to the endothelium and Ets-binding sites are not found in all endothelial genes [30, 31] suggesting that other factors must work in conjunction or independently of Ets for endothelial cell specification. Zebrafish *cloche* establishes molecular distinction and differentiation in a subset of endothelial cells. Although *cloche* mutants possess a limited number of trunk endothelial cells, they have no cranial endothelial cells nor any blood vessels, endocardium, or blood cells [18, 32]. Expression of the basic helix-loop-helix (bHLH) transcription factor, *scl*, can rescue *cloche* mutants suggesting *scl* falls downstream of *cloche* in differentiation of endothelial cells [32], but many signaling components in angioblast specification remain to be uncovered.

1.1.3.2 Development of vasculogenic cords

Isolated mesodermal cells expressing *Vegfr2* are classified as angioblasts [33]. Expression of this receptor is critical to the organization of the earliest vessel structures, with VEGF ligand acting as a powerful chemoattractant encouraging *Vegfr2*-mediated migration and coalescence. In *Xenopus*, *Vegfr2* expressing cells migrate from the lateral plate mesoderm towards high concentrations of VEGF at the midline to form the dorsal aorta [34], and avian embryos injected with soluble VEGF receptor, which acts as a decoy, show defects in vasculogenesis on the injected side [35]. The importance of *Vegfr2* is best illustrated in mice in which a single wild type allele of *Vegfr2* is insufficient and causes death by E8.5-9.5 from failure of early specified endothelial cells to form patterned vessels [36].

1.1.3.3 Lumen formation in vasculogenic vessels

During vasculogenesis, endothelial cells initially form solid cords of cells that must subsequently hollow into tubes. In the dorsal aorta, the process of lumen formation involves repulsion of endothelial cells at contacts within the newly formed cords, a change in endothelial cell shape, and a rearrangement of endothelial junctions. The process is initiated by expression of de-adhesive apical proteins coinciding with a translocation of junctions to lateral positions where they possess properties of both adherens and tight junctions through expression of vascular endothelial (VE)-cadherin and zonula occludens-1 (ZO-1), respectively [37, 38]. The repulsion of cells created by the localization of apical proteins is sufficient to begin lumenization, but requires additional myosin-dependent retraction of apical surfaces [39].

1.1.4 Angiogenesis

During development and into adulthood, blood vessels must be able to develop to meet the ever-changing oxygen and nutritional requirements of the body, and they do so by angiogenesis, which involves extensive remodeling and expansion of existing vascular networks. One important trigger for angiogenesis is hypoxia, as hypoxic tissues require oxygen delivery through blood supply for survival. The hypoxia-activated transcription factor, hypoxia inducible factor-1 α (HIF-1 α), acts to upregulate Vascular Endothelial Growth Factor A (VEGFA) [also known as Vascular Permeability Factor (VPF)], which typically serves as an initial cue for a vessel to sprout [1].

1.1.4.1 Tip cell selection

Within a quiescent vessel, certain endothelial cells possess enhanced ability to respond to environmental VEGFA in part due to increased surface expression of VEGF receptor 2 (VEGFR2), a receptor tyrosine kinase. These specialized cells, known as tip cells, commence migration using filopodial extensions to navigate towards high concentrations of VEGFA. Typically, the tip cell will be trailed by a group of proliferating endothelial cells comprising the stalk, which will elongate the vessel [40]. Alternatively, as in zebrafish intersegmental vessel (ISV) formation, tip cells may both proliferate and migrate [41]. Endothelial cells within a sprout dynamically compete for the tip position, with Notch-dependent lateral inhibition controlling levels of VEGFR2/VEGFR3 and thereby dictating which cell is best suited to acquire tip cell position: tip cells express high levels of Notch ligand, Dll4, whereas stalk cells express high levels of Notch receptor, and Notch signaling within stalk cells represses expression of *VEGFR2* and *VEGFR3* [42]. Genes of the Notch family encode large transmembrane receptors that

interact with membrane-bound ligands of the Delta/Serrate/Jagged family of genes. Ligand binding stimulates proteolytic cleavage of the Notch intracellular domain (ICD) which complexes in the nucleus with coactivator RBPJ to control target gene expression. *VEGFR3* expression is exclusive to the tip cell position and inhibition of VEGFR3 can suppress angiogenic growth completely [43]. *dll4* overexpression in zebrafish or mouse embryos can cause excessive endothelial cell sprouting that can be partially rescued by inhibition of VEGFR3 [41, 44]. In zebrafish embryos, downregulation of *vegfr3* expression by Notch signaling within the stalk is mediated by microRNA- (miR-) 221 [45]. Besides Notch, VEGFR1 also acts to antagonize the pro-angiogenic response of VEGFR2. A soluble isoform (sVEGFR1) may act as a high affinity decoy receptor, sequestering VEGF ligand and thereby inhibiting angiogenic potential. Membrane-bound VEGFR1 (mVEGFR1) also acts to suppress tip cell phenotype at least in part through interaction with Notch, as *vegfr1* knockdown reduces notch signaling components [46]. Abundance of sVEGFR1 is in part dictated by Semaphorin-PlexinD1 signaling which inhibits angiogenesis through upregulation of sVEGFR1 abundance [47].

1.1.4.2 Guidance of angiogenic sprouts

Navigation of growing angiogenic sprouts requires a proper balance of attractive and repulsive cues, which can be provided from matrix substrates, cell-cell contacts and soluble factors. As mentioned, VEGFA acts as the main soluble factor stimulating polarized filopodial extensions from tip cells while ephrinB2/EphB4 cues between endothelial cells encourage directed migration of sprouts [1, 48]. Transmembrane Neuropilins (NRP1 and NRP2) serve dual function, promoting migration through interaction with VEGFR2/VEGF₁₆₄ and regulating repulsive cues through Semaphorin/PlexinD1 [49]. Supporting a role for Semaphorin/PlexinD1 signaling in repulsion, knockdown of *plexinD1* in zebrafish or genetic loss in mice leads to aberrant

intersegmental sprout outgrowth into somites [50, 51], and SEMA3A can inhibit integrin function thereby inhibiting vessel migration [52]. Similarly, the transmembrane endothelial-specific receptor, Robo4, binds secreted Slit protein and acts to inhibit VEGF induced vascular migration, in part through interaction with Unc5b Netrin receptor [53, 54]. Another Netrin receptor, Netrin-1, elicits a retraction of filopodial projections [55]. In the adult mouse, *Robo4* is exclusively expressed in sites of active angiogenesis and areas exposed to hypoxia [56] and *Robo4*^{-/-} mice are viable but display VEGF-dependent hypervascularization in pathological settings [57]. In zebrafish, Slit/Robo is a necessary signaling pathway for intersegmental vessels (ISVs) sprouting off the dorsal aorta. In both *robo4* morphants and *robo4*-RNA injected embryos, ISVs are either truncated or follow an aberrant path off the dorsal aorta, infiltrating the somites [58]. (Figure 1)

1.1.4.3 Lumen formation in angiogenic vessels

Although vasculogenic vessels such as the dorsal aorta have been shown to lumenize via a cord hollowing mechanism [39], there is some debate as to whether angiogenic vessels lumenize by cord hollowing, cell hollowing, or a combination of the two mechanisms. Cell hollowing has been demonstrated in cultured endothelial cells and the intersegmental arteries of zebrafish and involves CDC42/Rac1-dependent pinocytosis and subsequent production of small vacuoles that fuse first to form large intracellular vacuoles and then intercellular, longitudinal vacuoles [59, 60]. A second mode for ISV lumen formation has been proposed that resembles that which takes place in larger vessels, where lumen formation occurs extracellularly at an apical pole interface between endothelial cells. Adherens junctions localize sialomucins/moesin/F-actin that drive separation of endothelial cells, and the process becomes further activated by VEGF-mediated activation of ROCK [39]. In the intersegmental vessels of zebrafish, Ve-cadherin and Moesin1

contribute to apical/basal polarity and are necessary in driving early separation of two endothelial cells [61].

1.1.4.4 Angiogenic resolution

The transformation from actively growing network to functional vascular bed requires the cessation of endothelial cell proliferation and migration, as well as stabilization through the recruitment of vSMCs and pericytes. Oxygenation of tissue caused by newly formed vessels downregulates environmental VEGFA, subsequently leading to a reduction in VEGFR2-mediated migration [1]. Besides a cessation of growth, new vessels must recruit support cells to maintain proper function and cope with hemodynamic stress. Some hypothesize that endothelial cells promote differentiation of mural precursor cells from surrounding mesenchyme through soluble factors during branching [62]. Tip cells secrete high levels of PDGFB, the ligand for pericyte-expressed PDGFR β , ensuring pericyte coverage over newly formed vessels [40]. Mural cell support is clearly a requirement for integrity and quiescence as deletion of *Tie-1*, *Tie-2*, *Ang-1*, or *PDGFR β* , all of which produce deficiency in vSMC and pericyte development or endothelial interaction, display vascular hemorrhaging phenotypes [63-66]. (Figure 1)

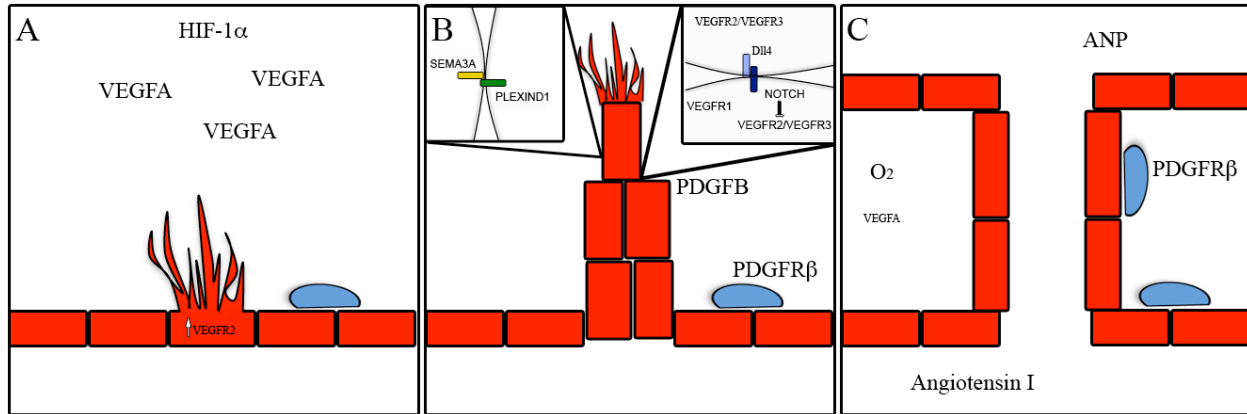


Figure 1: Steps of Angiogenesis

(A) Tip cells with high expression of VEGFR2 extend filopodial projections towards high concentrations of VEGFA ligand, produced in hypoxic tissues through the actions of HIF-1 α . (B) Endothelial cells compete for tip cell position through lateral inhibition. Tip cells have high expression of *Vegfr2/Vegfr3* and *Dll4*. Stalk cells have high expression of *Notch* and *Vegfr1*. Repulsive cues between the environment (SEMA3A) and endothelial cells (PlexinD1) serve to guide migration. Tip cells secrete PDGFB to promote pericyte attachment through PDGFR β expression. (C) Oxygen provided by new vessels leads to downregulation of *Vegf*. Pericytes cover newly formed vessels. Endocrine factors ANP and Angiotensin I control vasodilation/vasoconstriction respectively.

1.1.5 The role of blood flow in vessel development

Prior to lumen formation, the development of the vascular tree is dependent exclusively on cell type-specific transcription factors and paracrine molecular pathways, as described. However, once vessels have lumenized, endocrine factors and mechanical forces imparted by blood flow also come into play. This section will describe the role of endocrine factors in vascular development and homeostasis, the mechanistic basis of mechanosensation and mechanotransduction in endothelial cells, and the effects of mechanical forces on endothelial cell behavior and vascular architecture.

1.1.5.1 Endocrine factors in vascular development and homeostasis

Blood flow is critical in the distribution of endocrine factors that serve to control vessel constriction/dilation. Atrial natriuretic peptide (ANP), a potent vasodilator, is released into circulation from the atria of the heart in response to high blood pressure [67]. Opposing ANP, renin activation of angiotensin I occurs in circulation and serves as a vasoconstrictor [68]. Together, these opposing forces provide balance necessary for homeostasis (Figure 1). It is now known that even when the vasculature does not require change, vascular quiescence and homeostasis require active cellular signaling and must therefore depend on a host of circulating factors. Recently, sphingosine-1-phosphate (S1P), a product of erythrocytes and present at micromolar concentrations within blood, has been shown to serve as a vascular quiescence factor inhibiting VEGFR2 when bound to its endothelial receptor, S1P1R [69]. This is only one example however and many factors remain to be uncovered.

1.1.5.2 Hemodynamic forces in vascular development and homeostasis

The vasculature is a closed circuit with the heart acting as a pump and the vascular network needing to continuously respond to changes in flow and balance mechanical and chemical stimuli to maintain homeostasis and prevent disease. The framework of the vasculature subjects different regions of the network to different patterns of flow and thus different magnitudes and directions of mechanical forces. To maintain proper function, the endothelium has adopted means to respond to flow differences including altering of the cytoskeleton and cellular realignment, recruitment of vSMCs, and the regulation of gene expression [70]. Blood flow exerts a range of biomechanical forces upon the endothelium, including pressure, stretch, and shear stress. The best characterized of these forces is shear stress, which is the frictional force

that acts tangentially on the apical surface of endothelial cells and is directly proportional to the viscosity and velocity of blood but inversely proportional to the radius of the vessel. In straight tubes, shear stress is pulsatile and laminar (net forward-directed) and these vascular regions are generally quiescent, as characterized by low levels of proliferation, vasodilation, and expression of antioxidant and anti-inflammatory genes. If cardiac output and blood flow velocity increase, shear stress increases, and vessels dilate to bring shear stress down to a physiological set point. Conversely, vessels exposed to low shear forces will become smaller or in extreme cases will regress entirely. At the outer wall of bifurcations or the inner walls of curvatures, flow is not laminar and shear stress is disturbed (low and/or oscillatory). In these regions, endothelial cells mount a transcriptional program favoring proliferation, vasoconstriction, oxidation, and inflammation. These latter regions are highly prone to atherosclerosis [for review, see [70]].

1.1.5.2.1. Effects of laminar shear on vessel development

Molecularly, the biomechanical forces that blood flow imparts can dictate such diverse developmental processes as vascular remodeling, maintenance of arterial-venous identity, and collateral vessel formation. Mice with impaired heartbeat possess defects in yolk sac remodeling, a result that can be phenocopied by decreasing hematocrit and thus viscosity and shear stress [10]. In mammals, the natural rotation of the outflow tract exposes opposite sides of the branchial aortic arches to different flow patterns: specifically, rotation results in increased hemodynamic force on the left side, leading to regression of the right fourth and retention of the left four aortic arch such that the mature aortic arch forms on the left side. Inhibition of outflow tract rotation produces random retention and enlargement of aortic arches [71, 72]. The mechanical forces of blood flow also guide the hypoxia-independent process of arteriogenesis in

which preexisting collateral vessels are recruited to bypass vessels which have been impeded [73].

1.1.5.2.2 Mechanosensation of shear stress in endothelial cells

Endothelial cells must possess means by which to sense shear stress and ultimately transduce this force into a molecular response. Primary cilia, glycocalyx, and junctional complexes have all been implicated as mechanosensors on endothelial cells, transmitting force via the actin cytoskeleton to affect changes in gene expression and integrin activation, but whether one or all of these mechanisms is active in vivo is unknown. The primary cilium is a nonmotile apical appendage that consists of microtubules arranged in a 9+0 pattern, without ciliary dynein. These cilia can bend in response to blood flow, thereby opening a calcium channel, consisting of PKD1 and PKD2, that allows calcium entry into the cell. Genetic deletion of *Pkd1* in mice leads to vascular fragility in vivo, and primary cilia have been shown to be required for numerous flow responses in cultured endothelial cells [74, 75]. However, in mice and chick, primary cilia are only detected in atheroprone areas [76, 77], which are sites of disturbed shear stress but not in straight tubes that are exposed to pulsatile laminar shear stress where they quickly disassemble in response to flow. Furthermore, the primary cilia of human umbilical vein endothelial cells (HUVECs) quickly disassemble in response to laminar shear stress [78]. Together, these data suggest that primary cilia may be required for sensing of disturbed but not laminar shear stress.

The endothelial surface glycocalyx (ESG), a heterogeneous structure of proteoglycans and glycosaminoglycans, may work in conjunction with primary cilia and other mechanosensors to transduce mechanical signals into cellular responses [79]. The negatively charged components of the ESG can capture circulating plasma proteins necessary for signaling. Furthermore, the

ESG also provides a barrier on endothelial cells preventing them from experiencing direct shear stress and rather creating a torque on the EC surface [79]. Evidence for the ESG providing mechanosensory function includes findings that enzymatic degradation of the glycocalyx can directly effect production of vasodilatory nitric oxide (NO) and prevent flow dependent vasodilation [80].

There are several reported examples of vascular receptors acting in complex with endothelial cellular adhesion molecules in a ligand-independent manner to control vascular patterning in response to flow. Most notably, Vascular Endothelial (VE)-cadherin/ Platelet Endothelial Cell Adhesion Molecule (PECAM)/VEGFR2 have been shown to comprise an essential flow sensing signaling hub that controls integrin activation. Within this complex, PECAM acts to transmit mechanical force through Src activation and VE-cadherin serves as a crucial adaptor molecule for VEGFR2 to activate phosphatidylinositol-3-OH kinase (PI(3)K), thereby activating integrins [81]. In turn, integrins have been shown to facilitate cell alignment and transient induction of NF- κ B in response to flow [82]. Loss of either PECAM or VE-cadherin can abolish this response to flow in endothelial cells [82]. Conversely, transfection of PECAM, Ve-cadherin and VEGFR2 can confer flow-responsiveness to non-endothelial cells [81].

1.1.5.2.3 Mechanotransduction pathways in endothelial cells

Laminar and disturbed shear stress have differential effects on gene expression and cell behavior due in large part to activation of key transcription factors (Figure 2). The zinc finger DNA-binding Kruppel-like transcription factor 2 (Klf2) has emerged as a key component in mediating the effects of pulsatile laminar shear stress and promoting vascular quiescence. In HUVECs,

KLF2 expression is upregulated and maintained more than 20-fold when exposed to pulsatile laminar shear [83]. In zebrafish, *klf2a* expression is diminished in no flow, *silent heart (sih)* mutants [84], and murine carotid artery collar models show *Klf2* expression is directly related to the magnitude of laminar shear stress [84, 85]. Furthermore, *Klf2* provides a link between arterial shear stress and vasoconstrictive/vasodilatory genes: release of Endothelin-1 (EDN1), a vasoconstrictive peptide, from endothelial cells is repressed by laminar shear stress in a *Klf2*-dependent manner [85, 86], and endothelial nitric oxide synthase (eNOS), cyclooxygenase-2 (COX-2), and manganese-dependent superoxide dismutase, which generate vasodilatory nitric oxide (NO) and prostaglandins and scavenge damaging superoxide, respectively, are all upregulated by laminar shear stress in a *Klf2*-dependent manner [87]. Thus, *Klf2* orchestrates a gene expression program that promotes a dilated and low-oxidant state, which favors endothelial cell quiescence. Surprisingly, however, although *Klf2*^{-/-} mice die ~E12-E14.5 from high output cardiac failure, expression of flow-responsive, *klf2*-dependent genes, including *Edn1* and *eNOS*, is unchanged [88]. This observation may be explained by the fact that the related transcription factor, *Klf4*, may compensate for loss of *Klf2*. Like *Klf2*, *Klf4* is induced in HUVECs exposed to laminar shear and this serves an anti-inflammatory function, with silencing of *Klf4* leading to decreased eNOS and thrombomodulin [89, 90]. (Figure 2)

In contrast to laminar shear, areas of disturbed flow (complex geometries, outer wall of bifurcations) in which average shear forces are low due to forward-reverse flow cycles are characterized by transcriptional profiles that enhance cell turnover and proliferation [91]. This genetic profile favors prolonged signaling of pro-inflammatory and proliferative pathways and therefore makes areas of disturbed flow more susceptible to atherosclerosis. Constant shear stress works in part to deactivate mitogen-activated protein kinase (MAPK) and nuclear factor kappa-

light-chain enhancer of activated B cells (NF- κ B) signaling, which both trigger pro-inflammatory and proliferative responses [70]. Pig aortas at regions of disturbed shear display elevated levels of MAPK and NF- κ B in part due to low expression of negative regulators of these pathways [92]. The expression of NF- κ B subunits is also enhanced at regions of low shear which primes regions of these vessels for inflammatory stimuli [93].

Not surprisingly, the pathways activated by steady versus disturbed laminar shear oppose one another to maintain vessel homeostasis. Pulsatile shear stress-activated KLF2 may function to inhibit activating protein-1 (AP-1) superfamily members by downregulating MAPK signaling through upregulation of negative regulator, MAPK phosphatase-1 (MKP-1), and inhibition of ATF-2 nuclear localization [94, 95]. Also, KLF2 can sequester essential coactivators for NF- κ B, thereby limiting inflammatory responses [96]. Differences in shear rate may also induce different mechanisms for NF- κ B activity with high shear encouraging atheroprotective anti-apoptotic targets of NF- κ B [97].

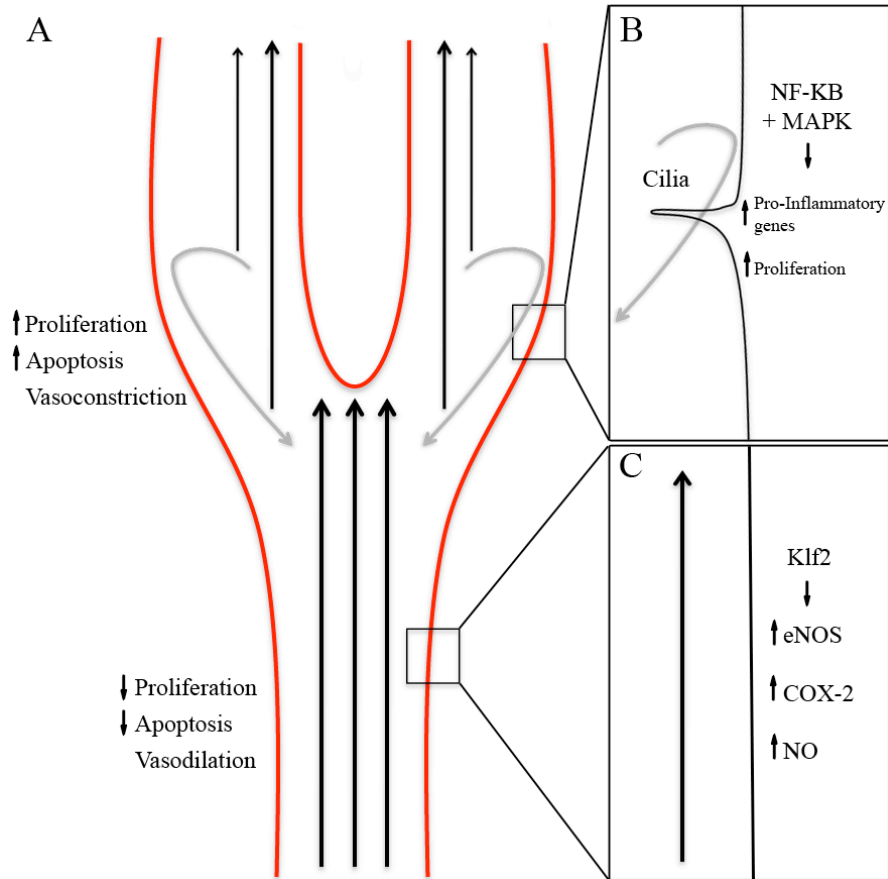


Figure 2: Differences in shear are present at vascular bifurcations.

(A) Cells on the outer wall of bifurcations experience disturbed shear, which favors increased proliferation, apoptosis, and vasoconstriction. Endothelial cells exposed to steady laminar shear show reduced proliferation, apoptosis, and favor vasodilation. (B) Cells exposed to disturbed shear upregulate pro-inflammatory genes and genes that favor proliferation in part through NF- κ B and MAPK. Flow sensing cilia may be present in areas of disturbed shear. (C) Transcription factor Klf2 is induced by laminar shear and upregulates vasodilatory factors, COX-2 and eNOS, which produces prostaglandins, and NO, respectively.

1.2 ARTERIOVENOUS MALFORMATIONS

Vascular malformations are prevalent in approximately 4.5% of the population [98]. Typically, they are present at birth and grow in proportion to the individual. Arteriovenous malformations (AVMs) consist of high-flow arteries or arterioles that lack an intervening capillary bed and instead lead into a tangled web of vessels, or nidus, which feeds directly into a neighboring draining vein. This architecture essentially allows high-pressure blood flow to travel from thick-walled arteries directly into thin-walled veins, creating extreme hemodynamic stress within the vein [99]. These fragile improper connections are susceptible to rupture and can lead to a range of clinical complications depending on size and location including epistaxis, hemorrhage, and stroke. AVMs appear in equal frequency in men and women and have been documented in almost every tissue and organ; when they occur in small mucous membrane or cutaneous vessels, they are known as telangiectasias [100]. It was originally thought that all AVMs formed during development; however it is now widely accepted that these connections can manifest in any vessels undergoing active angiogenesis. Some speculate that AVMs may arise due to failed regression of arteriovenous connections within primitive vascular plexuses [101, 102]. An alternative and currently more widely held explanation is that loss of arterial-venous identity leads to loss of artery-vein repulsion and therefore direct arteriovenous connections.

1.2.1 Arterial-venous specification and AVM development

Although maintenance of arterial identity requires pulsatile laminar shear stress, the acquisition of arterial and venous endothelial cell fate is determined prior to exposure to hemodynamic forces. In fact, it has been postulated that improper assignment of arterial and venous identities is a critical underlying cause of AVMs (Figure 3).

1.2.1.1 Arterial-venous specification

Arterial specification is dependent on the interplay between sonic hedgehog (Shh), VEGFA, Notch, and Ephrin signaling pathways. In zebrafish, Shh from the notochord instructs cells within the somites to produce Vegfa, which in turn acts upon endothelial Vegfr2 to enhance Notch activity in arterial endothelial cells. Notch activity, in turn, induces expression of *ephrinB2* [103, 104]. In support of this pathway, morpholino knockdown of *shh* or *vegfa* leads to a decrease in arterial markers, *ephrinB2* and *notch5*, whereas venous expression of *flt4* expands to arteries [104]. A variety of Notch signaling components have been shown to be expressed exclusively in arterial cells including receptors *Notch1* and *Notch4* and ligands *Jag1*, *Jag2*, and *Dll4* [105-108]. *Dll4*^{+/-} and *Notch1*^{-/-}/*Notch4*^{-/-} mouse embryos display reduced arterial *ephrinB2* expression and axial vessel defects similar to mice harboring mutations in Notch downstream effectors, *Hey1*, *Hey2* and *Rbpj* [109-111]. In zebrafish, *notch5* expression is restricted to the dorsal aorta, and similar to mouse mutants, notch signaling mutants (*mindbomb*, *mib*) lack arterial *ephrinB2* expression, while constitutively active Notch can repress expression of venous markers [103]. The zebrafish *Hey2* homologue, *gridlock* (*grl*) is induced by Notch1 and is essential for formation of the dorsal aorta, with morpholino-mediated knockdown of *grl* causing an expansion of venous markers [112, 113].

The Eph receptors belong to the largest family of Receptor Tyrosine Kinases (RTKs). Both Ephrin (Efn) ligands and Eph receptors are transmembrane proteins with signaling capabilities, and cases of both forward and reverse signaling have been documented [114]. Generally, Ephrin/Eph interactions lead to cell-cell repulsion via regulation of small GTPases that control cytoskeletal dynamics [115]. *Efnb2/Ephb4* were the first identified molecular discriminators of arterial and venous endothelial cells, with *Efnb2* restricted to arteries and

Ephb4 restricted to veins [116, 117]. Disruption of either *Efnb2* or *Ephb4* leads to defects in arteries and veins indicative of loss of arterial-venous identity [48, 117]. Endothelial cells do not acquire venous identity by default: rather, the orphan nuclear receptor superfamily member, NR2F2 (previously known as Coup-TFII), promotes venous identity through downregulation of Notch signaling components [118]. In cultured mouse endothelial cells, siRNA-mediated knockdown of *Nr2f2* leads to an acquisition of arterial cell markers, *Notch1*, *EphrinB2*, and *Np1* [119, 120]. *Nr2f2*^{-/-} embryos die at E10.5 with malformed cardinal veins and mispatterned atria and sinus venosus [121]. In summary, both arterial and venous endothelial cells are independently specified, and it has been postulated that the repulsive interaction between EfnB2 and EphB4 is required to prevent direct connections between arteries and veins, or arteriovenous malformations (AVMs).

1.2.1.2 Loss of arterial-venous identity can promote development of AVMs

One theory for AVM development is that they are caused by loss of arterial-venous identity, resulting in a lack of arterial-venous repulsion and thus improper connections between arteries and veins. Much of the evidence to support this notion comes from manipulation of Notch signaling, which plays a central role in specification of arterial identity. For example, zebrafish *mindbomb* mutants, which are defective in Notch signaling due to impairment of Delta internalization, lose expression of arterial markers and develop AVMs [103, 122]. Similarly, mice harboring heterozygous mutations in the Notch ligand, *Dll4*, or homozygous mutations in various Notch downstream effectors or targets, including *Rbpsuh*, *Hey1*, and *Hey2*, exhibit defective arterial specification and develop AVMs [110, 123]. The AVMs in these Notch mutants bear striking resemblance to AVMs seen in *Efnb2* [48] and *Ephb4* mutants [116, 117], further supporting the idea that Notch signaling is required for arterial specification and thus

AVM prevention. However, enhanced Notch signaling and arterial specification also can result in AVMs. In mice, conditional expression of Notch4 ICD specifically within endothelial cells is sufficient to arterialize veins (as characterized by increased *Efnb2* expression and increased association of vSMCs) and produce AVMs [124]. Interestingly, these AVMs are reversible: when transgenic expression of Notch4 ICD is turned off, venous cell fate is restored and AVMs resolve [125]. Together, these data indicate that proper Notch regulation is critical for functional artery-vein interfaces.

Like the Notch pathway, members of the SRY-related HMG-box (SOX) family of transcription factors are critical in proper demarcation of arteries and veins, and disruption has been shown to lead to AVMs. For example, in zebrafish, morpholino-mediated co-knockdown of *sox7* and *sox18*, which function redundantly to establish arterial cell fate, produces AVMs resembling Notch pathway morphants [126-128]. Similarly, *Ragged* mutant mice, which harbor mutations in *Sox18*, display enlarged surface capillaries akin to telangiectasias and die by E11.0 with blood and lymphatic vascular defects [129-131]. Notably, mutations in *SOX18* have been found in families with the autosomal dominant recessive disorder, hypotrichosis-lymphedema-telangiectasia (HLT), who exhibit, as the name implies, telangiectasias [132].

1.2.2 Genetic causes of AVMs

Although most telangiectasias and AVMs are sporadic, some percentage can be attributed to genetic disorders, including HLT (discussed above), capillary malformation-arteriovenous malformation (CM-AVM), ataxia-telangiectasia (AT), and hereditary hemorrhagic telangiectasia (HHT). Patients with CM-AVM develop arteriovenous fistulae in the capillaries of the skin and have been shown to possess mutations in *RASA1*, which encodes a p120Ras-GAP [133]. This

very rare autosomal dominant disorder affects approximately 1 in 100,000 people of northern European origin, with prevalence in other populations unknown [100]. The autosomal recessive neurodegenerative disorder AT is caused by mutations in the serine/threonine DNA damage checkpoint kinase, Ataxia Telangiectasia Mutated (ATM) [134]. Patients with AT display locomotor impairment during childhood and develop telangiectasias in the eye typically by age eight. Telangiectasias have also been reported in the bladder, skin, lungs, and liver [135]. This rare autosomal recessive disorder occurs in approximately 1 in 100,000 people worldwide. HHT is actually a family of autosomal dominant disorders affecting approximately 1 in 8,000 people worldwide [136], and thus much more prevalent than all of the other genetic causes of telangiectasia/AVM combined. My research has focused on better understanding the pathophysiology of HHT.

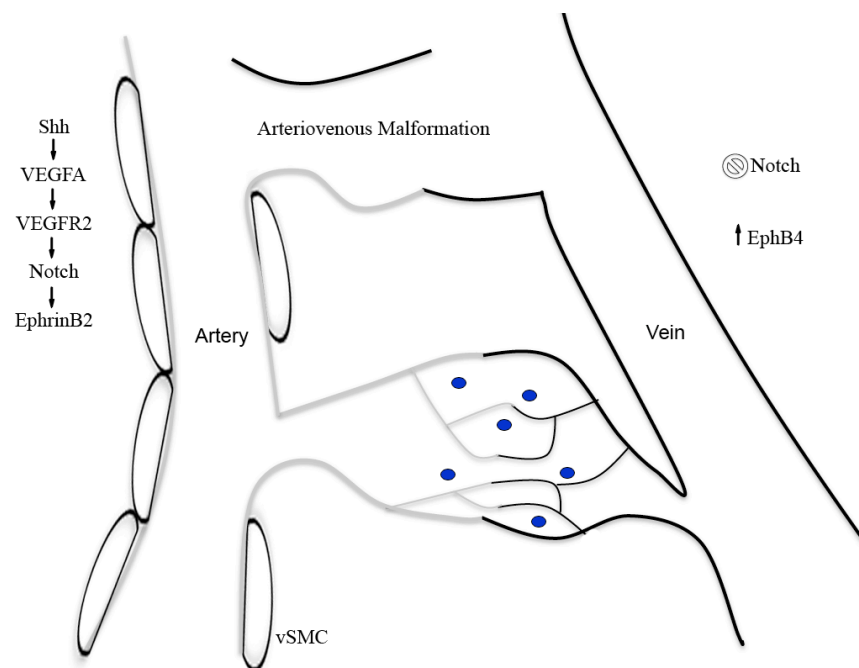


Figure 3: Artery-Vein differentiation and the formation of Arteriovenous Malformations.

Arteries (gray vessels) are specified by notochord-derived Sonic hedgehog (Shh) activating somitic VEGFA ligand which binds arterial endothelial cell VEGFR2, inducing Notch expression and upregulating EphrinB2 ligand. In veins (black vessels), inhibited Notch signaling leads to an increase in EphB4. Capillary beds allow for diffusion of oxygen and nutrients into surrounding tissue. Arteriovenous malformations (AVMs) are tortuous fragile connections between arteries and veins that possess deficient oxygen and nutrient exchange. Loss of arterial-venous identity may trigger AVM formation.

1.3 HEREDITARY HEMORRHAGIC TELANGIECTASIA

HHT, the most common cause of genetically-based AVMs and telangiectasias, is actually a family of disorders caused by mutations in TGF- β superfamily signaling components. HHT accounts for 70-80% of pulmonary AVMs in the general population [137], and a lesser but significant percentage of brain, liver, spinal cord, and gastrointestinal AVMs. HHT is characterized by highly variable age of onset and expressivity, with most HHT patients (~70%) experiencing severe and recurrent nosebleeds by age 20. In contrast, gastrointestinal bleeding typically affects patients at age 50 or over. Shunting of blood even prior to rupture can cause patients to suffer from transient ischemic attack, migraines, and hypoxemia [138-141]. Diagnosis is based on the following criteria: 1) epistaxis, 2) oral/dermal telangiectasias, 3) visceral AVMs, and 4) family history. Patients who meet three of the above “Curacao Criteria” are diagnosed as having HHT [136, 142, 143]. Below, I review the basics of TGF- β signaling and discuss the genetics of HHT. Finally, I summarize studies in animal models that have increased our understanding of the mechanism by which ALK1 signals in the endothelial cell to prevent AVMs, which have served as the foundation of my dissertation research.

1.3.1 Overview of TGF- β family signaling

In TGF- β signaling, a secreted ligand binds to a complex of two type I and two type II receptors, all of which are transmembrane serine/threonine kinases. Ligand binding may be facilitated by the presence of a non-signaling type III receptor, either betaglycan or endoglin. Type II and type I receptors typically exist as dimers but complex as heterotetramers upon ligand binding, allowing phosphorylation and thus activation of the type I receptor by the type II receptor, and subsequent type I-receptor mediated phosphorylation of Smad transcription factors. Activated Smads form a heterotrimeric complex with the common partner Smad, Smad4, enter the nucleus and activate or repress target genes (for review, see [144]). Specificity is imparted by cell-type specific coactivators or corepressors guiding Smad-mediated transcription [145]. Additional complexity is introduced in several ways: type I receptors can activate Smad-independent pathways [146]; Smad proteins can form non-traditional heterotrimeric complexes [145]; Smad proteins can play non-transcriptional roles [147]; and Smads may interact with other signaling pathways [148]. Below, I elaborate on the BMP arm of TGF- β signaling, which is directly relevant to HHT.

1.3.1.1 BMP ligands

There are 33 members of the TGF- β superfamily of ligands, including TGF- β s, activins, nodals, myostatin, anti-Mullerian hormone (AMH), growth and differentiation factors (GDFs), and Bone Morphogenetic Proteins (BMPs). BMP ligands represent the most abundant class of TGF- β family ligands, with 20 members. BMP precursor proteins are produced in the cytoplasm as 400-500 amino acid proteins containing an N-terminal signal peptide necessary for secretion, a prodomain, and a C-terminal mature peptide. Mature BMP ligands have seven cysteine residues,

with six participating in intrachain disulfide bonds and the seventh forming an additional disulfide bond with a second monomer [149]. Prior to secretion, BMPs are cleaved between the prodomain and the mature peptide by furin proteases, and the protein is secreted as a noncovalent complex consisting of two covalently-linked mature peptides that are noncovalently linked to two prodomains (Figure 4). Some ligands bound to their prodomain (for example, BMP4,5,7,9) can be active in solution because of the ability of type II receptors to compete with the prodomain for active ligand binding. Conversely, the prodomains of other ligands (for example, BMP10) render them inactive [150, 151]. The prodomain bestows structural stability and renders ligand active at greater distances [152] and may mediate dimer interactions to extracellular matrix molecules, thereby enhancing localization of action [153]. The activity of some BMPs can also be regulated through reversible interactions with extracellular antagonists (noggin, chordin, DAN) [154].

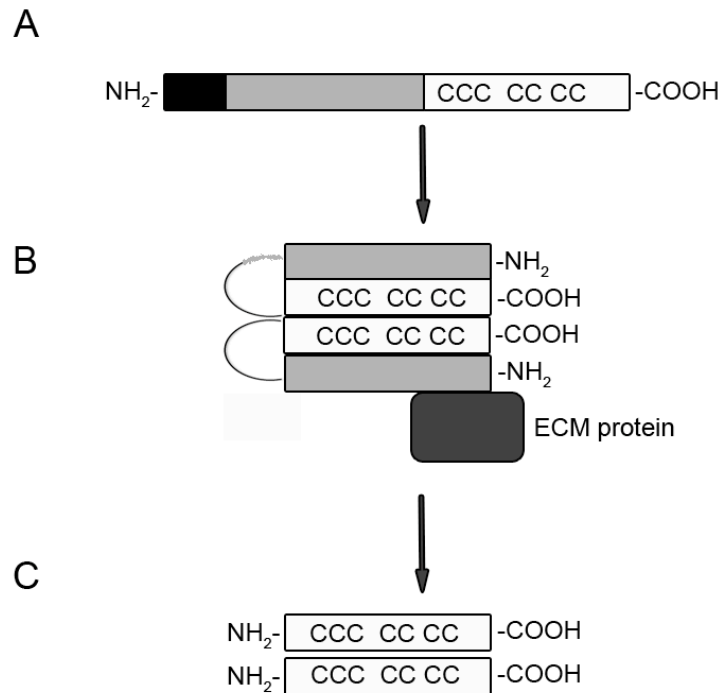


Figure 4: Processing of BMP ligands.

(A) BMP proteins include an N-terminal secretion signal (black box), a prodomain (grey box), and a C-terminal active peptide (white box). (B) Prior to secretion, the signal sequence and the prodomain are cleaved, but the latter remains noncovalently bound to the mature peptide. Some BMPs are active when bound to the prodomain, whereas others must be released from the prodomain (C).

1.3.1.2 BMP receptors

The TGF- β ligands signal through a heterotetrameric complex of two type II receptors and two type I receptors (Figure 5) all of which are single transmembrane spanning serine/threonine kinases with short cysteine rich extracellular domains [149]. There are seven type I receptors (activin receptor-like kinases, or Alk1-Alk7) and five type II receptors [activin type IIA receptor (ActRIIA), activin type IIB receptor (ActRIIB), BMPRII, TGF β R2, and anti-mullerian hormone type II receptor (AMHRII)]. BMPs are unique amongst TGF- β ligands in that they have the capacity to bind independently to either type II or type I receptor first, with choice dictated by relative affinity [155]. However, BMPs utilize only specific complexes with either BMPRII, ActRIIA, or ActRIIB serving as type II receptor and Alk1, 2, 3, or 6 serving as type I receptor [149]. Ligand binding can be facilitated by non-signaling type III receptors which are either transmembrane or glycosylphosphatidylinositol-anchored [156]. Upon ligand binding the type II receptor transphosphorylates the type I receptor on a conserved Gly-Ser (GS) domain allowing downstream transcription factors Smads1/5/9 to dock on the L45 loop of the type I receptor and become phosphorylated [145].

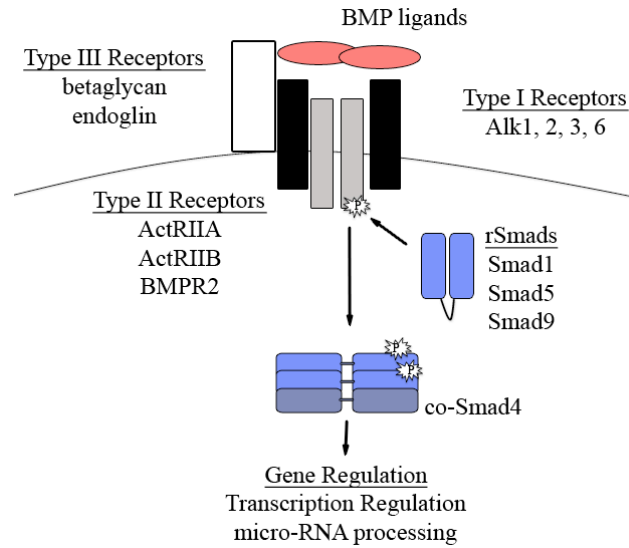


Figure 5: BMP signaling pathway

BMP ligands bind to a heterotetrameric complex of type I and type II serine/threonine kinase receptors. Ligand binding is facilitated by type III receptor. Type II receptor transphosphorylates the type I receptor leading to activation (release from autoinhibitory fold) of receptor Smads (rSmads1/5/9) which complex with co-Smad4 and regulate gene expression either at the transcriptional or post-transcriptional level.

1.3.1.3 BMP-related Smad proteins

Intracellular signaling by TGF- β s and BMPs is reliant upon Smad proteins. Smad protein family members are divided into receptor-regulated (rSmads), inhibitory Smads (iSmads), and the co-Smad, Smad4. rSmads can be subdivided based on the Type 1 receptors to which they bind. rSmads2 and 3 dock with T β RI/ALK5, ActRIB/ALK4, and ALK7 downstream of TGF- β binding, whereas rSmads1, 5 and 9 complex with ALK1, ALK2, BMPRIA/ALK3, and BMPRIIB/ALK6 upon BMP binding. Receptor recognition is governed by the L45 loop of the receptor and the L3 loop and α helix 1 (H1) of the Smad protein. Phosphorylation on the MH2 domain on a conserved SSXS motif [157] releases rSmads from their autoinhibitory fold

between MH1 and MH2 domains. Smad4 and two rSmads form a heterotrimer via binding of their MH2 domains, and enter the nucleus (Figure 6).



Figure 6: Domain structure of Smad proteins.

(A) r-Smads are comprised of MH1 and MH2 domains, which function to bind DNA and other Smad proteins respectively. The nuclear localization signal (NLS) on the MH1 domain helps target the r-Smad to the nucleus while the L3 loop on the MH2 domain is critical for recognition of type I receptor. Phosphorylation of r-Smads occurs on a conserved SSXS sequence. (B) co-Smad4 is also comprised of MH1 and MH2 domain with the H3/4 loop on the MH2 domain facilitating interactions with r-Smads.

Once within the nucleus, Smad complexes bind conserved Smad binding elements (SBEs, core sequence GTCT); however BMP-activated Smads recognize SBEs weakly and require additional GC-rich sequences known as BMP-Responsive Elements (BRE; GGCGCC) [158, 159]. GGCGCC palindromes are often 5 bp from GTCT or CGCC, which are bound by the r-Smad and co-Smad, respectively [160, 161]. Due to low affinity for these sites, multiple binding sites are often needed for effective induction of target genes. More often, these complexes rely on other DNA-binding partners to regulate tissue specific transcriptional responses [162]. For example, the MH2 domain of Smad1 can bind CREB binding protein

(CBP), helping to target to specific promoters [163]. Smads can act to modulate coactivators as in the case of Smad1 binding STAT via p300 in modulating expression of GFAP in astroglial cells [164]. The Smad MH2 can bind other proteins and work to repress their transcriptional function as with the case with Hoxc-8 [165]. R-Smads may also act independently of Smad4 to influence the processing of microRNAs through a physical interaction to Drosha by their MH2 domain and hypothesized selection of microRNAs by their MH1 domain [147, 166] (Figure 5).

1.3.2 Genetics of HHT

The HHT family of diseases is caused by mutations in various BMP signaling components, and all syndromes are autosomal dominant. Currently, there are five genetic loci linked to HHT, with three of those being known genes. HHT1 maps to chromosome 9 and is caused by mutations in the type III receptor, endoglin (*ENG*) [167] which facilitates ligand binding to TGF- β family receptors [168]. HHT2 is linked to the heterozygous loss of the TGF- β Type I receptor, activin receptor-like kinase 1 (*ALK1*) on chromosome 12 [169]. Of note, a subset of HHT2 patients will develop Primary Pulmonary Hypertension (PPH), a disease linked to the heterozygous loss of the TGF- β Type II receptor, bone morphogenetic protein receptor II (*BMPRII*) [170, 171] and characterized not by AVMs but by pulmonary vascular constriction. Mutations in *SMAD4*, a downstream effector of TGF- β signaling, have been linked to Juvenile Polyposis with HHT phenotypes [172]. Mutations in *ENG*, *ALK1*, and *SMAD4* account for 80-87% of HHT cases with similar frequency of mutations in *ENG* and *ALK1* (53% and 47%, respectively) [173]. It is also important to note that in each of the above cases, HHT results from haploinsufficiency. HHT1 and HHT2 are clinically distinguishable, with pulmonary AVMs much more common in HHT1 and hepatic AVMs more common with HHT2 [173-175]. The organ-specific nature of these diseases is not at all understood but suggests the intriguing possibility that *ALK1* and endoglin may not

actually function in the same molecular pathway, at least in certain vascular beds. HHT3 has been linked to a 5.4 cM disease gene interval on chromosome 5 [176], and HHT4 to a 7-Mb region on the short arm of chromosome 7 (7p14) [177]. As causative genes have not yet been identified in these locations, it remains to be determined whether these genes also function in BMP signaling.

1.3.3 ALK1 signaling in endothelial cells

ALK1 is an endothelial cell specific TGF- β type I receptor that is predominantly expressed in arteries, with strongest expression during embryonic development and very low expression in adult arteries, although areas of active angiogenesis, as in wound healing or in vascular pathologies, display increased *Alk1* expression [178, 179]. Although ALK1 is clearly required for normal vascular development and prevention of AVMs, the role of ALK1 in arterial endothelium is not understood. Constitutively active Alk1 ($Alk1^{CA}$) is able to increase proliferation of immortalized mouse endothelial cells, suggesting a role in angiogenic activation [180]. Conversely, siRNA-mediated knockdown of *ALK1* in human dermal microvascular endothelial (HMVEC-d) cells increases proliferation and migration, suggesting a role in angiogenic resolution [146]. In vivo systems strengthen the case for ALK1 functioning in angiogenic resolution. In zebrafish, *alk1* mutant embryos possess supernumerary endothelial cells in a subset of cranial arteries and develop arteriovenous malformations (AVMs) [181, 182]. Similarly, endothelial deletion of *Alk1* in mice causes enlarged arteries and AVM formation indicative of Alk1 being required for angiogenic resolution [183].

1.3.3.1 ALK1 ligands

TGF- β 1 and TGF- β 3 can bind ALK1 in concert with T β RII in cultured endothelial cells and trigger phosphorylation of Smad1/5 [180, 183, 184]. However, although mice lacking TGF β -1 or TGF β -3 possess dilations in the yolk sac vasculature reminiscent of Alk1 or Endoglin null mice, they do not develop AVMs [185, 186]. Furthermore, the binding and subsequent activation by TGF- β 1 and TGF- β 3 requires ALK5, which has been shown to be dispensable for in vivo Alk1 signaling in both mouse and zebrafish models [187]. Further evidence against a role for these ligands in ALK1 signaling comes from the fact that neither TGF- β 1 nor TGF- β 3 produces a prolonged phosphorylation of Smad1/5 in cultured endothelial cells [180]. Thus, roles for TGF β -1 or TGF β -3 in ALK1 signaling in vivo seem unlikely.

Of 29 TGF- β ligands (including TGF- β 1 and TGF- β 3) tested in BIAcore ALK1 binding assays, only BMP9 and BMP10, which are highly related ligands, bind to ALK1 with nanomolar affinity [188, 189]. It has also been shown that Bmp9 and Bmp10 have higher affinities for Alk1 than alternative BMP ligands have for their Type I receptor [149, 190-192]. At the protein level, BMP9 and BMP10 are 65% identical and share 16/24 residues that contact ALK1, with an additional five being conservatively substituted [193]. Both ligands can suppress HUVEC proliferation and migration [194, 195], similarly to ALK1^{CA}. Furthermore, BMP9 and BMP10 can suppress VEGF and FGF-2 induced angiogenesis in mouse sponge and chick allantois assays [196]. However, the role of these ligands in ALK1 signaling in vivo is not clear.

1.3.3.2 Signaling pathways downstream of ALK1

Historically, activity of ALK1 has been assessed by pSmad1/5/9 expression or activation of a pSmad1/5-responsive reporter, BRE-luciferase. Indeed, both BMP9 and BMP10 as well as

ALK1^{CA} can induce pSmad1/5/9 expression in cultured endothelial cells, and siRNA-mediated knockdown of *ALK1* abrogates the effect of BMP9/10 on pSmad1/5/9 [194-196]. However, the necessity of Smad1/5/9 phosphorylation downstream of ALK1 has not been well demonstrated. In human dermal microvascular endothelial cells, ALK1 can inhibit cell migration in a pSmad1/5/9-independent manner, relying instead on phosphorylation of MAP kinases, including p38 and ERK1/2 [146]. In mouse, *Tak1* (*Map3k7*) has been proposed to serve as a mediator of the Alk1 signal, with *Tak1*^{-/-} embryos suffering from yolk sac angiogenesis defects similar to *Alk1* mutant embryos. Similarly, co-knockdown of *tak1* and *alk1* in zebrafish produces enlarged cranial vessels, although the phenotype is quite dissimilar to that in *alk1* mutants [197]. Note that co-knockdown of *smad5* and *alk1* also reportedly produced a vascular phenotype similar to that in *alk1* mutants, suggesting that both MAPK and Smads may play roles downstream of ALK1 [182, 197].

1.3.3.3 Genes regulated downstream of Alk1.

Although Alk1 is essential to endothelial cell function, few genes have been identified as targets of its activity. In cell culture, expression of *Inhibitor of differentiation-1* (*Id1*) is a known readout of Alk1 activity, with *Alk1* knockdown leading to downregulation of Id1 promoter-driven luciferase and ID1 protein expression [194-196]. In mice, *Robo4* is upregulated five fold in *Alk1* mutants relative to wild type [54]. Recently, an intracellular transmembrane protein, *Tmem100* has been identified as a target for Alk1 signaling in vivo, with *Tmem100* expression diminished in *Alk1* mutant and *Tmem100* mutant mice possessing defects in arterial endothelial cell differentiation and vascular morphogenesis reminiscent of *Alk1* mutants [183, 198]. Finally, Alk1 activation of pSmad1/5/9 may contribute to activation of Notch targets *Hey1* and *Hey2* to

synergistically enhance expression of Notch target genes [199]. Interestingly, downregulation of *Hrt2/Hey2* is observed in the endothelium of both *Alk1* and *Tmem100* deficient mice [198].

1.3.4 Animal models of HHT

1.3.4.1 Mouse HHT models

Alk1 mutant mice die by E11.5 from angiogenic defects, including failure to remodel the primary capillary plexus and dilation of large vessels. *Alk1*^{+/-} mice also develop AVMs like HHT2 patients [183, 200, 201]. As expected, *Alk1* is required cell autonomously within endothelial cells, as endothelial-specific deletion of *Alk1* in mice leads to reduced pericyte and vSMC coverage of brain endothelial cells as well as AVMs in the lungs, brain, and yolk sac [187, 202]. *Alk1*^{+/-} mice also display signs of pulmonary hypertension, including right ventricular hypertrophy and increased thickness of pulmonary arterioles reminiscent of *Smad9*^{+/-} mice and a subset of HHT2 patients [171, 203, 204]. Interestingly, postnatal deletion of *Alk1* results in AVM formation and lethality, while wounding *Alk1*-deficient dermal vessels can precipitate AVM formation [179, 187]. Together, these data indicate that *Alk1* contributes to mature vessel homeostasis. In the mouse retinal vasculature, blockage of *Alk1* signaling via a soluble ligand sink, *Alk1*-Fc, results in increased tip cells and a hypersprouted phenotype [199]. Together, these animal models suggest a role for *Alk1* in favoring arterial endothelial cell quiescence, with questions remaining as to the pathway by which *Alk1* dictates endothelial cell behavior.

1.3.4.2 Zebrafish HHT2 model

The homozygous *alk1* zebrafish mutant, *violet beaugarde* (*vbg*), like its mammalian counterparts, develops AVMs and serves as a model for HHT2 [182]. *alk1* mutants develop an enlargement in a subset of cranial arteries proximal to the heart causing increased hemodynamic

load, and subsequently precipitating downstream AVMs [181, 182]. Zebrafish *alk1* mutants serve as a valuable model to dissect AVM development not only for reasons listed at the beginning of this chapter, but also because AVMs develop in a predictable, stereotypical fashion, connecting either the basal communicating artery (BCA) or basilar artery (BA) to the primordial midbrain channel (PMBC) or primordial hindbrain channel (PHBC), respectively. Zebrafish also afford a means to dissect the complex relationship between Alk1 and blood flow. Here, I have used the *alk1* mutant zebrafish model to elucidate the in vivo signaling pathway for Alk1 and provide insight as to how Alk1 acts within the endothelium to prevent AVMs.

1.3.4.3 *alk1*-positive arteries in zebrafish

By 1.5 dpf, the vessels affected in *alk1* mutants are fully formed and carrying blood flow. Blood enters circulation from the bulbus arteriosus in the heart into left and right first aortic arches (AA1). From AA1, blood flows caudally into the lateral dorsal aorta (LDA) and rostrally into the internal carotid arteries (ICA). The ICA will split at the eye and loop dorsally to form the caudal division of the internal carotid (CaDI). The CaDI from either side of the embryo meet dorsally and form the basal communicating artery (BCA) which will distribute blood into two posterior communicating segments (PCS) before meeting again in the basilar artery (BA) carrying blood caudally and distributing blood through the brain through central arteries before being returned to the heart via the primordial hindbrain channel (PHBC) (Figure 7A, for review, see [19]).

The cranial vessels of the zebrafish embryo first arise from angiogenesis from two pairs of bilateral clusters, the rostral organizing centers (ROC) and midbrain organizing centers (MOC). Both pairs of clusters arise from angioblasts derived from the anterior lateral plate mesoderm. Between 14-16s, a subset of endothelial cells from the MOC will give rise to the

aortic arches, which will meet the LDA being formed bilaterally from ventral posterior extensions of the MOC. Other MOC progenitors will migrate toward the midline where ventral anterior extensions will give rise to the primitive ICA. Contributions to the ICA also come from posterior extensions from the ROC at 16-18s stage. At the same time, ventral extensions from the ROC form the CaDI. Further contributions to the CaDI arise via migration of rostral angioblasts that form adhesions once reaching the CaDI (for review, see [205]).

1.5 DISSERTATION AIMS

To date, although TGF- β 1, TGF- β 3, Bmp9, and Bmp10 have all been shown to bind Alk1 [180, 190, 194-196], none have been identified as necessary ligands for Alk1 in AVM prevention. Furthermore, the mechanism by which Alk1 signals in endothelial cells has not been defined in vivo. Therefore, the Aims of my thesis research were to: 1) define the relevant in vivo Alk1 ligand(s), and 2) explore the role of phosphorylated Smads1/5/9 downstream of Alk1 signaling. Using zebrafish embryos as a model system, I used genetic and embryological approaches to systematically test the relevance of putative Alk1 ligands and r-Smad proteins in vertebrate embryonic vascular development, and generated a novel Smad1/5-responsive transgenic reporter line to further define the role of Smad activation in Alk1 signaling.

2.0 CIRCULATING BMP10 ACTS THROUGH ENDOTHELIAL ALK1 TO MEDIATE FLOW-DEPENDENT ARTERIAL QUIESCENCE.

Blood flow plays critical roles in vascular development, remodeling, and homeostasis, but the molecular pathways required for transducing flow signals are not well understood. In zebrafish embryos, arterial expression of *activin receptor-like kinase 1 (alk1)*, which encodes a TGF- β family type 1 receptor, is dependent on blood flow, and loss of *alk1* mimics lack of blood flow in terms of dysregulation of a subset of flow-responsive arterial genes and increased arterial endothelial cell number. These data suggest that blood flow activates Alk1 signaling to promote a flow-responsive gene expression program that limits nascent arterial caliber. Here, I demonstrate that restoration of endothelial *alk1* expression to flow-deprived arteries fails to rescue Alk1 activity or normalize arterial endothelial cell gene expression or number, implying that blood flow may play an additional role in Alk1 signaling independent of *alk1* induction. To this end, I define cardiac-derived Bmp10 as the critical ligand for endothelial Alk1 in embryonic vascular development, and provide evidence that circulating Bmp10 acts through endothelial Alk1 to limit endothelial cell number in and thereby stabilize caliber of nascent arteries. Thus, blood flow promotes Alk1 activity by concomitantly inducing *alk1* expression and distributing Bmp10, thereby reinforcing this signaling pathway that functions to limit arterial caliber at the onset of flow. Because mutations in *ALK1* cause arteriovenous malformations (AVMs), my findings suggest that an impaired flow response initiates AVM development.

2.1 INTRODUCTION

Blood flow imparts mechanical forces and distributes endocrine factors that influence vascular development and remodeling and allow maintenance of arterial-venous identity, but the molecular pathways that govern these flow-dependent processes are not fully understood [for review, see [206]]. Among the physical forces imparted by blood flow, shear stress, the frictional force that acts in the direction of blood flow, is the most extensively studied. Laminar shear stress induces expression of the transcription factor, *KLF2*, which coordinates expression of numerous flow-responsive genes that promote cell cycle arrest and vasodilation, thereby favoring vascular quiescence and conferring atheroprotection [83-85, 207]. In contrast, disturbed (low or oscillatory) shear stress activates the transcription factors NF- κ B and AP-1, which promote an atherogenic response characterized by inflammation and vasoconstriction [208-211]. However, the repertoire of flow responses that exist in vivo clearly extends well beyond these pathways.

Mounting evidence implicates the TGF- β family type I receptor, ALK1, as a key player in a flow-responsive signaling pathway that functions independently of KLF2 to promote quiescence in nascent arteries. In zebrafish embryos, *alk1* is expressed predominantly in arteries proximal to the heart, which experience relatively high magnitudes of mechanical forces, and preventing heartbeat eliminates *alk1* mRNA expression [181]. Furthermore, either loss of blood flow or loss of *alk1* results in increased expression of *cxcr4a*, which encodes a pro-angiogenic chemokine receptor, and decreased expression of *endothelin-1* (*edn1*), which encodes a vasoconstrictive peptide [181]. Both of these genes are flow-responsive in cultured endothelial cells [212, 213], suggesting that Alk1 might lie upstream of *cxcr4a* and *edn1* in a mechanosensitive signaling pathway. In support of this hypothesis, blood flow-mediated repression of *cxcr4a* correlates with

quieting of endothelial cell protrusive activity in nascent zebrafish arteries [214], and zebrafish *alk1* mutants, which exhibit abnormally high levels of arterial *cxc4a*, develop enlarged arteries containing supernumerary endothelial cells, suggestive of failed flow-induced suppression of endothelial cell migration or proliferation [181, 182]. Evidence from mice further supports the idea that Alk1 functions in a flow-responsive pathway to quiet nascent arteries. In mice, *Alk1* is expressed predominantly in embryonic arterial endothelial cells, with weak expression in adults [215, 216]. However, *Alk1* expression can be induced in adult mice during periods of active angiogenesis in arterial endothelial cells exposed to high shear stress [215]. Furthermore, recent mouse studies have implicated bone morphogenetic protein (BMP) signaling in general or Alk1 signaling in particular in maintenance of a quiescent endothelial stalk cell fate [199, 217]. Together, these data from both mouse and zebrafish support the hypothesis that Alk1 signaling mediates flow-dependent arterial endothelial cell quiescence. Notably, *alk1* acts independently of *klf2a* in zebrafish [181], suggesting that multiple flow-dependent pathways coordinate in vivo to control the activation state of the endothelium.

Alk1 signaling is critical for normal vascular development and homeostasis in mice and zebrafish, with loss of function resulting in embryonic lethality associated with development of direct connections between arteries and veins, or arteriovenous malformations (AVMs) [169, 182, 183, 201]. In humans, *ALK1* heterozygosity results in hereditary hemorrhagic telangiectasia type 2 (HHT2), a vascular disorder characterized by predisposition to development of telangiectases and AVMs [169, 218]. However, despite the clear link between ALK1 signaling and AVM prevention, the ALK1 signaling pathway remains poorly defined in vivo. In TGF- β family signaling, ligands bind to a heterotetrameric complex of two type II receptors and two type I receptors, both of which are serine/threonine kinases. The type II receptors phosphorylate

and thus activate the type I receptors, and the type I receptors then phosphorylate receptor-specific Smad proteins. Phosphorylated Smads complex with the common partner Smad, Smad4, enter the nucleus, and, together with a variety of transcription factors, regulate transcription of target genes [for review, see [219]]. With respect to ALK1, TGF- β 1, TGF- β 3, BMP9, and BMP10 ligands can induce ALK1-dependent phosphorylation of Smad1, Smad5, and/or Smad9 (hereafter referred to as Smad1/5/9) and stimulate activity of a phospho-Smad1/5/9 (pSmad1/5/9)-responsive reporter in cultured endothelial cells [180, 183, 188-190, 194-196, 220, 221]. However, although TGF- β -mediated activation of ALK1 requires ALK5 (canonical TGF- β 1 type I receptor) activity in cultured endothelial cells [221], endothelial cell-specific deletion of *Alk5* in mice or *Alk5* inhibition in zebrafish embryos does not affect *Alk1* activity [187], suggesting that TGF- β subfamily ligands are not relevant to *Alk1* signaling in embryonic development. In fact, BMP9 and BMP10 are the only TGF- β superfamily ligands that bind to ALK1 with high affinity in vitro, and they circulate at physiologically relevant concentrations [188, 189, 196, 222]. However, neither *Bmp9* [189, 196, 222] nor *Bmp10* [223] null mice phenocopy *Alk1* null mice [183, 201], which present with AVMs. Although the lack of AVMs could reflect ligand redundancy, interference with both ligands via blocking antibodies and/or ligand traps impairs mouse retinal angiogenesis but does not produce retinal AVMs [199, 222]. As such, the identity of the activating ALK1 ligand in vivo has remained elusive.

In this work, I use zebrafish embryos to demonstrate that *Alk1* kinase activity, in addition to *alk1* mRNA expression, requires blood flow, and I provide evidence that this newly-defined role for blood flow stems not from mechanical force but from distribution of the cardiac-derived circulating ligand, *Bmp10*. Taken together, my data define a novel endocrine pathway in which circulating *Bmp10* binds to endothelial cell *Alk1* to induce phosphorylation of Smad1/5/9, which

promotes a program of gene expression that limits endothelial cell number within nascent arteries in response to blood flow. Abrogation of this flow response results in enlarged arteries and ultimately AVMs.

2.2 RESULTS

2.2.1 Blood flow is required not only for *alk1* expression but also for Alk1 activity

In 36 hours post-fertilization (hpf) zebrafish embryos, *alk1* is expressed predominantly in endothelial cells within arteries proximal to the heart: the first aortic arch; the cranialward internal carotid artery, caudal division of the internal carotid artery (CaDI), and basal communicating artery (BCA); and the caudalward lateral dorsal aortae (Figure 7A). We previously demonstrated that *alk1* expression requires blood flow, and that loss of *alk1* mimics loss of blood flow in terms of changes in expression of *cxcr4a* and *edn1*: both *alk1* mutants, which have high flow through assayed vessels, and *cardiac troponin-t2a* (*tnnt2a*) morphants, which lack heartbeat and blood flow, exhibit increased *cxcr4a* expression and decreased *edn1* expression in *alk1*-expressing cranial arteries at 36 hpf [Figure 7B and [181]]. Given that mammalian orthologs *Cxcr4* and *Edn1* are flow-responsive in cultured endothelial cells [212, 213], these data suggest that Alk1 might act downstream of blood flow to control expression of these mechanoresponsive genes. Accordingly, if Alk1 signaling is sufficient downstream of blood flow, then restoration of *alk1* in the absence of flow might be expected to rescue expression of *cxcr4a* and *edn1*. To test this hypothesis, we generated a stable transgenic line, *Tg(fli1a:alk1-myc)*, which expresses Alk1-myc in all endothelial cells regardless of the presence of blood flow (Figure 8). This transgene restores wild type expression of *cxcr4a* and *edn1* during embryogenesis (Figure 7B), rescues *alk1* mutants to adulthood [n = 23 *alk1* mutants of 130 adults

from *alk1*^{+/-}; *Tg(fli1a:alk1-myc)* incrosses; 71% rate of rescue], and has no untoward effects on growth and development. However, flow-independent expression of endothelial cell *alk1* fails to normalize expression of *cxcr4a* or *edn1* in 36 hpf *tnnt2a* morphants (Figure 7B). There are two plausible explanations for this observation: Alk1 signaling may not be sufficient downstream of blood flow to control expression of these genes, or flow may be required for some aspect of Alk1 signaling in addition to *alk1* expression.

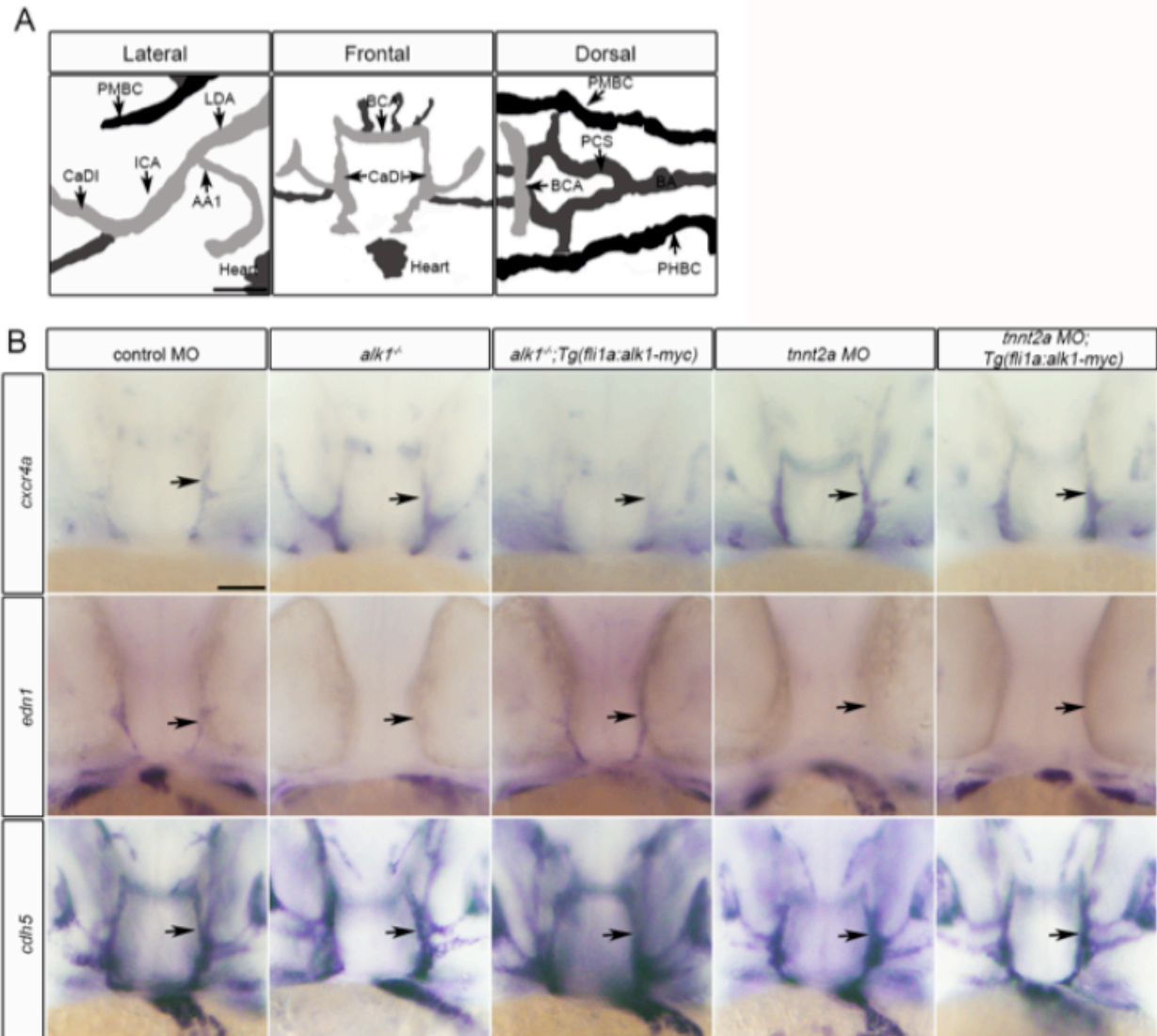


Figure 7: Restoration of *alk1* expression does not rescue *cxcr4a* and *edn1* expression in the absence of blood flow.

(A) Lateral, frontal, and dorsal views of the zebrafish cranial vasculature, 36 hpf. *alk1*-positive arteries are light gray, *alk1*-negative arteries dark gray, and veins black. Note *alk1*-positive arteries are closest to the heart. AA1, aortic arch 1; BA, basilar artery; BCA, basal communicating artery; CaDI, caudal division of the internal carotid artery; ICA, internal carotid artery; LDA, lateral dorsal aorta; PCS, posterior communicating segments; PHBC, primordial hindbrain channel; PMBC, primordial midbrain channel. Scale bar, 50 μ m. (B) Whole mount in situ hybridization for *cxcr4a*, *edn1*, and cadherin 5 (*cdh5*, pan-endothelial control) at 36 hpf in control morphants; *alk1*^{-/-}; *alk1*^{-/-} embryos in which *alk1* expression is restored by a blood flow-independent transgene, *fl1a:alk1-myc*; *tnnt2a*

morphants; and in *tnnt2a;Tg(fli1a:alk1-myc)* embryos. Frontal views, dorsal up. Arrows, *alk1*-positive CaDI. Scale bar, 50 μm .

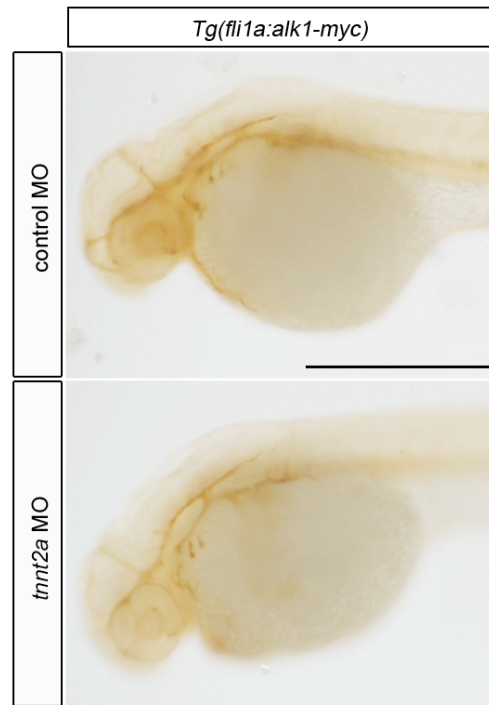


Figure 8: *Tg(fli1a:alk1-myc)* drives *alk1* expression in all endothelial cells independently of flow.

Immunohistochemistry for myc in 36 hpf *Tg(fli1a:alk1-myc)* embryos injected with either control or *tnnt2a* MO.

Lateral views, anterior left. Scale bar, 200 μm .

To determine whether restoration of endothelial *alk1* expression is sufficient to restore Alk1 signaling in the absence of flow, I assessed a direct measure of Alk1 activity, phosphorylated Smad1/5/9 (pSmad1/5/9). Because *alk1* expression is dependent on blood flow [181] and immunofluorescent detection of pSmad1/5/9 is dependent on *alk1* expression, detection of pSmad1/5/9 by immunofluorescence in these arterial endothelial cells should be dependent on blood flow. Indeed, pSmad1/5/9 immunofluorescence is not detectable in the CaDIs at 24 hpf, prior to the onset of flow through and *alk1* expression in these vessels (Figure 9A), and pSmad1/5/9 epitope is absent at 36 hpf in *tnnt2a* morphants (Figure 9B) but is robust in

sibling controls (Figure 9C). However, restoration of *alk1* expression via a *fli1a:alk1-myc* transgene in flow-deprived *tnnt2a* morphants fails to rescue detection of pSmad1/5/9 by immunofluorescence (Figure 9D), whereas endothelial-specific expression of a constitutively active (ligand- and type II receptor-independent) form of *alk1* via a *fli1a:alk1^{CA}-mCherry* (*fli1a:alk1^{CA}-mCh*) transgene restores pSmad1/5/9 epitope in the absence of blood flow (Figure 9E). Taken together, these data suggest that blood flow is required not only for *alk1* expression but also for some additional aspect of Alk1 activity, such as type II receptor expression and/or expression or distribution of Alk1 ligand.

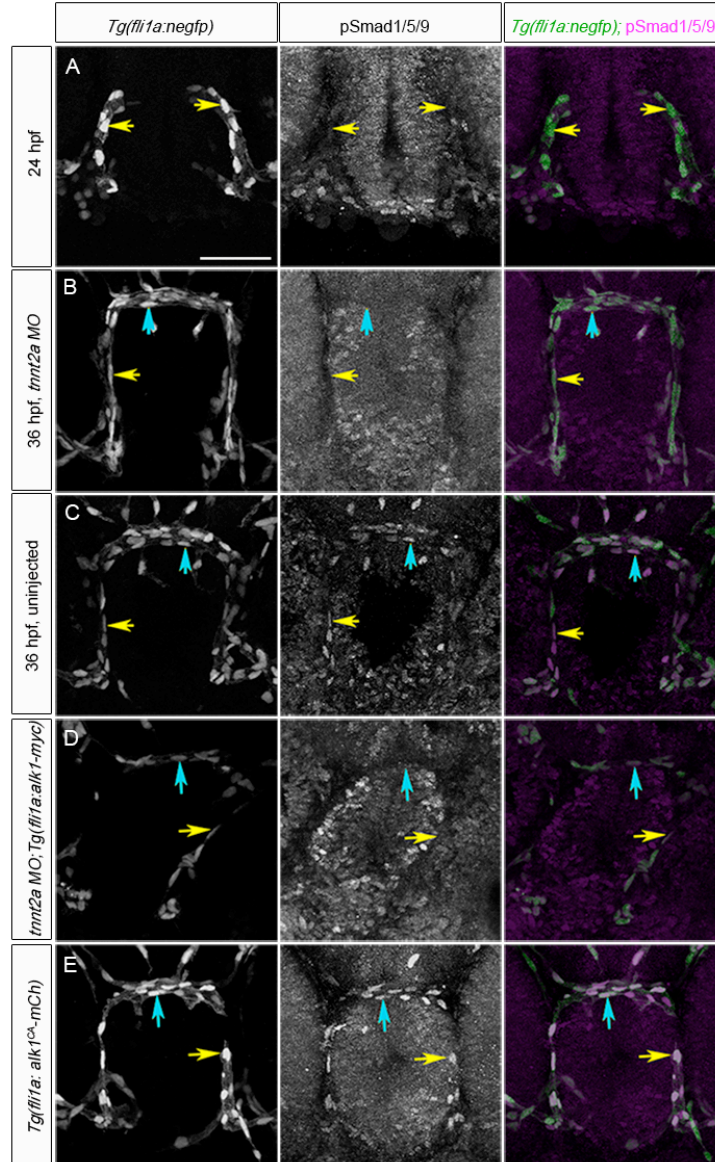


Figure 9: Alk1 activity is dependent on blood flow.

pSmad1/5/9 expression (middle column) in endothelial cells (nuclei marked by *fli1a:negfp* transgene, left column) at 24 hpf, prior to blood flow (A); in the absence (*tnnt2a* morphants, B) or presence (C) of blood flow at 36 hpf; in *tnnt2a* morphants harboring a *fli1a:alk1-myc* transgene (D); and in embryos harboring a *fli1a:alk1^{CA}-mCh* transgene (E). Note that *Tg(fli1a:alk1^{CA}-mCh)* embryos do not have blood flow in these vessels. In merge (right column), EGFP-expressing endothelial cell nuclei are green, pSmad1/5/9 immunofluorescence is magenta. Yellow and blue arrows point to endothelial cells in the CaDI and BCA, respectively. 2D confocal projections of 50 μ m frontal sections, dorsal up. Scale bar, 50 μ m.

2.2.2 *bmp10* knockdown phenocopies *alk1* mutants

To investigate the effect of blood flow on Alk1 ligand availability, I first needed to determine the physiologically relevant ligand during zebrafish embryonic vascular development. Therefore, I assessed vascular gene expression and architecture between 36 and 48 hpf in *bmp9* (ENSDARG00000059173) and *bmp10* (ENSDARG00000061769) morphants, and compared results to *alk1* mutants/morphants. Translation blocking (TB) morpholinos were validated in vivo as described in Materials and Methods (Figure 10).

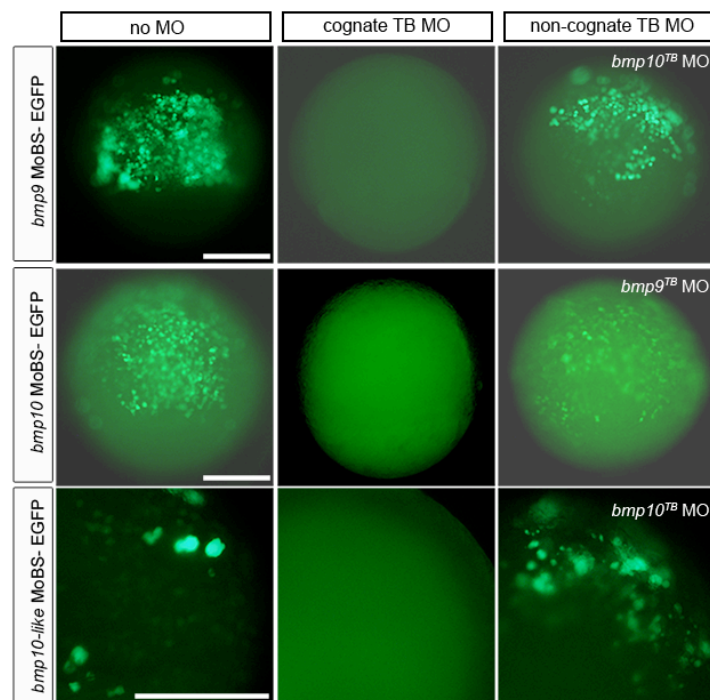


Figure 10: *bmp9*, *bmp10*, and *bmp10-like* knockdown their respective targets in vivo.

Wild type embryos injected at the one-cell stage with 50 pg CMV-driven EGFP constructs modified with morpholino binding sites (MoBS) inserted upstream of the ATG, with or without cognate or non-cognate morpholinos. *Bmp9* MO: 7 ng; *bmp10* MO: 20ng; *bmp10-like* MO, 3 ng. Embryos were observed at ~6 hpf for EGFP fluorescence. Scale bar, 500 μ m (top two rows) or 250 μ m (bottom row).

Injection of *bmp9^{TB}* morpholino had no effect on detection of pSmad1/5/9 by immunofluorescence in the 36 hpf CaDI/BCA (Figure 11A) nor any effect on cranial vascular architecture at 48 hpf (Figure 11B), but reproducibly generated a venous remodeling defect in the tail that was phenocopied by injection of *bmp9* splice blocking (SB) morpholino (data not shown).

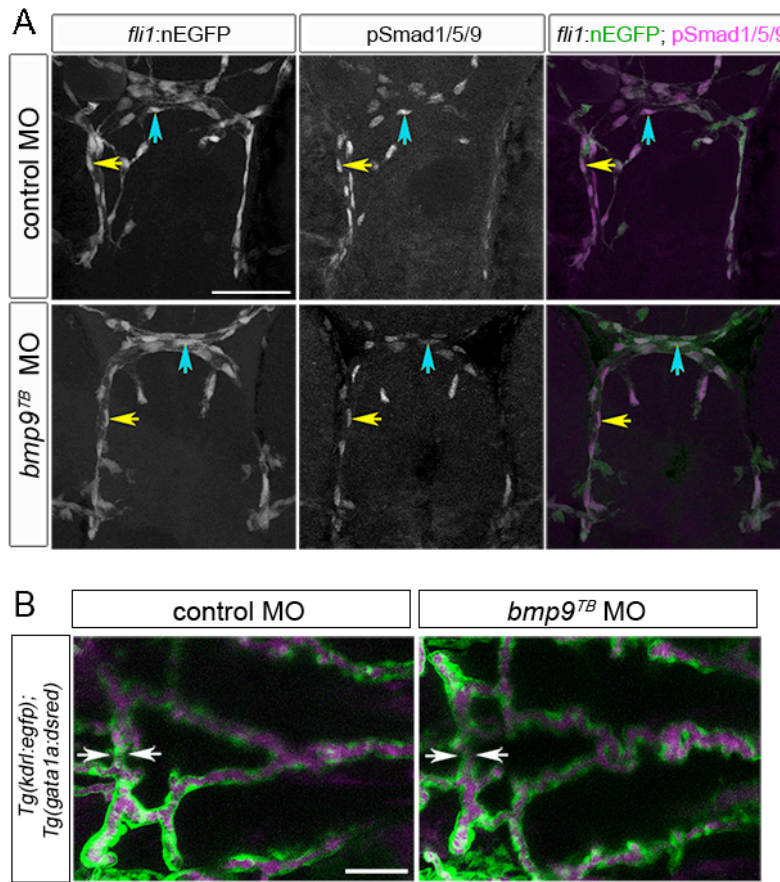


Figure 11: *bmp9* knockdown does not phenocopy *alk1* mutants.

(A) pSmad1/5/9 expression (middle column) in endothelial cells (nuclei marked by *fli1a:negfp* transgene, left column) in 36 hpf control and *bmp10^{TB}* morphants. In merge (right column), EGFP-expressing endothelial cell nuclei are green, pSmad1/5/9 immunofluorescence is magenta. Yellow and blue arrows denote endothelial cells in the CaDI and BCA, respectively. 2D confocal projections of 50 μ m frontal sections, dorsal up. Scale bar, 50 μ m.

(B) Cranial vasculature in 48 hpf control and *bmp9* morphant embryos. Endothelial cells are green, red blood cells magenta. 2D confocal projections, dorsal views, anterior left, Scale bar, 50 μ m

In contrast, at 36 hpf, *bmp10^{TB}* morphant CaDIs/BCAs were enlarged and contained supernumerary endothelial cells, a phenotype indistinguishable from *alk1* morphants (Figure 12A,B). Furthermore, in the 36 hpf CaDI/BCA, *bmp10^{TB}* morphants exhibited severely downregulated detection of pSmad1/5/9 by immunofluorescence (17/19, 89%; Figure 12C), increased expression of *cxc4a* (50/53, 94% Figure 12D), and decreased expression of *edn1* (15/15, 100%; Figure 12D). These effects were similar to effects observed in *alk1* mutants. In addition, *bmp10^{TB}* morphants developed AVMs connecting the arterial system underlying the midbrain and hindbrain to adjacent veins, strongly resembling *alk1* mutants/morphants (Figure 12E). However, the *bmp10* morpholino-induced AVM phenotype was observed with relatively weak penetrance (21/43, 49%; Figure 12F) and low expressivity at a maximum tolerated dose (20 ng), suggesting that an additional ligand might be compensating for *bmp10* at later time points. Examination of the zebrafish genome uncovered *bmp10-like* (ENSDARG00000045632), which is most closely related to *bmp10* (64% identity in the active peptide) and likely represents a *bmp10* paralog that arose during a teleost whole genome duplication [224]. Therefore, I knocked down both *bmp10-like* and *bmp10* and assessed the zebrafish vasculature at 48 hpf. Injection of *bmp10-like* morpholino (3 ng) or *bmp10^{TB}* morpholino (10-15 ng) alone had almost no effect on cranial vascular architecture (n = 61 and 47, respectively), whereas co-injection of these two morpholinos at these same doses robustly phenocopied *alk1* morphants in terms of AVM development (122/146, 84%; Figure 12E,F), suggesting a strong genetic interaction. Similar results were observed with a *bmp10^{SB}* morpholino, with no AVMs at 15 ng (n = 48) but AVMs upon co-injection with 3 ng *bmp10-like* morpholino (46/57, 81%). In contrast, co-injection of *bmp9^{TB}* morpholino (7 ng) with *bmp10^{TB}* morpholino (15 ng) failed to elicit AVMs (0/29), and co-injection of *bmp9^{TB}* morpholino (7 ng), *bmp10^{TB}* morpholino (15 ng), and *bmp10-*

like morpholino (3 ng) did not increase percent phenotype (20/31, 65%) beyond combined injection of *bmp10^{TB}* morpholino and *bmp10-like* morpholino. These results demonstrate that *bmp10-like* acts redundantly with *bmp10* and that Bmp10 but not Bmp9 is the critical in vivo Alk1 ligand required for arterial quiescence and AVM prevention during zebrafish embryonic vascular development.

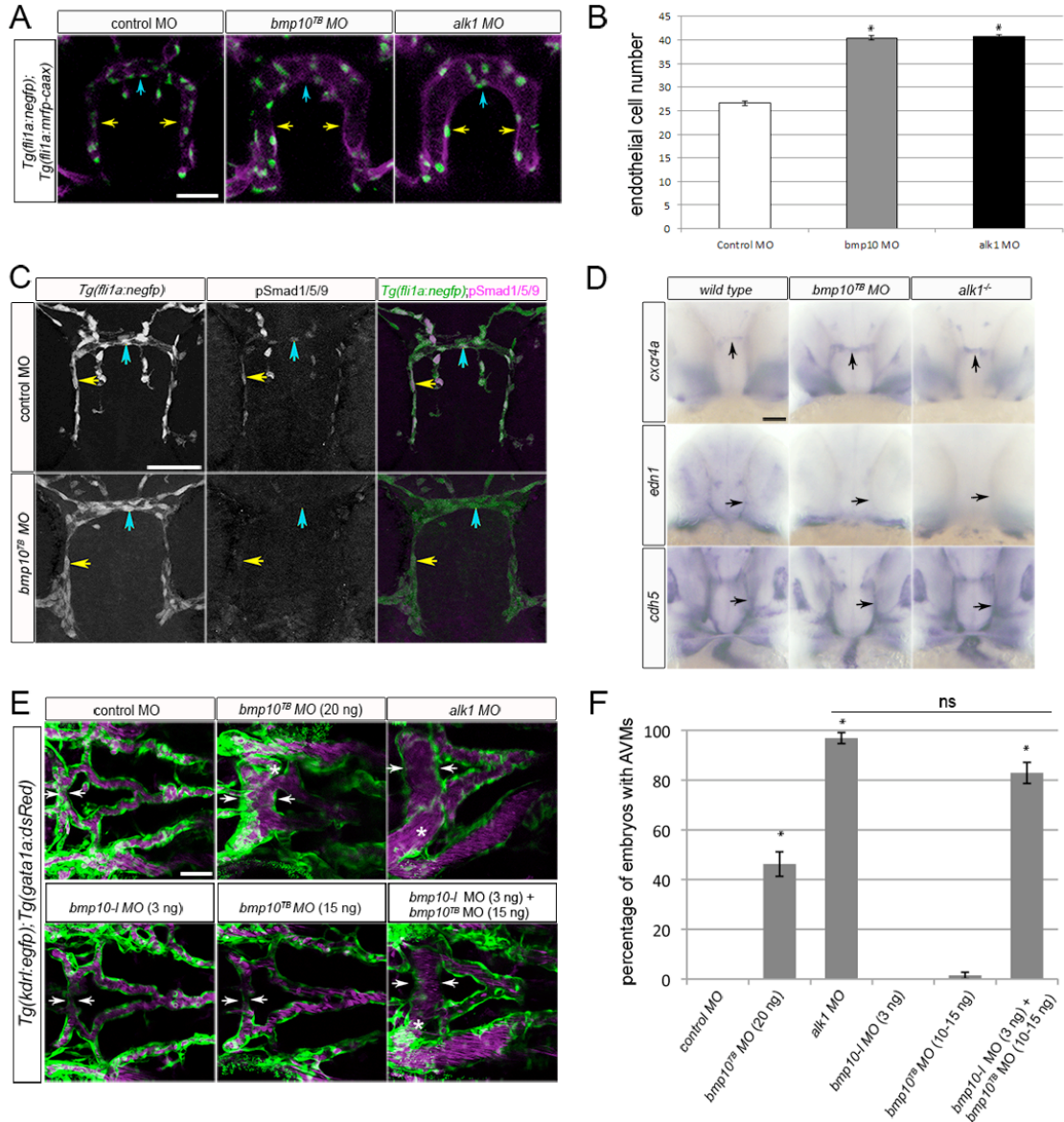


Figure 12: Knockdown of *bmp10* phenocopies zebrafish *alk1* mutants.

(A) CaDIs (yellow arrows) and BCA (blue arrows) in 36 hpf *Tg(fli1a:mrfp-caax);Tg(fli1a:negfp)* embryos injected with 20 ng control, 20 ng *bmp10^{TR}*, or 2.5 ng *alk1* morpholino. Endothelial cell membranes are magenta; nuclei are green. 2D projections of 10 optical sections (Z-step, 2 μm), frontal views, dorsal up. Scale bar, 50 μm. (B) Endothelial cell number in the CaDI/BCA in control, *bmp10*, and *alk1* morphants. n = 7 to 10 in 3 independent experiments. Values are mean ± SEM. Student's *t*-test: **P*<0.001. (C) pSmad1/5/9 expression (middle column) in endothelial cells (nuclei marked by *fli1a:negfp* transgene, left column) in 36 hpf control and *bmp10^{TR}* morphants. In merge (right column), EGFP-expressing endothelial cell nuclei are green, pSmad1/5/9 immunofluorescence is

magenta. Yellow and blue arrows denote endothelial cells in the CaDI and BCA, respectively. 2D confocal projections of 50 μ m frontal sections, dorsal up. Scale bar, 50 μ m. **(D)** Whole mount in situ hybridization for *cxcr4a*, *edn1*, and *cdh5* (pan-endothelial control) at 36 hpf. Frontal views, dorsal up. Arrows point to BCA (up) or CaDI (right). Scale bar, 50 μ m. **(E)** Cranial vasculature in 48 hpf *Tg(kdrl:gfp);Tg(gata1a:dsRed)* embryos injected with *bmp10^{TB}* morpholino (15-20 ng, as indicated), *alk1* morpholino (2.5 ng); and/or *bmp10-like* morpholino (3 ng). Arrows highlight width of BCA; asterisk denotes AVM. Endothelial cells are green, red blood cells magenta. 2D confocal projections, dorsal views, anterior left. Scale bar, 50 μ m. **(F)** Quantification of AVM development in 48 hpf morpholino-injected embryos. n = 43-146. Values are mean \pm SEM. Student's *t*-test: **P*<0.001; ns, not significant:

2.2.3 *bmp10* paralogs are expressed exclusively in the heart

I have demonstrated that concomitant knockdown of *bmp10* and *bmp10-like* phenocopies *alk1* mutants. *bmp10* expression becomes detectable in the heart at 24 hpf and is independent of mechanical force (Figure 13).

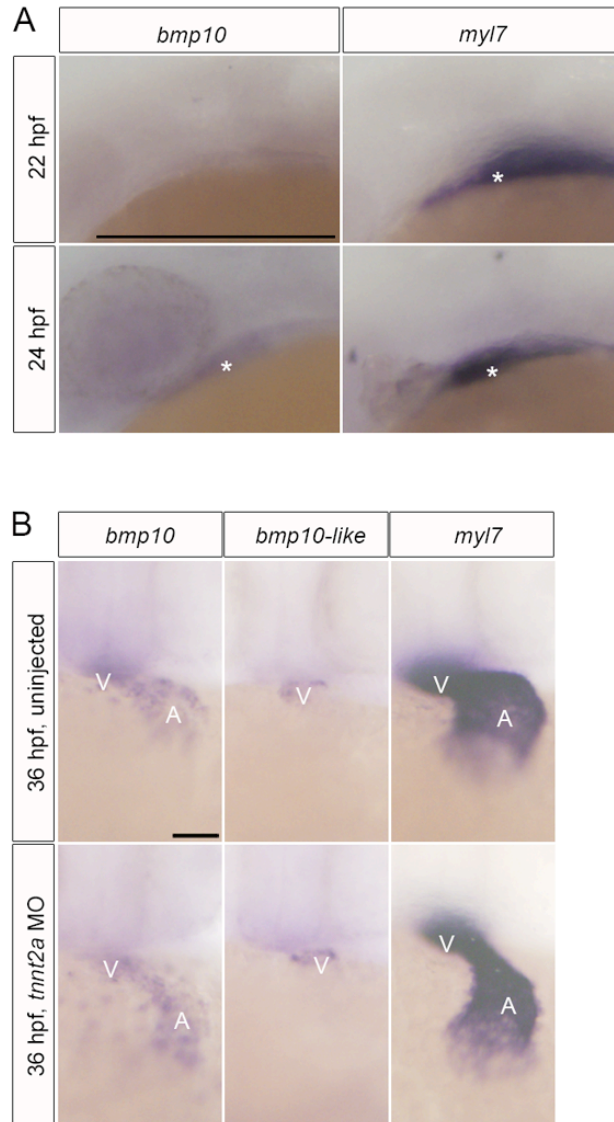


Figure 13: *bmp10* and *bmp10-like* expression is independent of flow.

(A) Whole mount in situ hybridization for *bmp10* and *myl7* (myosin light chain 7, previously known as cardiac myosin light chain) at 22 and 24 hpf. Lateral views, anterior left. Asterisk denotes location of heart. Scale bar, 500 μm (B) Whole mount in situ hybridization for *bmp10*, *bmp10-like*, and *myl7* at 36 hpf. in uninjected and *tnnt2a* morphant embryos. Frontal views, dorsal up. Scale bar, 50 μm

By 28 hpf, *bmp10* is expressed throughout the heart tube, with predominant expression in the ventricle at 36 hpf (Figure 14A). By 48 hpf, expression is in both heart chambers but absent from the atrioventricular canal (Figure 14A). Double staining for *bmp10* mRNA and sarcomeric myosin protein revealed that *bmp10* is expressed strongly in endocardium but is largely absent from myocardium at 36 hpf (Figure 14B). *bmp10-like* is undetectable in the heart at 28 hpf but is expressed at 36 and 48 hpf in distal ventricular myocardium (Figure 14A,B). No additional discrete expression domains of either *bmp10* or *bmp10-like* were detected (data not shown). The temporal difference in ligand expression suggests that Bmp10-like might compensate for Bmp10 after 36 hpf, providing a plausible explanation for the observation that knockdown of *bmp10* alone robustly phenocopies *alk1* mutants at 36 hpf, but double knockdown of *bmp10* and *bmp10-like* is required for robust phenocopy at 48 hpf (Figure 12). Furthermore, these data demonstrate that the heart is the most likely source of both Bmp10 and Bmp10-like and suggest that cardiac-derived Bmp10 ligands might be carried by blood flow to arterial endothelial Alk1.

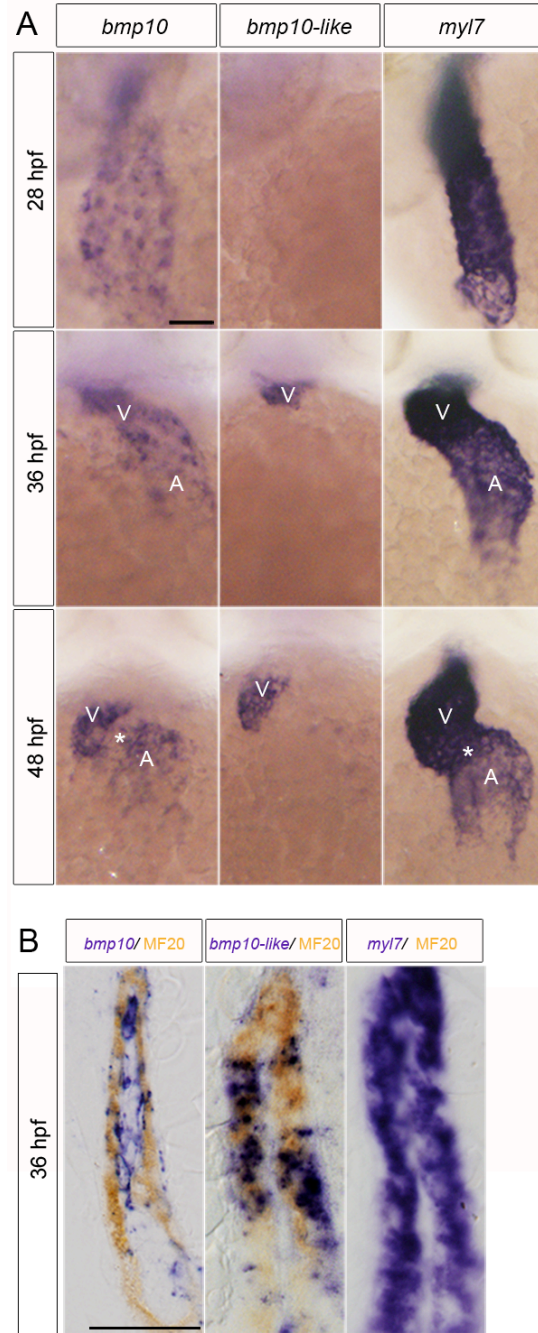


Figure 14: *bmp10* and *bmp10-like* are expressed in the heart.

(A) Whole mount in situ hybridization for *bmp10*, *bmp10-like*, and *myl7* (myosin light chain 7, previously known as cardiac myosin light chain) at 28, 36, and 48 hpf. Frontal views, dorsal up. Scale bar, 50 μ m. (B) Eight-mm sagittal sections through the heart of 36 hpf embryos co-stained with *bmp10*, *bmp10-like*, or *myl7* (purple) and MF20 (sarcomeric myosin; brown). Scale bar, 25 μ m.

2.2.4 Circulating Bmp10 acts via Alk1 to limit endothelial cell number in nascent arteries

Given that *bmp10* orthologs are detectable only in the heart in zebrafish (Figure 14) and mouse [223, 225] and that Bmp10 circulates in embryonic mouse plasma [222], it stands to reason that blood flow may be required to transport Bmp10 to arterial endothelial cell Alk1, explaining why restoration of *alk1* gene expression alone is insufficient to rescue defects in arterial endothelial cell *cxcr4a*, *edn1*, and detection of pSmad1/5/9 by immunofluorescence in the absence of flow (Figures 7,9). To test this hypothesis, I injected *tnnt2a* morpholino into *Tg(fli1a:alk1-myc)* embryos, once again generating embryos that lack heartbeat but nonetheless express endothelial *alk1*. At 28 hpf, I injected tracer (phenol red or quantum dots) alone or together with recombinant human (rh) BMP10 directly into the base of one CaDI. Note that rhBMP10 can act through zebrafish Alk1 to activate BMP responsive element (BRE)-driven luciferase activity in transfected C2C12 cells with an EC₅₀ similar to that required for activation of human ALK1 (Figure 15A). Neither *tnnt2a* morphant;*Tg(fli1a:alk1-myc)* embryos injected with tracer alone nor rhBMP10 injected siblings lacking *Tg(fli1a:alk1-myc)* showed detection of pSmad1/5/9 by immunofluorescence in the CaDI (0/17, 0/11 respectively) whereas injection with tracer plus rhBMP10 induced detection of pSmad1/5/9 by immunofluorescence near the site of injection (12/17, 71%; Figure 15B). Furthermore, injection of rhBMP10 into *tnnt2a* morphant;*Tg(fli1a:alk1-myc)* embryos decreased expression of *cxcr4a* (13/23, 57%) and increased expression of *edn1* (14/22, 64%) on the injected side, driving expression of these genes toward levels observed in the presence of blood flow (Figure 15C). In addition, similarly restoring Alk1 signaling to one CaDI in flow-deprived *tnnt2a* morphant embryos significantly decreased endothelial cell number within the injected CaDI and BCA but not the uninjected CaDI, normalizing endothelial cell number in the injected CaDI/BCA to that observed in the

presence of blood flow (Figure 15D). Because expression of *Cxcr4* and *Edn1* can be repressed or induced, respectively, by mechanical force in cultured endothelial cells [212, 213], these results support the idea that Bmp10/Alk1/pSmad1/5/9 signaling may be critical in transducing a mechanical signal into a biochemical response in arterial endothelial cells in vivo. In total, my results define a novel blood flow responsive signaling pathway – in which blood flow is required for *alk1* expression as well as, via circulating Bmp10, Alk1 activity – that is critical for flow-dependent limitation of endothelial cell number in and therefore caliber of nascent arteries.

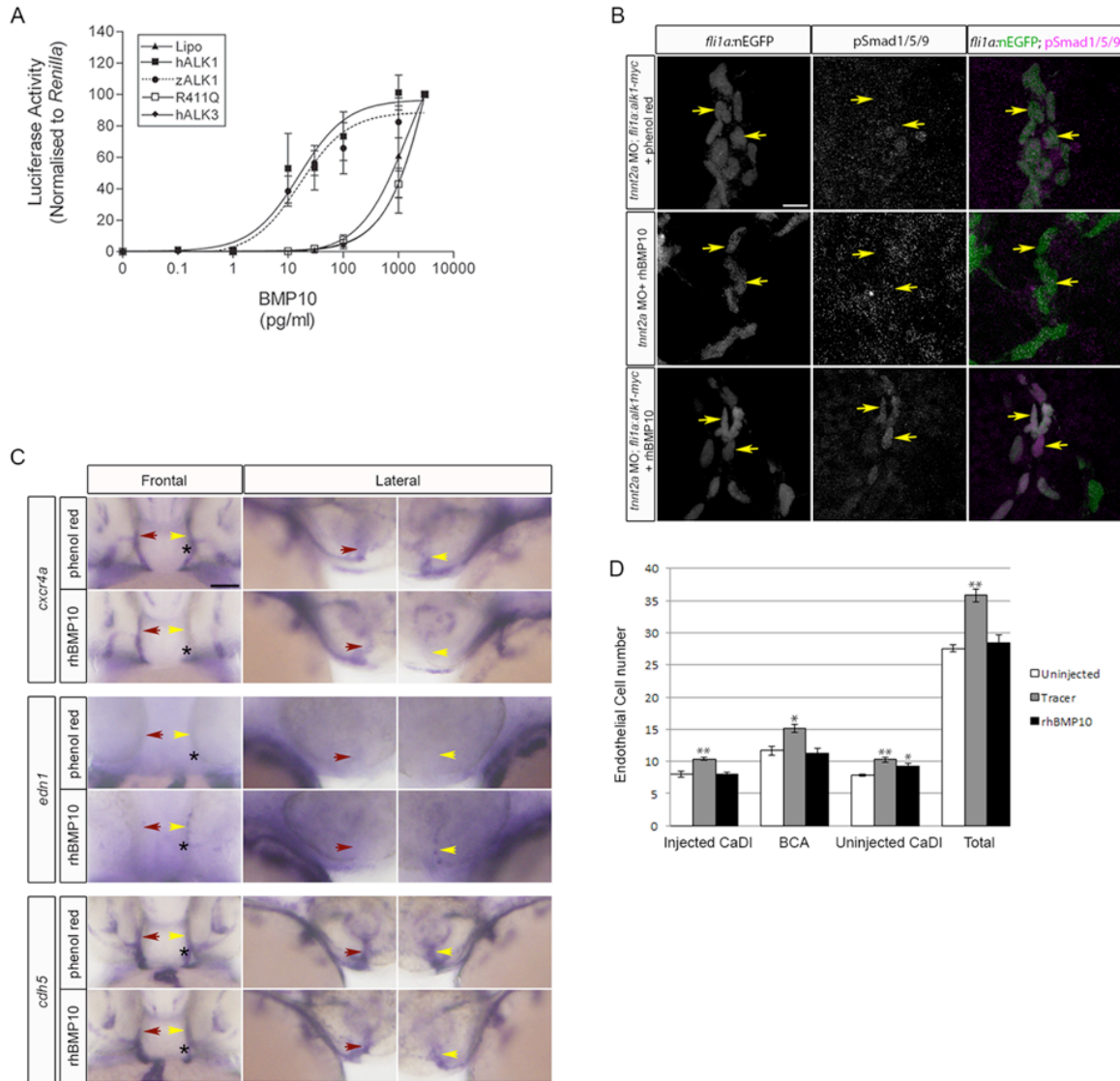


Figure 15: Bmp10/Alk1 lies downstream of blood flow in regulation of pSmad1/5/9, *cxcr4a*, and *edn1*.

(A) BRE:luciferase activity in C2C12 cells transfected with human (h)*ALK1*, zebrafish (*z*)*alk1*, *hALK1* kinase dead mutant (R411Q), *hALK3* (which does not bind BMP10), or Lipofectamine (lipo), and treated with rhBMP10. Data are normalized to pTK-*Renilla* luciferase activity. (B) pSmad1/5/9 expression (middle column) in endothelial cells (nuclei marked by *fli1a:negfp* transgene, left column) of the CaDI of 36 hpf *tnnt2a* morphants injected with 2 nl of 10 μ M rhBMP10 or *tnnt2a* morphant;*Tg(fli1a:alk1-myc)* embryos injected directly into the base of the CaDI with tracer alone or in combination with 2 nl of 10 μ M rhBMP10 at 28 hpf. In merge (right column), EGFP-expressing endothelial cell nuclei are green, pSmad1/5/9 immunofluorescence is magenta. Yellow arrows point to endothelial cells in the injected CaDI. 2D confocal projections of 50 μ m frontal sections, dorsal up. Scale bar, 10 μ m. (C)

Whole mount in situ hybridization for *cxcr4a*, *edn1*, and *cdh5* (pan-endothelial control) in 36 hpf *tnnt2a* morphant;*Tg(fli1a:alk1-myc)* embryos injected at 28 hpf into the base of the left CaDI with 2 nl tracer with or without 10 mM rhBMP10. Yellow arrow designates injected CaDI, red arrow uninjected CaDI. Asterisk denotes injection site. Frontal views, dorsal up; or lateral views, right (uninjected) side or left (injected) side. Scale bar, 50 μ m. **(D)** 36 hpf *Tg(fli1a:negfp)Tg(fli1a:alk1-myc)* embryos left uninjected or injected with *tnnt2a* MO at the one to four-cell stage, then injected directly into the base of the right CaDI with tracer alone or in combination with 2 nl of 10mM rhBMP10 at 28 hpf. Yellow arrow, injected CaDI; red arrow, uninjected CaDI; blue arrow, BCA. 2D confocal projections, frontal views, dorsal up. Scale bar, 50 μ m. **(E)** Quantitation of endothelial cell number in the right (injected) CaDI, BCA, and left (uninjected) CaDI in embryos described in D. N=10-12 in 2 independent experiments. Values are mean \pm SEM. Student's *t*-test: **P*<0.05; ***P*<0.001; ns, not significant.

2.3 DISCUSSION

Early embryonic blood vessel development is controlled largely by paracrine signaling interactions that orchestrate endothelial cell migration and proliferation and coalescence into vascular cords, as well as subsequent angiogenic sprouting that serves to elaborate the primitive vascular network. However, once blood vessels form a lumen, biomechanical forces and endocrine factors also come into play. In this work, I present evidence that blood flow is critical for limiting endothelial cell number within nascent arteries, and that Alk1 acts downstream of blood flow in mediating this effect. Furthermore, I demonstrate that blood flow is required not only for *alk1* expression but also for Alk1 activity, and that the latter requirement is met by provision of circulating ligand, Bmp10. Thus, flow-dependent induction of *alk1* and distribution of ligand synergize to enhance Alk1 activity.

It is well established that both BMP9 and BMP10 bind ALK1 with high affinity and can induce Smad1/5/9 phosphorylation and pSmad1/5/9-dependent transcriptional responses in

cultured endothelial cells [188, 194, 196]. However, my work is the first to unequivocally define Alk1 ligands in vivo. I have demonstrated in zebrafish that *bmp10* paralogs are required for Alk1 function during embryonic development, whereas *bmp9* is dispensable. In contrast, neither *Bmp9* nor *Bmp10* mouse nulls exhibit AVMs. *Bmp9* null mice live to adulthood without apparent vascular abnormalities [222], whereas ventricular hypoplasia and impaired trabeculation but not AVMs have been reported in *Bmp10* nulls [223]. There are two possible explanations for this discrepancy between zebrafish and mice. First, *Bmp9* and *Bmp10* may act redundantly in mouse embryonic vascular development, reflecting a difference in the spatial and/or temporal ligand requirement in mouse versus zebrafish vasculature. Indeed, treatment of *Bmp9* null mice with Bmp10 blocking antibodies results in early postnatal retinal vascular defects, hinting at functional redundancy, although AVMs were not noted in these vessels [222]. Furthermore, like rhBMP10, rhBMP9 was effective in restoring detection of pSmad1/5/9 by immunofluorescence in the CaDI/BCA in *tnnt2a* morphant;*Tg(fli1a:alk1-myc)* zebrafish embryos (data not shown), suggesting that Bmp9 and Bmp10 may function redundantly in vivo if available to Alk1 contemporaneously. In zebrafish, *bmp9* is first detected in liver around 48 hpf (C. Mansfield and B. Shrivage, data not shown) and the liver is first vascularized around 55 hpf [226], supporting the idea that Bmp9 is not redundant with Bmp10 between 24 and 48 hpf, the time period during which AVMs develop in *alk1* mutants [181, 182]. A second possible reason for the discordance between mice and zebrafish in terms of definition of Alk1 ligand stems from the fact that slowed heartbeat and impaired circulation precede death of *Bmp10* mouse nulls at embryonic day (E)9.5-E10.5 [223]. Thus, it is reasonable to hypothesize that the absence of AVMs in *Bmp10* nulls is due to the earlier death of *Bmp10* nulls versus *Alk1* nulls (E10.5-11.5) and/or insufficient circulation to precipitate AVM formation, which we have demonstrated to be a flow-dependent

process [181]. Because trabeculation in zebrafish does not occur until 60-72 hpf in zebrafish [227, 228], it is not surprising that I noted no defects in heart development or function through 48 hpf in *bmp10* or *bmp10-like* morphants (data not shown).

In cranial arterial endothelial cells, both blood flow and Bmp10/Alk1 function are required for phosphorylation of Smad1/5/9, repression of *cxcr4a*, and induction of *edn1*, and concomitant restoration of endothelial *alk1* expression and injection of Bmp10 normalizes these molecular endpoints and restores arterial endothelial cell number in the absence of flow. These data strongly suggest that Alk1 acts downstream of blood flow to limit endothelial cell migration, proliferation, and possibly vascular tone and thus limit arterial endothelial cell number and vessel caliber. However, changes in expression of *cxcr4a* and *edn1* cannot account for defects in vessel architecture resulting from loss of *alk1*. Although Alk1 signaling can repress *Cxcr4* or induce *Edn1* in cultured endothelial cells [229-231], supporting our in vivo data, previous work has demonstrated that increased *cxcr4a* is not necessary nor is loss of *edn1* sufficient for AVM development [181], and additional work has demonstrated that concomitant increase in *cxcr4a* and loss of *edn1* is insufficient to generate AVMs (E. Rochon and B. Roman, unpublished). Thus, further work is required to define the molecular mechanisms and cellular behaviors that lead to arterial enlargement in the absence of *alk1*.

The multifaceted regulation of Alk1 signaling by blood flow is remarkable, with flow required for both *alk1* expression and Alk1 activity. Given that mammalian *Cxcr4* and *Edn1* respond to shear stress and/or cyclic strain in cultured endothelial cells [212, 213], it seems likely that Alk1 is important in transducing mechanical force into a biochemical signal in vivo. However, the mechanism by which blood flow upregulates *alk1* expression is currently unknown, and it remains formally possible that the flow-dependence of *alk1* expression stems at

least in part from a circulating factor. Circulation of ligand clearly contributes to the dependence of Alk1 activation on blood flow: blood flow distributes cardiac-derived circulating Bmp10 to arterial endothelial cell Alk1, thereby explaining the blood flow-dependence of Smad1/5/9 phosphorylation in these cells. However, a recent study reported that mechanical force induces Smad1/5/9 phosphorylation in intact mouse endothelium and cultured endothelial cells in a ligand-independent manner [232], contradicting my conclusions. This discrepancy may be explained by the fact that ligand-independence in that study was examined via treatment with Noggin, which sequesters most BMP ligands, but not BMP9 or BMP10 [233]. Alternatively, oscillatory shear stress applied in that study may have different effects on BMP signaling than pulsatile laminar shear stress, which acts within zebrafish cranial arteries [234], or the type I receptor responsible for oscillatory shear-induced pSmad1/5/9 may not be Alk1. Further work is required to better define the roles of and probe interactions between endocrine factors and mechanical force in the regulation of Alk1 signaling.

In summary, my data demonstrate that blood flow induces *alk1* expression and provides Bmp10 to arterial endothelial cell Alk1, thereby activating Smad1/5/9 phosphorylation, decreasing *cxc4a* expression, and inducing *edn1* expression. These changes in gene expression, along with changes in expression of yet to be identified genes, serve to dampen angiogenic behavior and stabilize arterial endothelial cell number and caliber at the onset of blood flow. Taken together with our previous work [181], my data suggest that loss of Alk1 function abrogates this important flow response and results in increased nascent arterial caliber, which in turn leads to increased hemodynamic forces within downstream arteries. In an attempt to normalize these hemodynamic forces, downstream vessels mount an Alk1-independent flow response that causes normally transient conduits between this overloaded arterial system and

neighboring veins to be retained and enlarged, thereby forming high flow AVMs. Thus, my model suggests that in HHT patients, abrogation of one flow response—due to impaired ALK1 signaling—leads to activation of an independent flow response that acts to normalize hemodynamic forces, ultimately leading to AVMs.

3.0 PHOSPHORYLATED SMADS1/5/9 ARE PRESENT AND ACTIVE DOWNSTREAM OF ALK1 IN THE ZEBRAFISH ENDOTHELIUM.

Loss of *ALK1* results in aberrant endothelial cell behavior and subsequently the formation of fragile improper connections between arteries and veins, AVMs. To date, the intracellular mediators for ALK1, critical in promotion of vascular quiescence and AVM prevention, remain unknown. Here, I demonstrate that pSmads1/5/9 are present and active in *alk1*-positive arteries and that Alk1 activity is necessary and sufficient for their expression. Furthermore, use of a phospho-Smad1/5 reporter, *Tg(BRE:EGFP)*, provides preliminary evidence that pSmads1/5/9 may play a non-canonical role downstream of Alk1. Finally, I show that inhibition of Alk1 kinase activity produces AVMs reminiscent of *alk1* mutants. Taken together, these data reveal pSmads1/5/9 to be a readout of Alk1 signaling in vivo during embryonic development, and demonstrate that activation may be critical in AVM prevention.

3.1 INTRODUCTION

In TGF- β signaling, ligand binds to heterotetrameric complexes of type I and type II serine/threonine kinase receptors which phosphorylate Smad1, Smad5, and Smad9 (hereafter referred to as pSmads1/5/9), allowing them to complex with Smad4, enter the nucleus, and regulate expression of downstream genes [235]. The importance of TGF- β signaling in vascular

development is highlighted by the HHT family of diseases in which haploinsufficiency of coreceptor *endoglin* (*ENG*) causes HHT1 [167], haploinsufficiency of Type I receptor, *ALK1* leads to HHT2 [169], and mutations in *SMAD4* cause Juvenile Polyposis with HHT phenotypes [172].

Although cases of HHT clearly indicate Alk1/Endoglin are necessary in endothelial cell behavior and AVM prevention, the in vivo intracellular mediators of this signal remain poorly understood. pSmads1/5/9 are the best characterized substrates for Alk1 [183]. However, Alk1 can also signal via phosphorylation of non-Smad substrates, including mitogen activated protein kinases (MAPKs) ERK1/2 and p38 [199, 229]. In fact, several lines of evidence suggest that pSmad1/5/9 is not required downstream of Alk1 in vivo. For example, Alk1-mediated inhibition of migration in human dermal microvascular endothelial cells is reportedly Smad-independent [146]. Furthermore, inducible knockout of *Endoglin* causes retinal AVMs; however, pSmad1/5/9 expression is unchanged in affected vessels [236]. In support of a role for MAPKs in Alk1 signaling in vivo, deletion of the *TGF- β activated kinase 1* (*Tak1*) produces mispatterned and dilated vessels in the yolk sac and embryo proper including, but not limited to, the dorsal aorta which is reminiscent of *Alk1* mutant embryos, and *tak1* and *alk1* knockdown in zebrafish synergize to reportedly exacerbate *alk1* knockdown phenotypes [197]. In some contexts, Alk1 may stimulate multiple pathways. In human pulmonary endothelial cells, BMP9/ALK1 upregulates *Edn1* through both Smad1 and p38 MAPK [229], and in zebrafish, *smad5* and *alk1* knockdown reportedly synergize to produce vascular malformations, similar to *tak1/alk1* knockdown [197]. Clearly, the intracellular mediators of Alk1 may be context-specific and warrant further investigation in vivo.

In vivo models demonstrate critical roles for Smad-mediated signaling in vascular biology. *Smad1*^{-/-} and *Smad5*^{-/-} mouse embryos both die between E9.5-11.5. *Smad5*^{-/-} mice display defective vasculogenesis in the yolk sac, and the dorsal aorta and vitelline vessels of the embryo proper are dilated and fragile [237]. Surprisingly, however, endothelial-specific deletion of Smad5 does not produce vascular phenotypes [238] although these data could be explained by the functional redundancy of Smad1 and Smad9. *Smad1*^{-/-} mice possess less severe vascular phenotypes compared to their *Smad5*^{-/-} counterparts, with vasculogenesis proceeding normally, but do possess disorganized vessels in the allantois prior to death at E10.5 [239]. *Smad1* and *Smad5* double heterozygotes proceed through vasculogenesis, but die by E9.5 with severe angiogenic defects characterized by hypersprouting [217]. *Smad9*^{-/-} mice serve as a model for Pulmonary Arterial Hypertension (PAH), with increased proliferation in pulmonary vSMCs leading to medial thickening in distal pulmonary vessels [204]. Finally, endothelial deletion of *Smad4* is embryonic lethal by E10.5 with embryos presenting with reduced capillary vessels, narrowed lumens and poor pericyte coverage in the yolk sac and embryo proper [240].

Despite these numerous studies implicating an importance for Smad-mediated signaling in vascular development, their mode of action, upstream activators, and involvement in Alk1 signaling remain poorly defined. Recently, reports have shown that pSmad1/5/9 activation can promote stalk cell phenotype through interaction with Notch intracellular domain (NICD) [217] and that Alk1-mediated pSmads1/5/9 synergizes with Notch signaling components to prevent hypervascularization, in part through VEGFR2 inhibition [199]. However, it should be noted that none of these *Smad* mutants present with AVMs that are characteristic of *Alk1* mutant embryos [181].

In the following studies, I provide evidence from zebrafish that pSmads1/5/9 are present in *alk1*-positive arteries during development and that *alk1* expression and activity are necessary for Smad1/5/9 phosphorylation. I further demonstrate that loss of pSmads1/5/9 correlates with AVM development and thus may be required downstream of Alk1. However, I see no pSmad1/5-mediated transgene expression in *alk1*-positive arterial endothelial cells, suggesting that if pSmads are functioning downstream of Alk1, their mode of action may be via a non-canonical pathway.

3.2 RESULTS

3.2.1 Detection of pSmad1/5/9 by immunofluorescence is dependent on *alk1*

To first address whether pSmad1/5/9 was present in *alk1*-positive arteries, I collected frontal sections of 36 hpf wild type embryos and stained for pSmad1/5/9. pSmad1/5/9 is detectable by immunofluorescence in the *alk1*-positive caudal division of the internal carotid artery (CaDI) and basal communicating artery (BCA) (n=26/26). In contrast, detection of pSmad1/5/9 is not present in *alk1* mutant embryos (n=0/17) but restored in these arteries when *alk1* is driven under the control of an endothelial specific promoter, *Tg(fli1a:alk1-myc)* (Figure 16, n=11/11)

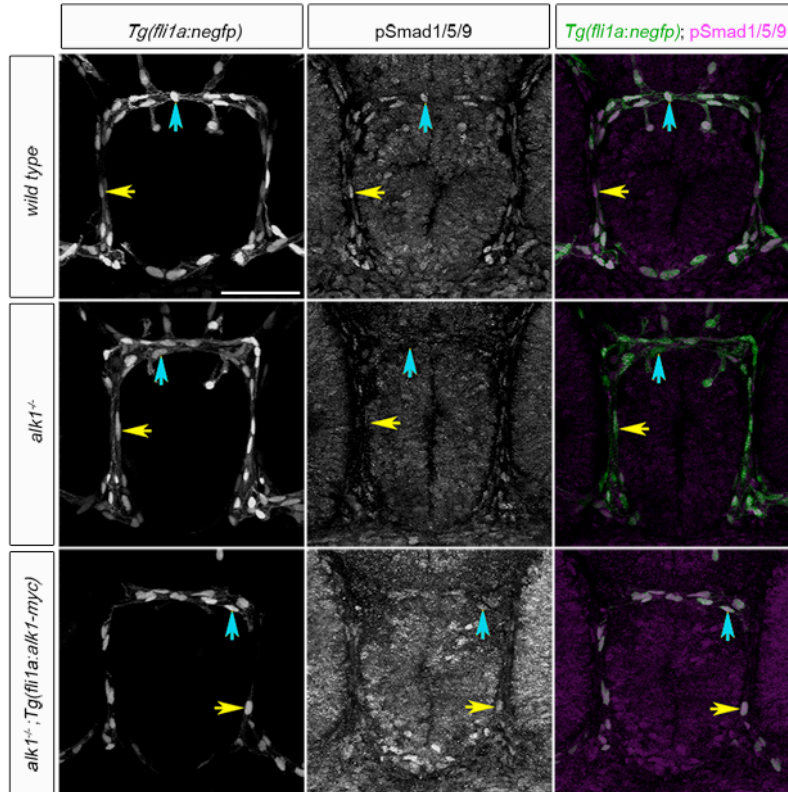


Figure 16: pSmad1/5/9 expression in *alk1*-Positive Endothelial Cells Depends on *alk1*.

pSmad1/5/9 expression (middle column) in endothelial cells (nuclei marked by *fli1a:negfp* transgene, left column) at 36 hpf, in wild type (top row), *alk1* mutants (middle row), and *alk1^{-/-}; Tg(fli1a:alk1-myc)* (bottom row) embryos. In merge (right column), EGFP-expressing endothelial cell nuclei are green, pSmad1/5/9 immunofluorescence is magenta. Blue and yellow arrows point to endothelial cells in the BCA and CaDI respectively. 2D confocal projections of 50 μ m frontal sections, dorsal up. Scale bar, 50 μ m.

Because Alk1 may also signal through the MAP kinase, ERK1/2 [199], I also examined diphospho-ERK1/2 (dpERK1/2) expression in wild type and *alk1* mutant embryos. Although dpERK1/2 is expressed in CaDI and BCA endothelial cells, expression is independent of *alk1* (Figure 17), suggesting that disruption of dpERK1/2 does not lead to enlarged arteries and AVMs in *alk1* mutants.

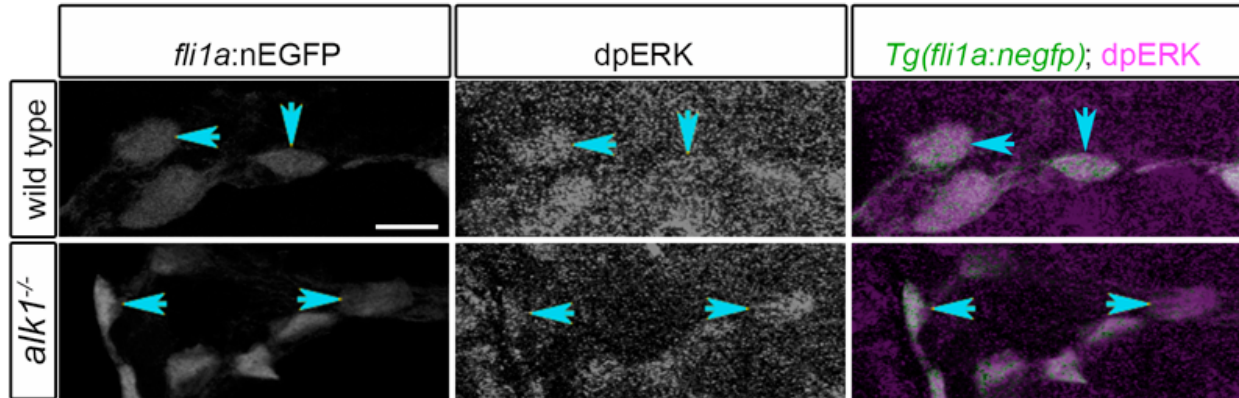


Figure 17: dpERK expression is not dependent on *alk1* expression.

dpERK expression (middle column) in endothelial cells (nuclei marked by *fli1a:negfp* transgene, left column) at 36 hpf, in wild type (top row) and *alk1* mutants (bottom row). In merge (right column), EGFP-expressing endothelial cell nuclei are green, dpERK immunofluorescence is magenta. Blue arrows point to endothelial cells in the BCA. 2D confocal projections of 50 μ m frontal sections, dorsal up. Scale bar, 50 μ m.

3.2.2 Detection of pSmad1/5/9 by immunofluorescence is dependent on Alk1 activity

Since detection of pSmad1/5/9 by immunofluorescence is dependent on *alk1* expression, I reasoned that it would similarly be dependent upon Alk1 kinase activity. To address this hypothesis, I treated zebrafish embryos with pharmacological inhibitors of BMP type I receptors, LDN-193189 and dorsomorphin [241-244], and assayed arterial pSmad1/5/9 by immunofluorescence. Because these inhibitors had not been characterized with respect to zebrafish Alk1 inhibition, our collaborator (Dr. Charles Hong, Vanderbilt University) first performed in vitro kinase assays to determine their efficacy against Alk1 compared to other known targets. LDN-193189 potently inhibited zebrafish Alk1 (IC_{50} ~13 nM) and Alk2 (IC_{50} ~41 nM) but was considerably less effective against vascular endothelial growth factor receptor-2 (VEGFR2, IC_{50} ~215 nM). In contrast, dorsomorphin was highly effective against VEGFR2 (IC_{50} ~22 nM), moderately effective against Alk2 (IC_{50} ~148 nM), and minimally effective

against Alk1 ($IC_{50} \sim 484$ nM). For my in vivo assays, drug exposure began at 23 hpf, prior to the onset of *alk1* expression. LDN-193189 exposure resulted in undetectable levels of pSmad1/5/9 (n = 16, Figure 18) but no change in dpERK1/2 (n = 6, Figure 19), similar to changes observed in *alk1* mutants (Figures 16). In contrast, treatment with 30 μ M dorsomorphin had no effect on pSmad1/5/9 (Figures 18) despite causing agenesis of the midline cranial arterial system (data not shown) and loss of dpERK1/2 (Figure 19), which are predicted outcomes of VEGFR2 inhibition. These results support the idea that the molecular endpoint documented in LDN-193189-treated embryos does in fact reflect inhibition of Alk1 kinase activity. These data demonstrate that activation of Smad1/5/9 is dependent on Alk1 kinase activity.

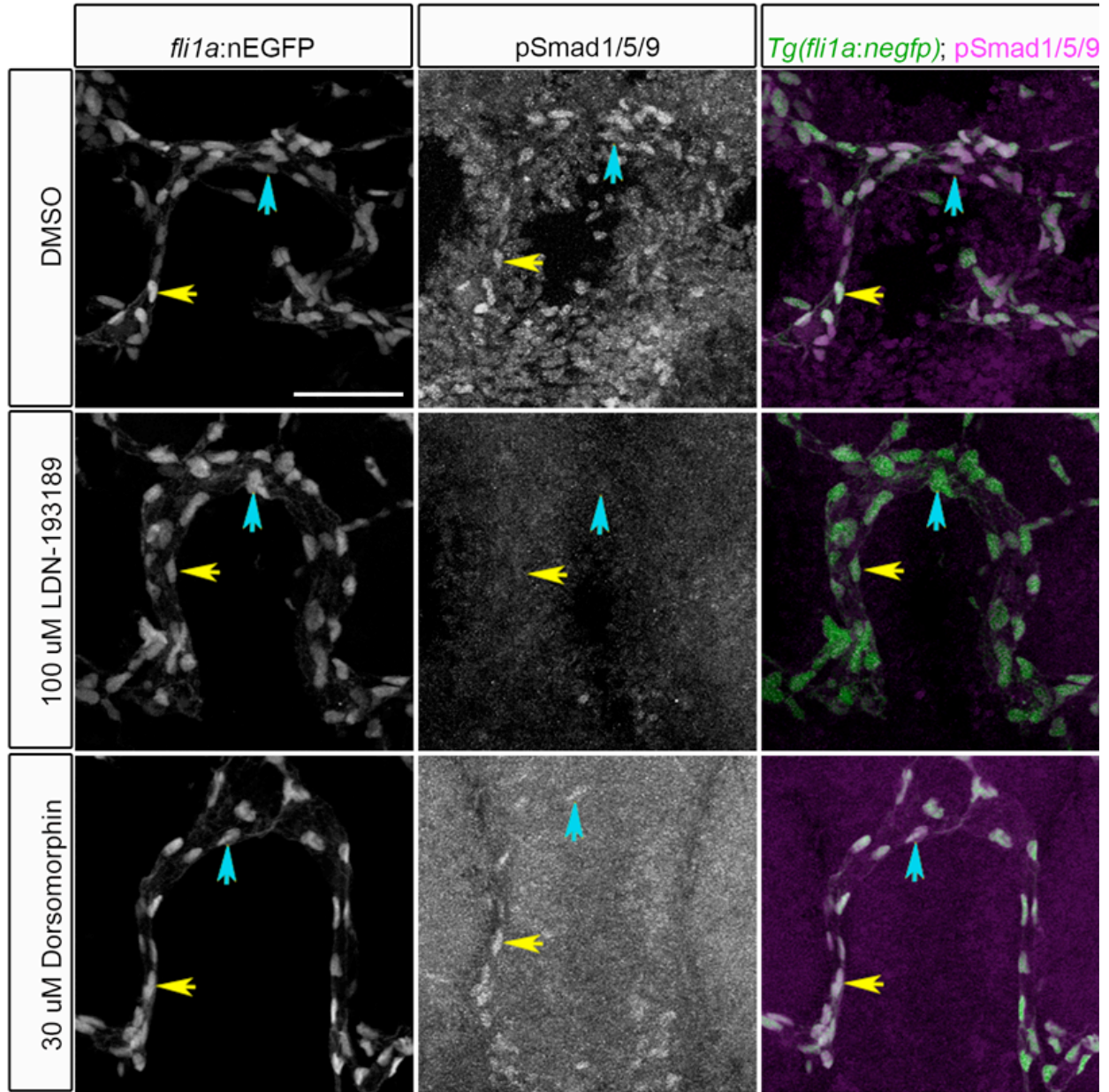


Figure 18: pSmad1/5/9 expression is dependent on Alk1 activity.

pSmad1/5/9 expression (middle column) in endothelial cells (nuclei marked by *fli1a:negfp* transgene, left column) at 36 hpf, in DMSO, 100 μ M LDN-103189, 30 μ M Dorsomorphin, treated embryos. In merge (right column), EGFP-expressing endothelial cell nuclei are green, pSmad1/5/9 immunofluorescence is magenta. Blue and yellow arrows point to endothelial cells in the BCA and CaDI, respectively. 2D confocal projections of 50 μ m frontal sections, dorsal up. Scale bar, 50 μ m.

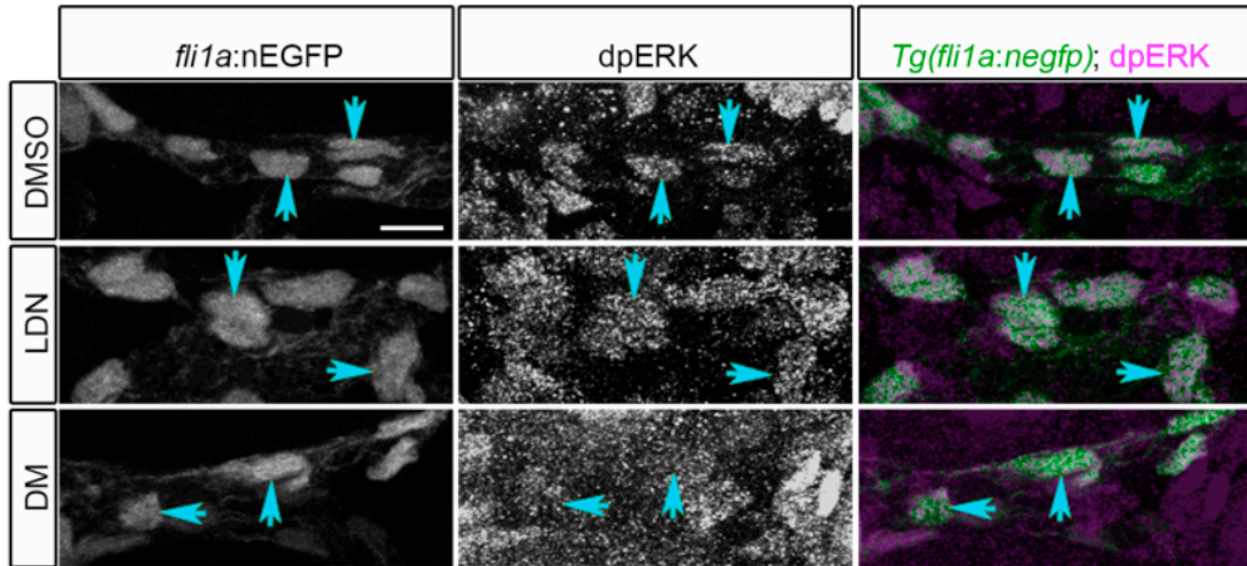


Figure 19: dpERK expression is not dependent on Alk1 activity.

dpERK expression (middle column) in endothelial cells (nuclei marked by *fli1a:negfp* transgene, left column) at 36 hpf, in DMSO, 100 μ M LDN-103189 (LDN), and 30 μ M Dorsomorphin (DM) treated embryos. In merge (right column), EGFP-expressing endothelial cell nuclei are green, dpERK immunofluorescence is magenta. Blue arrows point to endothelial cells in the BCA. 2D confocal projections of 50 μ m frontal sections, dorsal up. Scale bar, 50 μ m.

3.2.3 Individual *smad* transcripts are undetectable in *alk1*-positive arteries

Immunofluorescence with α -pSmad1/5/9 does not allow deciphering which rSmad or combination of rSmads is required downstream of Alk1 in the endothelium. To examine whether *smad1*, *smad5*, and/or *smad9* were present in *alk1*-positive arteries, I conducted whole mount *in situ* hybridization (WISH) for each of these transcripts at 36 hpf, a time point at which we know Alk1 to be active in the endothelium. *smad1* and *smad9* show discrete expression in many domains known to require BMP signaling including the heart, retina, pharyngeal endoderm, and trigeminal ganglia. Expression within the *alk1*-positive CaDI, however, is undetectable (Figure

20). In contrast to *smad1* and *smad9*, *smad5* is expressed ubiquitously within the head, precluding analysis of the cranial vasculature (Figure 20).

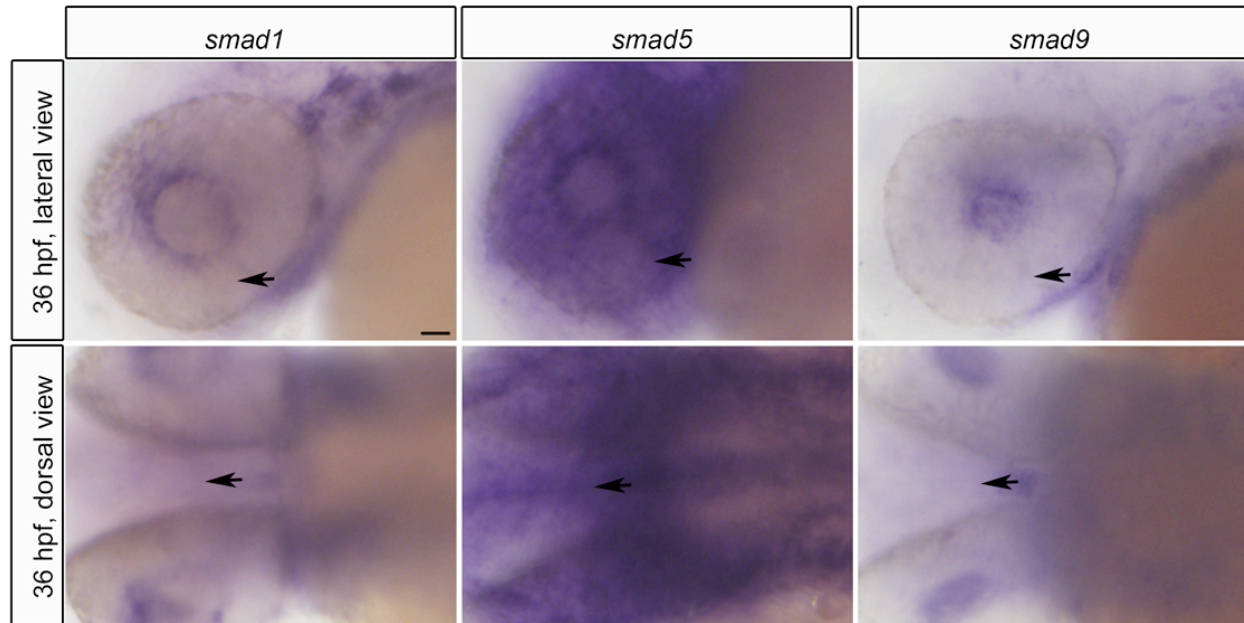


Figure 20: *smad1*, *smad5*, and *smad9* are undetectable in *alk1*-positive arteries.

Whole mount in situ hybridization for *smad1*, *smad5*, and *smad9* at 36 hpf. Top row: Lateral views, dorsal up. Bottom row: dorsal views,, anterior left. Arrows point to approximate location of CaDI and BCA in lateral and dorsal views, respectively. Scale bar, 50 μ m.

To improve detection limits and overcome interference by ubiquitous staining, I conducted double fluorescent *in situ* hybridization (FISH) coupling digoxigenin-labeled *smad* riboprobes with a FITC-labeled *kdrl* (pan-endothelial marker) riboprobe. Despite detecting both *smad1* and *smad5* transcripts in domains present in WISH (retina, pharyngeal endoderm), *smad1* and *smad5* transcripts did not colocalize with *kdrl* in *alk1*-positive vessels (Figure 21). However, as a positive control, colocalization was obtained with *kdrl* and the promigratory chemokine

receptor, *cxcr4a* (Figure 21). There are two possible explanations for these results: *smad* transcripts may truly not be present in *alk1*-positive arteries, or the protocols being used may not be adequate to detect low levels of transcripts. Note that double FISH has not yet been performed with *smad9/kdrl*.

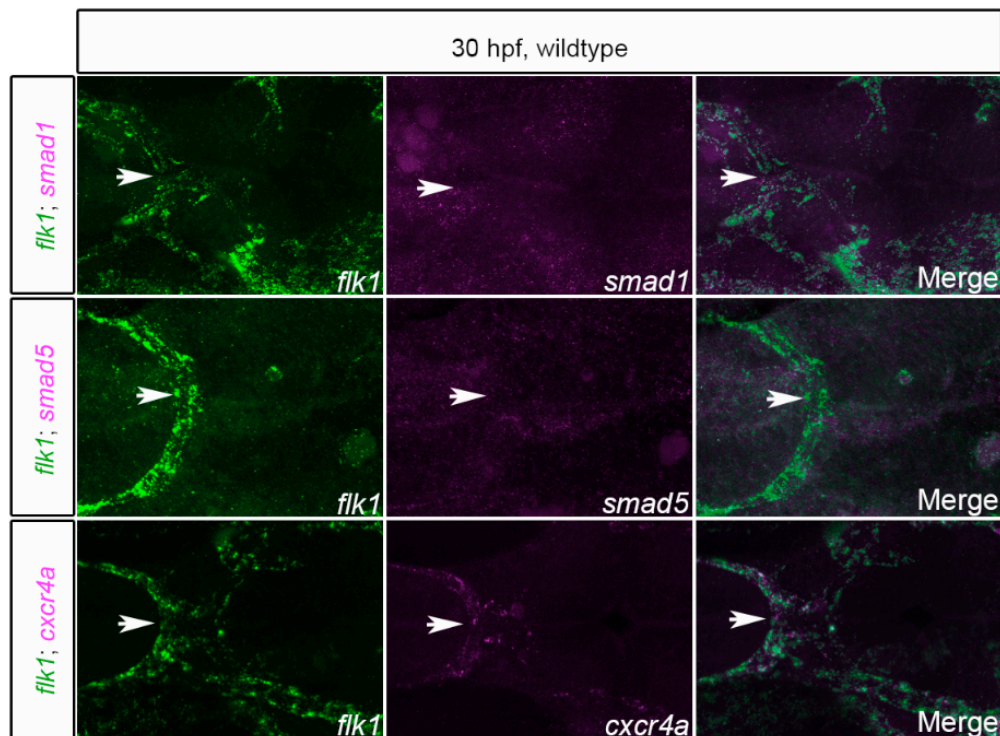


Figure 21: *smad1* and *smad5* are undetectable by FISH in *alk1*-positive arteries.

Whole mount double fluorescent in situ hybridization for *smad1*, *smad5*, and *cxcr4a* with *kdrl* (pan-endothelial marker) at 30 hpf. Dorsal views, anterior left. Arrows point to *alk1*-positive BCA. In all images, *kdrl* expression is green, *smad1*, *smad5*, or *cxcr4a* is magenta.

3.2.4 pSmad1/5/9 mediated *Tg(bre:egfp)* expression is undetectable in *alk1*-positive arteries

Given that Alk1 knockdown inhibits pSmad1/5 activated BRE-luciferase [194], I reasoned that pSmads1/5/9 played transcriptional roles downstream of Alk1 in promoting vascular quiescence. In addition, because pSmads1/5/9 immunostaining only provides a snapshot of Alk1 activity

during development, I desired a dynamic, live readout of Alk1 activity. To this end, I generated an in vivo phospho-Smad1/5/9 reporter, *Tg(bre:egfp)* [characterization and validation discussed in Chapter 4]. If pSmads1/5/9 were acting transcriptionally downstream of Alk1, I expected to detect *Tg(bre:egfp)* expression within *alk1*-positive arteries. Surprisingly, *Tg(bre:egfp)* expression is undetectable within the *alk1*-positive BCA of wild type embryos (Figure 22). Similarly, *alk1* mutants have no detectable *Tg(BRE:EGFP)* expression in their BCA (Figure 22). These results were consistent between two independent transgenic lines generated by different P₀ founders. Furthermore, examination of a BRE-driven transgenic, independently created [245], reveals no detectable pSmads1/5/9-driven EGFP in *alk1*-positive arteries (data not shown).

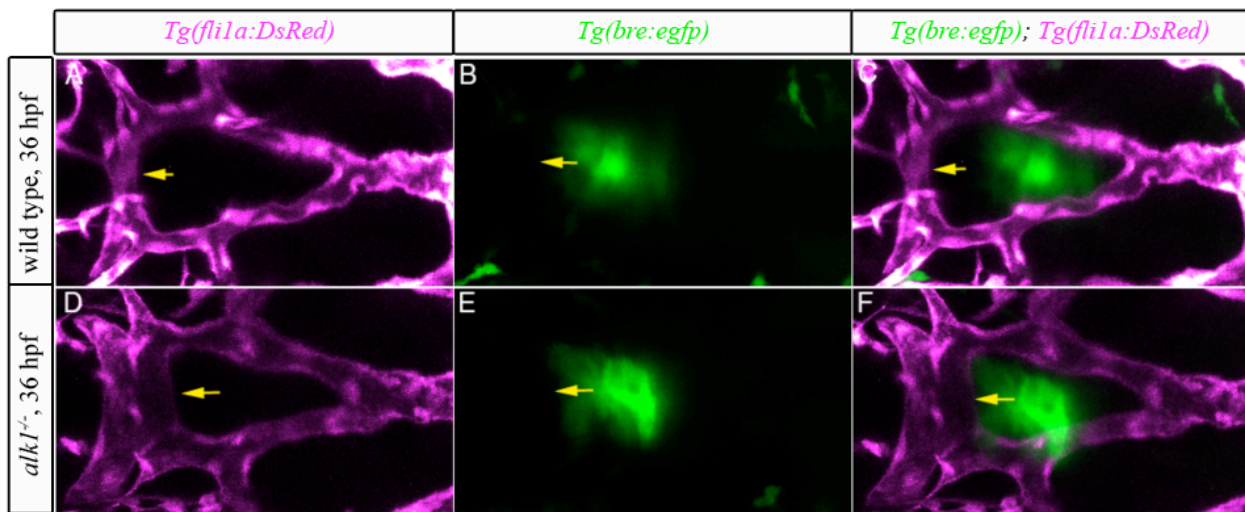


Figure 22: *Tg(bre:egfp)* expression is absent in *alk1*-positive arteries.

Cranial vasculature of wild type and *alk1* mutants at 36 hpf. In all images green is bre-driven EGFP expression, magenta is endothelial (*fli1a*) driven DsRed. Yellow arrows point to *alk1*-positive basal communicating artery. Dorsal views, anterior left. 2D confocal projections.

The lack of BRE-driven EGFP in *alk1* positive arteries could reflect technical issues. For example, at 36 hpf, EGFP may not have had sufficient time to fold and fluoresce at detectable levels. However, although Alk1 function is required as early as 32 hpf [181], *egfp* mRNA is undetectable at 36 hpf by WISH (Figure 23A); EGFP protein is undetectable by whole mount immunofluorescence at 36 hpf (Figure 23B); and *alk1*-positive arteries at later timepoints (40-48 hpf) still lack detectable EGFP expression (Figure 23C). Together, these data indicate that lack of expression is not a result of EGFP-folding delay. It remained possible, however, that BRE activation was so low as to be undetectable endogenously. Therefore, I intravascularly injected the Alk1 ligands, recombinant human (rh)BMP10 and rhBMP9, into *Tg(bre:egfp)* embryos to hyperactivate Alk1 signaling (Figure 24). However, injections failed to induce *Tg(bre:egfp)* in the CaDI or BCA despite inducing ectopic expression in the central arteries and primordial hindbrain channel (Figure 24). Since these latter vessels are *alk1*-negative, rhBMP9 and rhBMP10 must be acting through alternative type I receptors. Interestingly, endothelial-specific expression of a constitutively active form of Alk1, which requires neither ligand nor Type II receptor for activity, produces robust *Tg(bre:egfp)* expression in all vessels at 36 hpf, including the CaDI and BCA (Figure 24), proving that the machinery necessary for BRE activation is in fact in place in *alk1*-positive arteries. Together, these data suggest that BRE-driven transcription may not be an in vivo response to Bmp10/Alk1 signaling. Therefore, if phosphorylated Smad1/5/9 is in fact required downstream of Alk1 signaling, these Smads may bind non-traditional enhancer elements or activate an alternative Smad-dependent pathway such as miRNA processing in arterial endothelial cells.

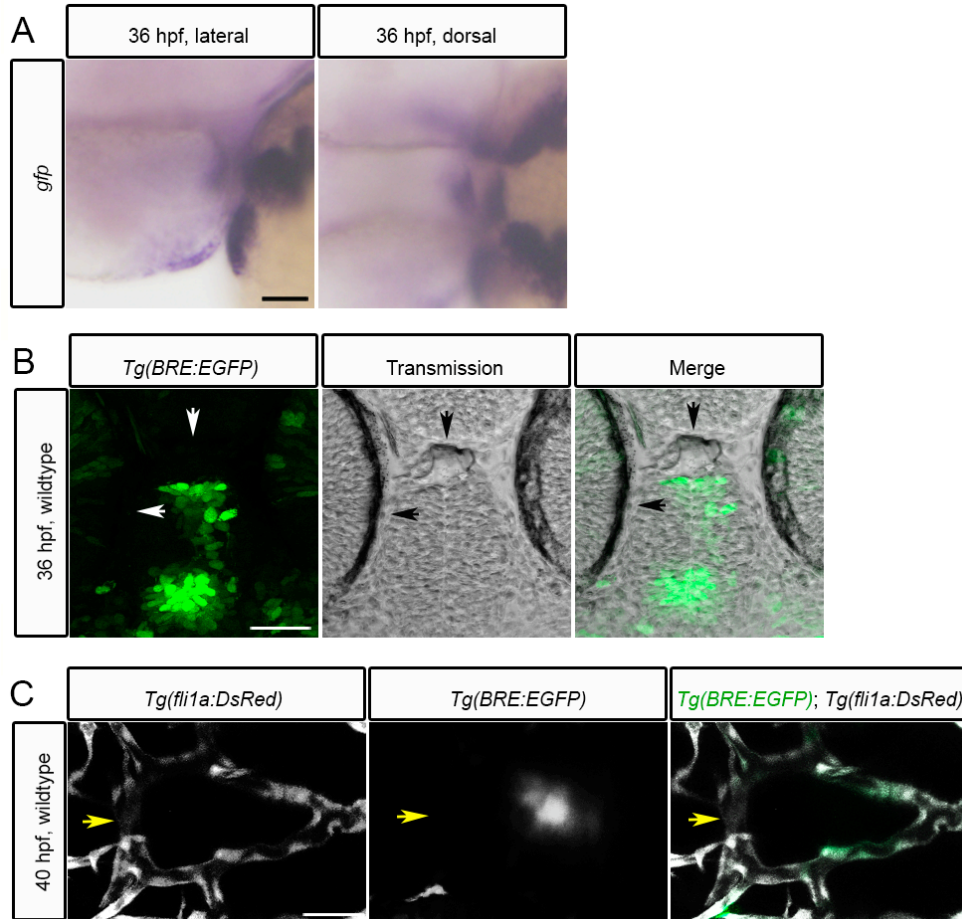


Figure 23: *Tg(bre:egfp)* expression is not detectable in *alk1*-positive arteries at later time points or by in situ hybridization or immunofluorescence.

(A) Whole mount in situ hybridization for *gfp* at 36 hpf. Scale bar, 50 μ m. (B) EGFP expression in 36 hpf wild type embryos. In all images, EGFP immunofluorescence is green. White and black arrows point to locations of CaDI and BCA. 2D confocal projections. Scale bar, 50 μ m. (C) Cranial vasculature of wild type embryos at 40 hpf. In all images green is bre-driven EGFP expression, gray is endothelial (*fli1a*) driven DsRed. Yellow arrows point to *alk1*-positive basal communicating artery. Dorsal views, anterior left. 2D confocal projections

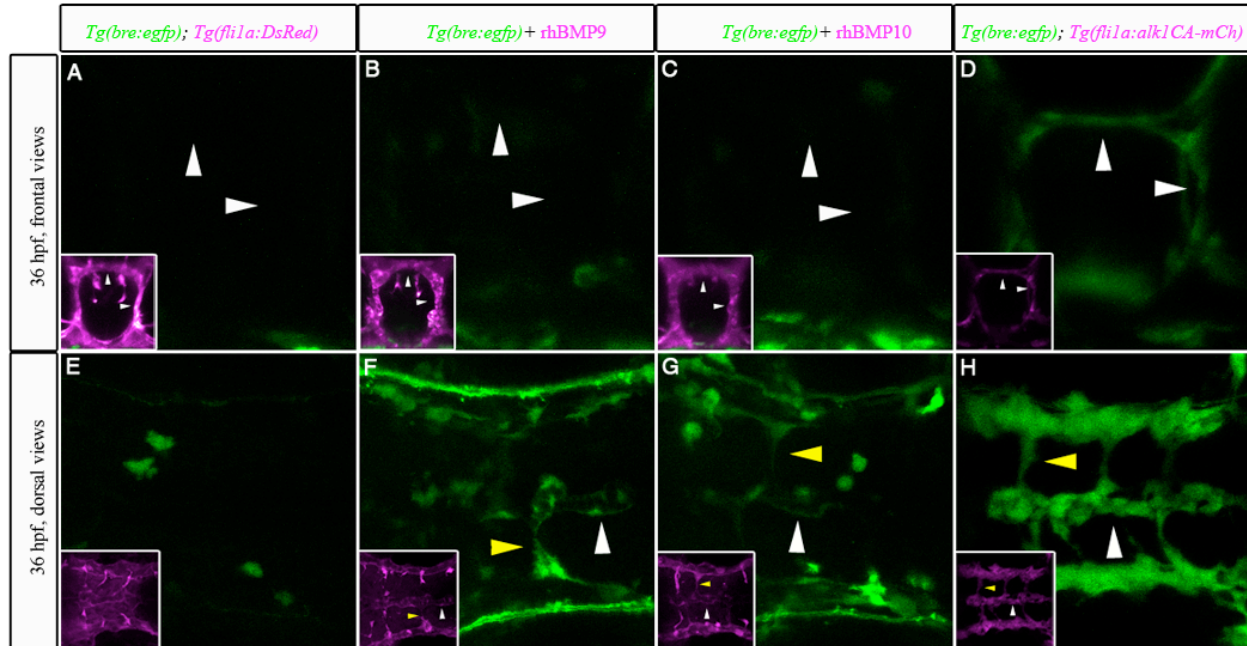


Figure 24: rhBMP9 and rhBMP10 do not induce *Tg(bre:egfp)* expression.

Cranial vasculature of 36 hpf wild type embryos either left uninjected, injected with 2 nL of 10 μ M rhBMP9, injected with 2 nL of 10 μ M rhBMP10, or crossed to *Tg(fli1a:alk1^{CA}-mCh)*. In all images green is *bre*-driven EGFP expression. Magenta is endothelial (*fli1a*) driven DsRed (A,E), intravascularly-injected Qdots 655 (B-C,F-G), or *Tg(fli1a:alk1^{CA}-mCh)* expression (D,H). Top panels: frontal views, dorsal up. White arrows point to locations of CaDI and BCA. Bottom panels: dorsal view, anterior left. White and yellow arrows point to basilar artery and central arteries respectively. In all images, insets show locations of vessels. 2D confocal projections.

3.2.5 Inhibition of pSmad1/5/9 partially rescues *alk1* mutants

Regardless of intracellular mechanism of action, I have demonstrated that pSmad1/5/9 expression is dependent on *alk1* expression and Alk1 kinase activity. I reasoned that if pSmad1/5/9 are the necessary transducers of the Alk1 signal in AVM prevention, knockdown of these critical signal transducers would phenocopy *alk1* mutants in AVM formation and endothelial cell number. To test this hypothesis, I performed MO knockdown experiments. Although injection of *Smad1^{TB}* MO or *Smad5^{TB}* MO produced yolk sac extension defects [246]

or dorsalized phenotypes [247] respectively and as expected, *smad1^{TB}*, *smad5^{TB}*, and *smad9^{TB}* all fail to produce AVMs (Figure 25A). *smad1* and *smad5* knockdowns also fail to phenocopy *alk1* mutant embryos in terms of increases in endothelial cells comprising the basal communicating artery and posterior communicating segments (Figure 25C). One might expect functional redundancy between the Smad protein family members; however, coinjection of *smad1^{TB}* /*smad5^{TB}* did not phenocopy *alk1* mutants in AVM formation (Figure 25B) or endothelial cell counts (Figure 25C). In fact, contrary to expectations, knockdown of *smad1*, *smad5*, or *smad1/smاد5* reduced cell counts in wild type embryos and partially restored *alk1* mutant embryos to wild type cell numbers (Figure 25C). These surprising results could be attributed to developmental defects including dorsalization, which is observed with *smad1* and *smad5* knockdown. Injection of 4 ng *smad1* or *smad5* morpholino produced head necrosis or dorsalization respectively, in all injected embryos. Because these developmental defects inhibited analysis of cranial vascular architecture, lower doses of morpholinos were used (2 ng) for the above experiments. With smaller doses, I cannot ensure that *smad1* and *smad5* transcripts were knocked down fully, and therefore, absence of phenotype may be attributed to residual Smad1 or Smad5 activity. Remaining to be seen is whether knockdown of all three *smad* transcripts is required to produce *alk1* mutant phenotypes, as they may all act redundantly within the endothelium downstream of Alk1 signaling.

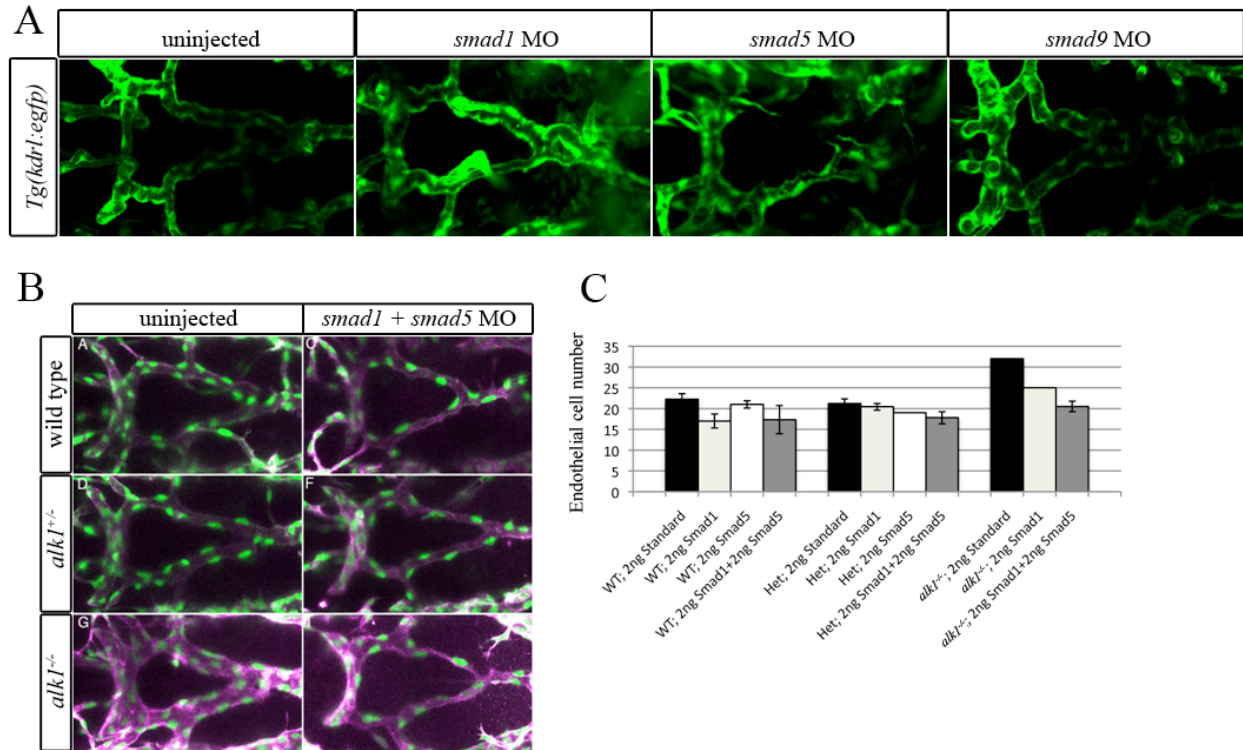


Figure 25: *smad1/smاد5/smاد9* knockdown does not phenocopy *alk1* mutants.

Cranial vasculature of uninjected, *smad1* (2 ng), *smad5* (2 ng), or *smad9* (4 ng) morphants at 48 hpf. Green is endothelial EGFP. Dorsal views, anterior left. **(B)** Cranial vasculature of 48 hpf uninjected or *smad1+smad5* morphants. In all images green is endothelial nEGFP, magenta is endothelial mRFP. Dorsal views, anterior left. **(C)** Endothelial cell counts of the BCA and PCS at 48 hpf in wild type, *alk1*^{+/-}, or *alk1* mutant embryos injected with *smad1*, *smad5*, or *smad1+smad5* morpholino. N= 1- 9 over 1 experiment. Error bars represent S.E.M. All values are not significant relative to standard controls using unpaired student's t-test.

Early gastrulation defects caused by *smad* morpholinos may mask effects on the vasculature. Therefore, we treated *Tg(kdr1:gfp);Tg(gata1:DsRed)* embryos with inhibitors of BMP receptor kinase activity, including LDN-193189 and dorsomorphin: both of these drugs inhibit numerous BMP receptors and dorsomorphin also inhibits VEGF receptor, but only LDN-193189 effectively inhibits Alk1 ([243], Charles Hong, personal communication). Embryos were exposed at 23 hpf and the cranial vasculature was evaluated at 48 hpf. Enlarged cranial

vessels and AVMs were documented in embryos exposed to LDN-193189 (22/34, 65%; Figure 26) but not dorsomorphin (n = 30) or DMSO (n = 34). However, dorsomorphin treatment resulted in agenesis of the midline vasculature, a predicted outcome of VEGFR2 inhibition, so its effect on this system could not be evaluated. Although we cannot rule out the possibility that LDN-193189 may diminish Alk1 kinase activity directed against targets other than Smad1/5/9 [241], the lack of effect of LDN-193189 on dpERK1/2 expression (Figure 19) suggests that pSmad1/5/9 is likely required downstream of Alk1 to prevent arterial enlargement and development of AVMs.

As a complementary approach to examining the role of pSmad1/5/9 downstream of Alk1, if pSmads1/5/9 were the main intracellular mediators of the Alk1 signal necessary for AVM prevention, I hypothesized that *smad* overexpression may bypass a requirement for Alk1 and rescue endothelial cell number in *alk1* mutants. To examine this possibility, *smad5* mRNA (100pg) was injected and endothelial cell number in wild types and *alk1* mutants was assessed; however, *smad5* injection had no effect on the number of endothelial cells comprising the BCA and PCS at 34 hpf (Figure 27). Failure to rescue may be attributed to inadequate dosage of *smad5* mRNA. 100pg of *smad5* did not produce ventralized phenotypes. Therefore, additional experiments, in which a dose response is performed, would need to be conducted to better study whether misexpression of *smad5* transcript can rescue *alk1* mutants.

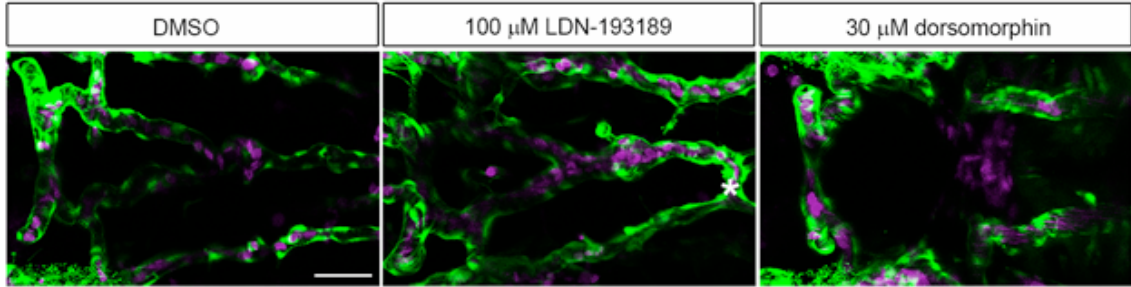


Figure 26: Inhibition of Alk1 kinase activity phenocopies *alk1* mutants.

Cranial vasculature in 48 hpf *Tg(kdrl:gfp);Tg(gatal:dsRed)* embryos treated with 0.05% DMSO, 100 μ M LDN-193189, or 30 μ M dorsomorphin. Asterisk denotes AVM. Endothelial cells are green, red blood cells magenta. 2D confocal projections, dorsal views, anterior left, Scale bar, 50 μ m.

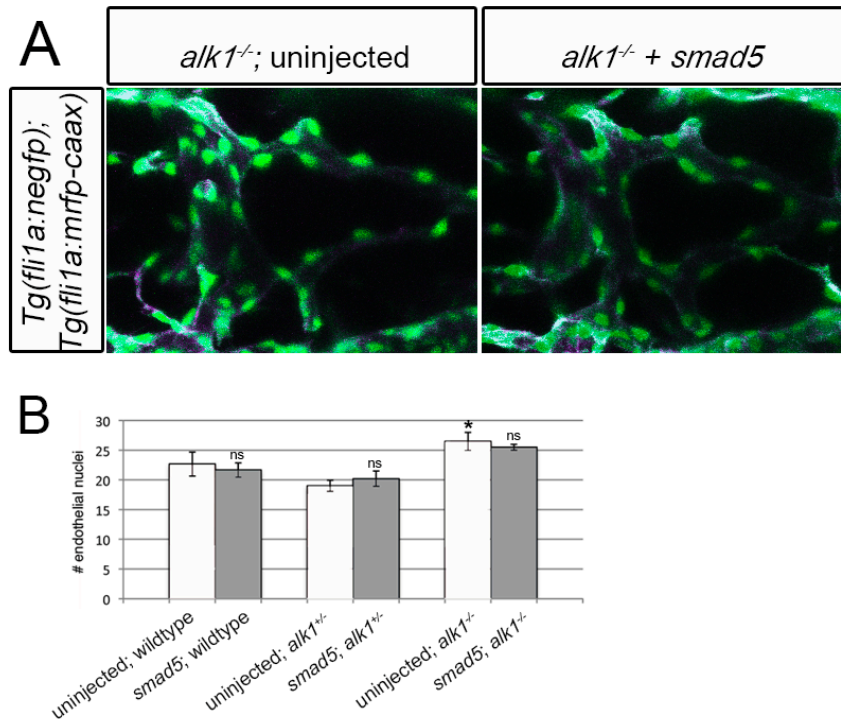


Figure 27: *smad5* misexpression does not rescue *alk1* mutant embryos.

(A) Cranial vasculature of 34 hpf *alk1* mutants left uninjected or injected with 100 pg *smad5* mRNA. Green is endothelial nEGFP, magenta is endothelial mRFP. Dorsal view, anterior left. 2D confocal projections. (B)

Endothelial cell counts in wild type, heterozygous, and *alk1* mutants, N = 3-6 for each group over 1 experiment. ns, not significant by student's unpaired t-test . *= p<0.05. Error bars represent S.E.M.

3.3 DISCUSSION

It has long been speculated that pSmad1/5/9 act downstream of Alk1 but that activation may depend on cellular context. Given the discrepancy in the literature, however, my results are significant in that they are the first to demonstrate that pSmad1/5/9 can serve as a readout for Alk1 activity in vivo during embryonic development. Here, I demonstrate that pSmad1/5/9 and dpERK1/2 expression are detectable by immunofluorescence in *alk1*-positive arteries, but only pSmad1/5/9 is dependent on *alk1* expression and Alk1 kinase activity. Interestingly, absence of *Tg(bre:egfp)* suggests that pSmads1/5/9 act in non-canonical fashion downstream of Alk1. Finally, I provide preliminary evidence that Alk1 kinase activity and is required for AVM prevention, likely functioning at least in part through Smad1/5/9.

Bmp9, Bmp10, and Alk1^{CA} can all lead to pSmad1/5/9 activation [194-196] in different cellular contexts. However, Alk1 may also trigger activation of MAPKs (dpERK1/2) to control endothelial cell behavior [199, 229]. Data presented here suggests an in vivo role for pSmads1/5/9 downstream of Alk1 in embryonic vascular development. Conversely, persistent expression of dpERK1/2 in *alk1* mutants and upon Alk1 kinase inhibition suggests dpERK1/2 is not a necessary substrate for Alk1 in vascular development.

Throughout development, different r-Smad protein locations and expression levels vary widely, indicating that although in some cellular contexts they may be functionally redundant, in others they may serve unique functions [248]. In zebrafish, although Smad1 and Smad5 each

contribute to zebrafish dorsal-ventral patterning, their expression is regulated independently of one another, and *smad1* can rescue *bmp2b* mutants whereas *smad5* cannot [249]. The endothelium of mouse embryos possesses high Smad5 protein levels but weak Smad1 protein levels [248], and Smad1 is not upregulated in *Smad5* mutants [237]. My early attempts to decipher which Smad was responsible for Alk1 signaling proved unsuccessful. Expression of *smad1* was undetectable at 36 hpf in *alk1*-positive arteries perhaps corroborating lack of detectable endothelial Smad1 protein in E15 mouse embryos [248]. Ubiquitous expression of *smad5* inhibited analysis of the cranial vasculature; however FISH results suggest that like *smad1*, *smad5* may be absent. Whether *smad9* is present in *alk1*-positive endothelial cells remains unclear; WISH results were inconclusive, and double FISH has not yet been performed. Because pSmad1/5/9 antibody recognizes Smad1, Smad5, and Smad9 on equivalent phosphorylated sites (Ser463/465), immunofluorescence prohibits us from discerning which of the Smad protein family members is responsible for transducing the Alk1 signal. However, immunofluorescence coupled with *smad* knockdown experiments may serve useful. Neither *smad1* nor *smad5* knockdown seems to affect pSmads1/5/9 staining (data not shown), but besides the potential for functional redundancy, we may also not be able to achieve sufficient knockdown due to early developmental defects.

It remains plausible that detection limits may explain the failure to detect *Tg(bre:egfp)* expression in *alk1*-positive arteries of wild type embryos. However, I neither detected basal *Tg(bre:egfp)* nor could I induce expression with intravascular injection of rhBMP10. Others have shown that complexed BMP10 can induce Alk1 activity during postnatal retinal vascularization without activating a pSmad1/5 BRE-reporter [222]. Together, these data allow for the speculation that pSmad1/5/9 are acting independent of transcription within the endothelium,

perhaps at a post-transcriptional step. Indeed, roles for pSmad1/5/9 have been demonstrated in the processing of microRNAs [147]. Alternatively, my results may imply that pSmad9 is the main mediator of the Alk1 signal as pSmad9 has been shown to be less effective in activating the BRE-reporter [250].

LDN-193189 is able to inhibit detection of pSmad1/5/9 by immunofluorescence and induce AVM formation but does not affect dpERK1/2 expression. These results make it seem plausible that pSmad1/5/9 activation downstream of Alk1 is necessary, at least in part, in AVM prevention. Despite this finding, weak phenocopy and confounding evidence from morpholino knockdown experiments make additional experiments, to test the necessity and sufficiency of Smads downstream of Alk1, vital. Failure of *smad* morphants to phenocopy *alk1* mutant embryos could be attributed to several confounding factors. First, high doses of *smad5* morpholino severely dorsalizes the embryo (> 2 ng) [[251] and data not shown], meaning utilized doses may not have been sufficient to generate vascular phenotypes. Second, earlier developmental defects may mask later effects on the vasculature. Finally, *Tg(bre:egfp)* embryos show robust pSmad1/5/9 activity within the heart [245, 252], deletion of *Smad5* causes defects in the myocardium [238], and *smad1/smad5* morphants and LDN-193189 treated embryos possess weak heart beats, suggesting that the resultant weak circulation may not be sufficient to precipitate AVMs, which we have shown to be dependent on flow [181]. Similarly, cell counts were collected at 48 hpf, a time point at which increases in endothelial cell number in *alk1* mutants are exacerbated by flow [181] again suggesting that failure to phenocopy may be attributed to poor circulation. While poor circulation is a plausible explanation, it also remains possible that *smad9* may functionally compensate for loss of *smad1/smad5*, and knockdown of all three Smad proteins is necessary to achieve AVMs. It should be noted, however, that *Smad5*^{-/-}

mice do not show compensatory increase in *Smad1* [253]. Weak penetrance of LDN-193189 may also be partially attributed to its off-target effects [VEGFR2, IC₅₀~ 215 nM], globally inhibiting angiogenesis and subsequently AVM formation. It should be noted however, that I did not detect loss of vessels or inhibition of ISV sprouting and therefore, inhibition of VEGFR2 signaling by LDN-193189 seems unlikely.

My results prove pSmads1/5/9 are an in vivo marker of Alk1 activity. Taken together with my previous data, these results place pSmads1/5/9 downstream of blood flow, Bmp10, and Alk1 in mediating a necessary pathway in promoting vascular quiescence. The exact roles for pSmads1/5/9 downstream of Bmp10/Alk1, whether they may be transcriptional or post-transcriptional, remain to be uncovered but may provide interesting examples of unique functions in endothelial cell biology.

4.0 DYNAMIC ANALYSIS OF BMP-RESPONSIVE SMAD ACTIVITY IN LIVE ZEBRAFISH EMBRYOS

Bone morphogenetic proteins (BMPs) are critical players in development and disease, regulating such diverse processes as dorsoventral patterning, palate formation, and ossification. These ligands are classically considered to signal via BMP receptor-specific Smad proteins 1, 5, and 9. To determine the spatiotemporal pattern of Smad1/5/9 activity and thus canonical BMP signaling in the developing zebrafish embryo, I generated a transgenic line expressing EGFP under the control of a BMP responsive element. EGFP is expressed in many established BMP signaling domains and is responsive to alterations in BMP type I receptor activity and *smad1* and *smad5* expression. This transgenic Smad1/5/9 reporter line will be useful for determining ligand and receptor requirements for specific domains of BMP activity, as well as for genetic and pharmacological screens aimed at identifying enhancers or suppressors of canonical BMP signaling.

4.1 INTRODUCTION

Bone morphogenetic proteins (BMPs), which are members of the transforming growth factor- β (TGF- β) ligand superfamily, play numerous roles in development and disease. For example, in vertebrate development, BMP signaling is required for dorsoventral axis formation and ventral cell fate specification during gastrulation, tailbud and somite formation, cardiomyocyte

differentiation, pharyngeal arch development, dorsal retina specification, and upper lip and palate fusion, among other processes [247, 254-264]. Furthermore, disruption of BMP signaling is associated with several human diseases, including pulmonary arterial hypertension, hereditary hemorrhagic telangiectasia, and fibrodysplasia ossificans progressiva [265-268]. While this diverse family of more than 20 ligands has been studied in many different contexts, discoveries of functional redundancies, promiscuous receptor binding, and non-canonical downstream effector activation have complicated elucidation of the molecular nature of BMP signaling pathways in specific developmental processes and disease states.

BMPs and other members of the TGF- β superfamily bind as homo- or heterodimers to a heterotetrameric complex consisting of two type II receptors and two type I receptors, both of which are serine/threonine kinases [269]. Ligand binding facilitates receptor complex formation, allowing the constitutively active type II receptor to phosphorylate the type I receptor within a glycine- and serine-rich (GS) motif. The now-active type I receptor then phosphorylates Smad proteins at a C-terminal SSXS motif [157]. Phosphorylation releases these receptor-specific Smads (R-Smads) from an autoinhibitory fold [270], allowing them to heterodimerize with the common partner Smad, Smad4, translocate to the nucleus, and, in concert with coactivators and corepressors, regulate transcription of target genes [271].

Typically, TGF- β , nodal, and activin ligands complex with type I receptors (Alk4, Alk5, or Alk7) that phosphorylate Smads 2 and 3. In contrast, BMPs complex with type I receptors (Alk1, Alk2, Alk3, or Alk6) that phosphorylate Smads1, 5, and 9. The specificity of type I receptor/Smad interaction is governed by the type I receptor L45 loop, and the L3 loop and α -helix1 within the Smad C-terminal MH2 domain [272-276]. More recently, TGF- β has been shown to induce Smad1/5 phosphorylation in many different cell types [180, 277-282], whereas

BMP9 has been shown to induce Smad2 phosphorylation in endothelial cells [283]. In some cases, these seemingly non-canonical responses are actually dependent on canonical type I receptor/Smad interactions, with TGF- β inducing the formation of mixed complexes containing both Smad2/3- and Smad1/5-specific type I receptors [221, 278]. However, in other cases, these responses seem to rely instead on novel activities of type I receptors, with Smad1/5-specific receptors phosphorylating Smad2, and Smad2/3-specific receptors phosphorylating Smad1/5 [279, 280, 283]. These findings challenge the notion of type I receptor Smad specificity and introduce further complexity into TGF- β family signaling pathways.

Phosphorylated R-Smad/Smad4 complexes regulate gene expression by binding to specific sequences within DNA and recruiting co-activators or co-repressors. While the specificity of DNA binding is not fully understood, it is clear that TGF- β -responsive Smads and BMP-responsive Smads activate different sets of genes. For example, phosphorylated Smad3 (pSmad3)/Smad4 binding to Smad Binding Elements (SBEs; GTCT) in the *plasminogen activator inhibitor-1 (PAI-1)* promoter is required for TGF- β -induced gene expression, and SBE multimers, in concert with a minimal promoter, confer responsiveness to TGF- β [284]. In contrast, pSmads1, 5, and 9 can, in concert with Smad4, induce expression of *inhibitor of differentiation-1 (Id1)* via binding to specific sites in its promoter [250, 285]. A so-called BMP responsive element (BRE) containing two regions of the mouse *Id1* promoter (-1052 to -1032; -1105 to -1080), ligated together and arranged as an inverted repeat, confers BMP responsiveness to a minimal promoter [285]. However, pSmad1/Smad4 can also regulate gene expression independently of canonical BMP responsive elements, either by binding directly to noncanonical *cis* elements [286] or by interacting with non-Smad transcription factors to mediate gene expression through their cognate *cis* elements [287, 288].

BMP signaling is negatively regulated at multiple levels, including ligand sequestration by soluble antagonists such as chordin and noggin; competition between R-Smads and inhibitory Smads (Smads 6 and 7) for binding to type I receptors or to Smad4; phosphatase-mediated dephosphorylation of type I receptors and R-Smads; ubiquitination and degradation of type I receptors, R-Smads, and Smad4; phosphorylation of Smads at sites other than the SSXS motif; and availability of nuclear co-activators and co-repressors [289]. Therefore, while BMP ligand, BMP receptor, and Smad expression patterns are informative, expression of pathway components cannot be equated with BMP activity. To better localize canonical BMP activity during development, BMP reporter mice have been generated that express β -galactosidase or GFP under the control of a BRE [250, 290, 291]. These models define sites of Smad1/5/9-mediated transcription in developing mice, including the dorsal optic vesicle, midbrain and hindbrain, anterior branchial arches, forelimb bud, heart, and tail mesenchyme at E9.5; and forebrain, snout, trigeminal ganglia, dorsal root ganglia, gut, kidney, liver, lung, heart, vasculature, skin, and limb at later stages. Generally, these domains correspond to the presence of pSmad1/5. To our knowledge, these models have not been exploited to determine ligand or receptor dependence of these activity domains, nor have they been used to identify novel genes or small molecules that impinge upon BMP signaling.

To expand the repertoire of models available for studying BMP signaling in vivo, I generated a transgenic zebrafish Smad1/5/9 reporter line using the BRE, in concert with a minimal promoter, to drive expression of EGFP. *Tg(bre:egfp)* embryos express EGFP in multiple domains known to require BMP activity, and EGFP expression is responsive to both activation and inhibition of Smad1/5 phosphorylation, suggesting that EGFP expression faithfully reports BMP activity. Because zebrafish embryos are externally fertilized, transparent,

and undergo rapid embryogenesis, this zebrafish BMP reporter line will allow mapping of endogenous BMP signaling over the course of development in live animals. Furthermore, because they are amenable to embryonic manipulations such as overexpression and knockdown, they can be used to define ligand-, receptor-, and Smad-dependence of different activity domains. Finally, *Tg(bre:egfp)* embryos can be used in genetic and chemical screens to identify novel players that either enhance or inhibit BMP signaling, either globally or in specific domains. These attributes may allow discovery of small molecules with specificity for particular ligands, receptors, or Smads involved in BMP signaling, providing finely-tuned tools for probing specific developmental processes and targeting specific BMP-related diseases.

4.2 RESULTS

4.2.1 Generation of transgenic zebrafish lines expressing EGFP under the control of a BRE

We assembled a DNA construct containing a BRE upstream of an adenovirus minimal *e1b* promoter and carp *b-actin* transcriptional start site [292], followed by EGFP coding sequence and a polyA signal. This construct, flanked by *Tol2* transposon arms [293, 294], was injected along with transposase mRNA into one-cell stage zebrafish embryos. Transient expression was observed in many structures that proved positive in stable transgenics (detailed below), whereas injection of a similar construct lacking the BRE was silent (data not shown). I identified 13 P0 founders, which ranged in germline transmission rates from 3-92%. Careful examination of two independent F1 lines, *Tg(bre:egfp)^{pt509}* and *Tg(bre:egfp)^{pt510}*, revealed identical patterns of EGFP expression, suggesting that expression domains are not reflective of the genomic context of the insertion.

4.2.2 *bre:egfp* expression correlates with many established domains of BMP activity

EGFP expression is first faintly detectable in the tailbud of developing *Tg(bre:egfp)* embryos at the 6 somite (6s) stage (12 hours post-fertilization or hpf; Figure 28a). While expression in this domain is weak at 6 somites, it is quite strong in the tailbud and has extended into the developing tail somites by the 12s stage (15 hpf; Figure 28b). The presence of BMP activity in the tailbud and somites correlates with expression of *smad1* and *smad9* and presence of pSmad1/5/9 in zebrafish, and corroborates the established role for BMP signaling in zebrafish tailbud and somite development [295-297]. A second early expression domain in 12s *Tg(bre:egfp)* embryos resides in the presumptive myeloid progenitor domain, just caudal to the eye (Figure 28b). By the 18s stage (18 hpf; Figure 28c), EGFP-positive myeloid cells can be seen migrating bilaterally away from their origin. Expression in this domain corroborates the established requirement for *smad1* in zebrafish macrophage and granulocyte development [246].

By 1 day post-fertilization (dpf), BRE activity has expanded to many new domains (Figure 28d), including the heart (Figure 28g-i). At this time, the entire endocardium is strongly EGFP-positive, colocalizing with *flil1a*-driven dsRed expression in both the atrium and ventricle (Figure 28g-g''). Sparse expression is also evident in the myocardium, which surrounds the endocardium (Figure 28g, g'). By 2 dpf, this expression pattern has inverted, with EGFP expressed most strongly in myocardial cells, as evidenced by colocalization with *myosin light chain 7 (myl7)*-driven nuclear-dsRed, and more weakly in endocardial cells, as evidenced by minimal colocalization with *flil1a*-driven dsRed (Figure 28e, h-h''). Between 2 and 3 dpf (data not shown), expression wanes in the endocardium to nearly undetectable levels and coalesces within the myocardium to the level of the atrioventricular canal, persisting in this pattern until at least 4 dpf (Figure 28f, i-i''). *bre*-driven transgene expression in mice [290] and pSmad1

expression in chick [298] have been reported in both endocardium and myocardium, and expression in these domains corroborates known roles of BMP signaling in endocardial cushion formation [299, 300], cardiomyocyte survival [301], and cardiomyocyte-specific *tbx20* expression [286].

Moving posteriorly from the heart, another strong domain of *bre*-driven EGFP expression is encountered in ventrolateral regions of the pharyngeal arches at 1 dpf (Figure 28d, j, j'). At this time, no segmentation is evident, whereas by 2 dpf, segmentation delineates ventrolateral regions of each pharyngeal arch (Figure 28e, k, k'). By 3 dpf (not shown), pharyngeal expression is no longer bilateral but instead has coalesced at the ventral midline, with expression persisting in this midline domain until at least 4 dpf (Figure 28f, l-l''). Closer examination reveals two distinct EGFP expression domains within the ventromedial pharyngeal arches. One domain surrounds and is closely apposed to the ventral aorta (Figure 28l'-l''), and is likely vascular smooth muscle, which first appears in this region around 3-4 dpf [302]. The second, segmented domain is more ventral and likely corresponds to the medial basihyal and basibranchial/hypobranchial cartilages (Figure 28l''). Pharyngeal arch expression correlates with reported expression of *bre*-driven GFP in mouse pharyngeal arches [250] and corroborates the established role of BMP signaling in development of zebrafish pharyngeal arches [260].

bre-driven EGFP is expressed in the dorsal retina at 1 dpf (Figure 28d, m, m'), but is no longer detectable by 2 dpf (Figure 28e). This expression domain corroborates the established requirement for GDF6a (BMP-13)-mediated signaling in zebrafish dorsal retina specification [264]. Just caudal to the eyes, the trigeminal ganglia also express EGFP at 1 dpf (Figure 28m, m''), with expression intensifying over the course of the day and persisting until at least 4 dpf. In mice, dorsal trigeminal neuron identity requires cell-autonomous BMP activity [303],

supporting my observation that only dorsal axonal projections emanating from this ganglion report pSmad1/5-mediated EGFP expression in zebrafish. Additional anterior domains of BRE-mediated EGFP expression at 1 dpf include the pineal gland/epiphysis (Figure 28d, n), which lies at the midline of the dorsal diencephalon and functions as a circadian pacemaker; and the ventral diencephalon, or hypothalamic rudiment (Figure 28d, o). Expression in these domains is also transient, waning during day 2. While I could find no published role for BMP signaling in the pineal gland, this structure is known to express *idl*, the gene from which the BRE was derived, in rat and zebrafish [304, 305]. Furthermore, BMP signaling is known to be required for hypothalamic patterning in chick embryos [306]. Thus, these two domains would be expected to report pSmad1/5 activity.

In the trunk and tail of 1 dpf *Tg(bre:egfp)* embryos, EGFP is expressed in the most ventral aspect of the embryos, including the mesenchyme underlying the yolk extension and the forming common kidney/gastrointestinal opening, the cloaca (Figure 28d, p, p'). Cloacal expression wanes over the course of the day, decreasing from a peak around the 26-28 somite stage (22-23 hpf). Interestingly, cloacal expression re-appears at 3-4 dpf (Figure 28f, q, q'). Expression timing correlates with connection of the kidney tubules (28 somites) and gut tube (4 dpf) to this common opening, and supports the established role of BMP signaling in cloacal development [307]. Also in the trunk, EGFP continues to be expressed in the somites through 4 dpf (Figure 28d-f, r, r'). While the intensity of EGFP expression in this domain decreases between 1 and 2 dpf, expression increases between 2 and 3 dpf and remains strong in most embryos at 4 dpf. The somitic expression domain is the most variable domain in *Tg(bre:egfp)^{pt510}*, with approximately 90 and 70% showing intermediate to strong somite expression at 1 and 4 dpf, respectively.

bre-driven EGFP expression continues at 2 dpf in the heart, pharyngeal arches, trigeminal ganglia, pineal gland, hypothalamus, and somites, as described above. In addition, clear expression is now evident in the developing mouth opening, or stomodeum, within the first pharyngeal arch (Figure 28s). The dorsoanterior expression domain of the stomodeum represents the maxillary process, whereas the ventroposterior expression domain of the stomodeum represents the mandibular process, which together delineate the forming mouth opening. Weaker expression is also seen in an adjacent horseshoe-shaped, slightly more dorsal-anterior domain that follows the contours of the ventral diencephalon (Figure 28s). The maxillary and mandibular processes thin along the dorsoventral axis and elongate along the left/right axis by 4 dpf to form the mouth opening (Figure 28t). Interference with BMP signaling results in cleft lip and cleft palate in mice, suggesting a critical conserved role for BMP-mediated pSmad1/5 activity in oral cavity development [261].

At 2 dpf, *bre*-driven EGFP expression is also strong in the pectoral fin bud, at the base of the fin as well as at the apical ectodermal ridge (Figure 28e, u). This expression domain is substantiated by the requirement for BMP signaling through the type I receptor, Alk8 (homologous to mammalian ALK2), in pectoral fin development [308]. Additionally, strong EGFP expression is apparent in many cells in the median fin fold, particularly in the ventral region (Figure 28e, v). These cells have a dendritic appearance similar to that described for neural crest-derived mesenchymal cells that give rise to fin rays, or lepidotrichia [309]. Finally, several spinal cord neurons are EGFP-positive at 2 dpf (Figure 28w). Cell bodies are positioned approximately at the midline, midway along the dorsoventral axis of the spinal cord, and axons extend bidirectionally, parallel to the anterior/posterior axis. Pectoral fin, median finfold, and spinal neuron *bre*-driven EGFP expression domains persist until at least 4 dpf.

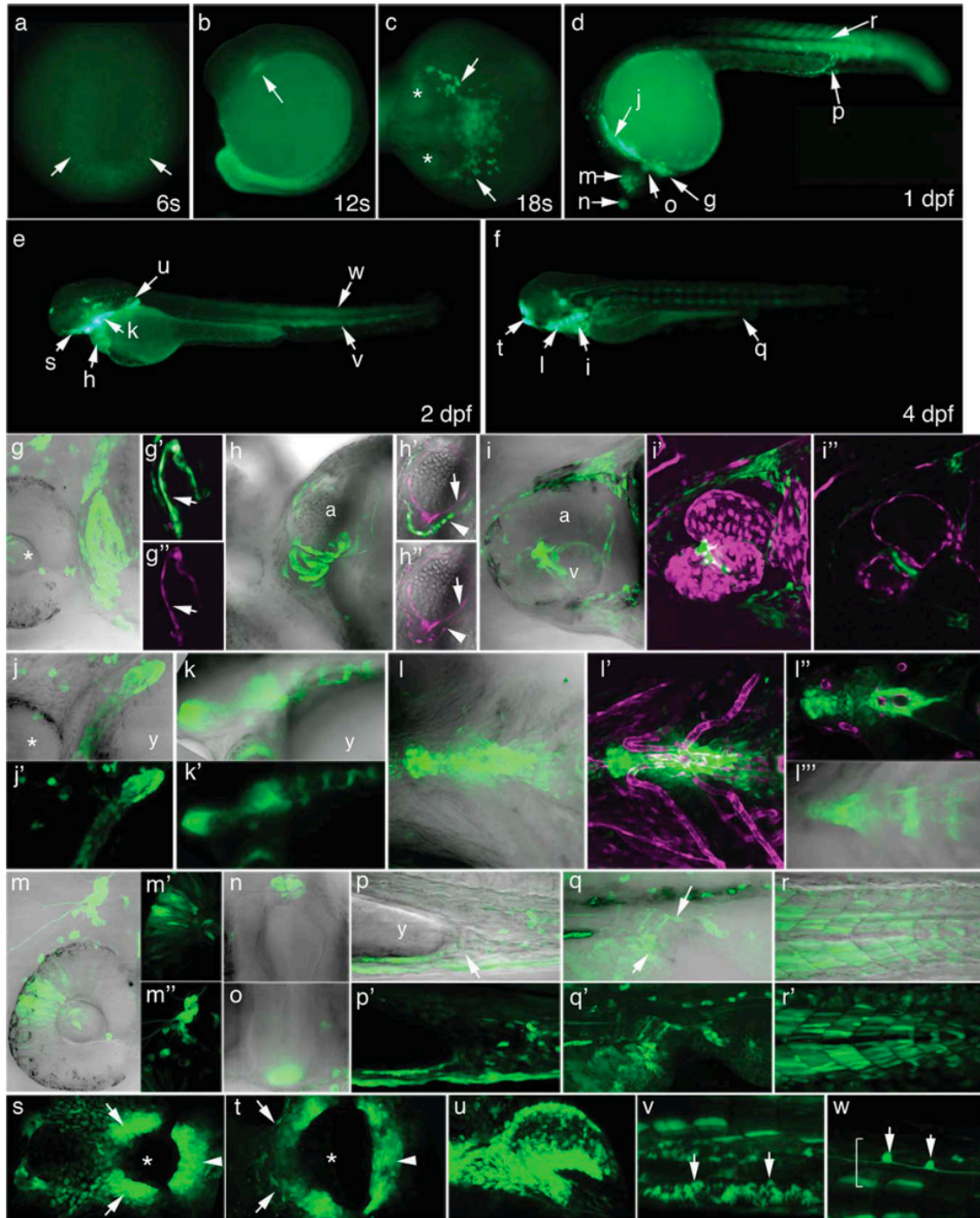


Figure 28: Developmental profile of pSmad1/5/9-mediated transcriptional activity in *Tg(bre:egfp)^{pt510}* embryos.

In all images, green represents *bre*-driven EGFP expression. Magenta represents endothelial expression of *Tg(fli1ep:dsRedEx)^{um13}* or myocardial expression of *Tg(-5.1myl7:nDsRed2)^{f2}*, as noted below. g-r, h', h'', l''':

Fluorescence/transmission overlays. a–f: Macro images. a: Six somites. Arrows point to tailbud. b: Twelve somites. Arrow points to myeloid progenitors. c: Eighteen somites. Asterisks denote eyes; arrows point to myeloid cells. d–f: Embryos at 1 (d), 2 (e), and 4 (f) dpf. Lettered arrows denote expression domains highlighted in correspondingly lettered panels below. g–w: 2D projections of confocal Z-series, except h', h'', i'', and l'', which represent single optical sections extracted from the corresponding Z-series. Magnification, 400x. g–g'': Heart at 1 dpf. Asterisk denotes eye. g' and g'' are matched substacks showing EGFP/*fli1ep:dsRedEx* (overlay) and *fli1ep:dsRedEx* expression, respectively. Arrows denote endocardium. h–h'': Heart at 2 dpf. h' and h'' are matched optical sections of EGFP/*fli1ep:dsRedEx/-5.1myl7:nDsRed2* (overlay) and *fli1ep:dsRedEx/-5.1myl7:nDsRed2*. Arrows denote endocardium; arrowheads denote myocardium. i–i'': Heart at 4 dpf. i' and i'' show overlays of EGFP with *fli1ep:dsRedEx*, 2D projection and single optical section, respectively. j–j': Pharyngeal arches, 1 dpf. Asterisk denotes eye. k,k': Pharyngeal arches, 2 dpf. l–l''': Pharyngeal arches, 4 dpf. l', l'': Overlays of EGFP with *fli1ep:dsRedEx*, 2D projection, and single optical section, respectively. l''': Substack of image shown in l. m–m'': Dorsal retina (m') and trigeminal ganglion (m''), 1 dpf. n: Pineal gland, 1 dpf. o: Hypothalamus, 1 dpf. p, p': Ventral mesenchyme and cloaca (arrow), 2 dpf. q, q': Cloaca, 4 dpf. Arrows delineate cloacal opening. r, r': Somites, 1 dpf. s: Stomodeum, 2 dpf. Asterisk, presumptive mouth opening; arrows, maxillary process; arrowhead, mandibular process. t: Stomodeum, 4 dpf. Asterisk, open mouth; arrows, maxillary process; arrowhead, mandibular process. u: Pectoral fin bud, 2 dpf. v: Mesenchymal cells of the median finfold (arrows), 2 dpf. w: Spinal cord neurons (arrows), 2 dpf. Spinal cord is bracketed. a: Dorsoposterior view, posterior down. b, d–g, j, k, m, p–r, u–w: Lateral view, anterior left, dorsal up. c: Dorsal view, anterior left. h, i, l: Ventral view, anterior left, left up. n: Dorsal view, left to the right. o: Frontal view, left to the right. s, t: Frontal view, left up. a, atrium; v, ventricle; y, yolk.

4.2.3 Temporal correlation between pSmad1/5/9 expression and *bre*-driven EGFP fluorescence

Because EGFP takes time to fold and fluoresce and is a stable protein [310], the temporal pattern of EGFP fluorescence in *Tg(bre:egfp)* embryos would not be expected to precisely reflect the temporal activity of pSmad1/5/9. To gauge the offset between pSmad1/5/9 activity and transgene expression, I assessed pSmad1/5/9 expression, *egfp* mRNA expression, and EGFP

fluorescence in the dorsal retina, a relatively transient EGFP expression domain, between 10 and 38 hpf (Figure 29). pSmad1/5/9 expression first appears in the dorsal retina at 12 hpf, *egfp* mRNA at 14 hpf, and EGFP fluorescence at 16 hpf, demonstrating an approximately four hour delay between the appearance of pSmad1/5/9 and EGFP fluorescence. A similar delay was seen in the trigeminal ganglia (Figure 29) and heart (data not shown) and in other zebrafish transgenic studies [311]. By 28-30 hpf, pSmad1/5/9 and *egfp* mRNA are barely detectable in the dorsal retina, while EGFP fluorescence disappears between 36 and 38 hpf (Figure 29). Thus, EGFP perdures in this domain for approximately eight-to-ten hours after pSmad1/5/9 is lost. While this perdurance is short compared to other published work demonstrating EGFP stability in vivo on the order of a day or even weeks [312], nearly all *bre*-driven EGFP expression domains are either dynamic or transient, suggesting that in these domains, EGFP is either less stable than previously described or that cell turnover is high.

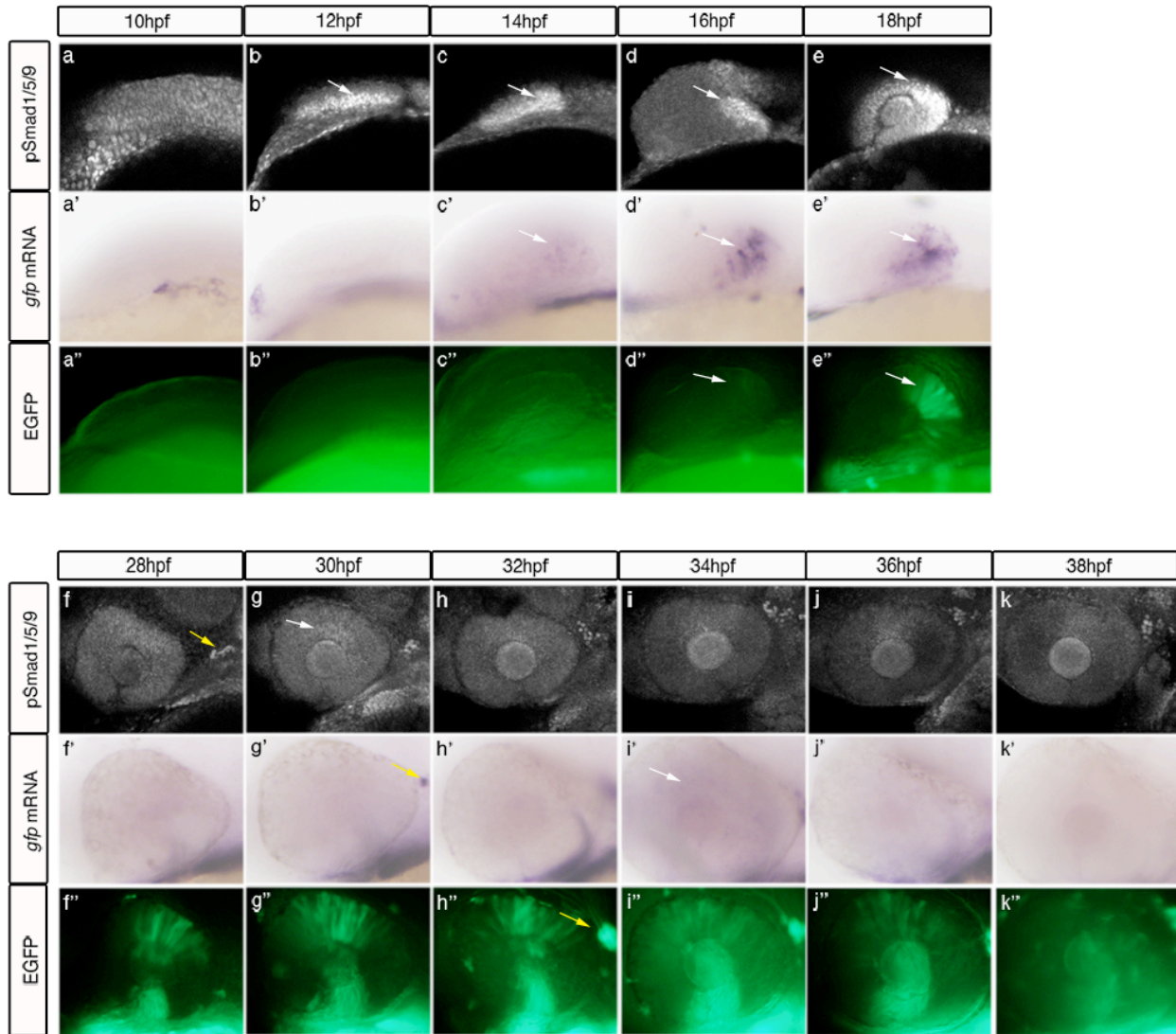


Figure 29: Temporal relationship between pSmad1/5/9 activity and EGFP fluorescence in *Tg(bre:egfp)* embryos.

Embryos were collected every 2 hr between 10–18 hpf and 28–38 hpf and assayed for pSmad1/5/9 via immunofluorescence (a–k), 100×; egfp mRNA via in situ hybridization (a'–k'), 80×; and EGFP fluorescence (a''–k''), 80×. Results demonstrate a 4-hr delay between pSmad1/5/9 expression and EGFP fluorescence, and an 8–10-hr perdurance of EGFP after pSmad1/5/9 is lost. Green indicates *bre*-driven EGFP expression, 80× magnification. White arrows, dorsal retina; yellow arrows, trigeminal ganglia. All images lateral view, anterior left.

4.2.4 *bre:egfp* transgene expression is responsive to changes in Smad1/5/9 phosphorylation

While EGFP expression in *Tg(bre:egfp)* embryos correlates well with known domains of BMP activity, I sought to further validate this model by manipulating phosphorylation of BMP-responsive Smads and assaying effects on EGFP expression. In shield stage *Tg(bre:egfp)* embryos, I can only faintly and variably detect EGFP via fluorescence or in situ hybridization, though pSmad1/5/9 is detectable by immunohistochemistry (Figure 30a-c). However, injection of one- to two-cell embryos with 5 pg mRNA encoding a constitutively active form of the zebrafish BMP type I receptor, Alk1 (Alk1^{CA}), induces EGFP expression at shield stage, as visualized by fluorescence and by in situ hybridization, correlating with a marked increase in nuclear-localized pSmad1/5/9 (Figure 30d-f). In contrast, injection of up to 100 pg mRNA encoding a constitutively active form of the zebrafish TGF- β type I receptor, Alk5 (Alk5^{CA}), fails to induce *bre:egfp* transgene expression or phosphorylation of Smad1/5/9 (Figure 30g-i), consistent with this receptor's established propensity to phosphorylate Smad2/3.

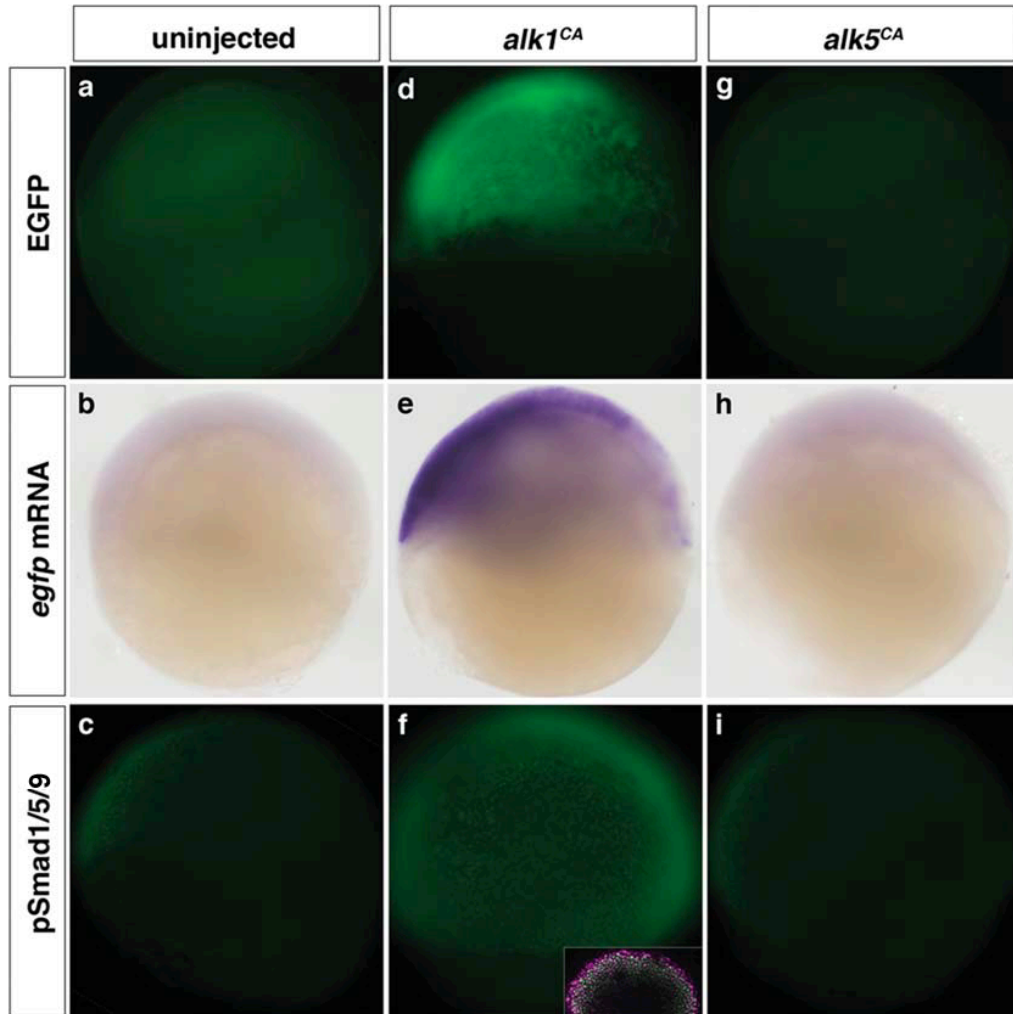


Figure 30: Expression of the *bre:egfp* transgene is responsive to changes in BMP type I receptor signaling.

Embryos were left uninjected (a–c) or injected with 5 pg *alk1^{CA}* mRNA (d–f) or 100 pg *alk5^{CA}* mRNA (g–i) at the one- to two-cell stage and assayed at shield stage (6 hpf). a, d, g: Expression of *bre*-driven EGFP fluorescence in live embryos. b, e, h: Expression of *bre*-driven *egfp* mRNA assayed by in situ hybridization. c, f, i: Expression of pSmad1/5/9 assayed by immunofluorescence. Inset in f is pSmad1/5/9 (green)/DAPI (magenta) merge. Lateral views, animal pole up, dorsal right. Original magnification 80x except inset, 200x.

To further confirm that *bre:egfp* transgene expression is dependent upon BMP signaling, I treated embryos at tailbud stage (10 hpf) with 10 μ M dorsomorphin, a small molecule that inhibits BMP type I receptor-mediated Smad1/5/9 phosphorylation [313]. Treatment at this time

avoids dorsalization resulting from treatment prior to gastrulation, allowing me to assess transgene expression during organogenesis. Dorsomorphin treatment reduced EGFP expression in all domains at 1 dpf, most notably in the retina, hypothalamus, heart, pharyngeal arches, somites, and cloaca (Figure 31e, f, i-r and Table 1), without greatly affecting general morphology (Figure 31a, b). Furthermore, treatment with 10 μ M DMH1, a more potent dorsomorphin analog that, unlike dorsomorphin, does not affect vascular endothelial growth factor receptor (VEGFR) activity [242], essentially eliminated EGFP expression in all domains (Figure 31c, g), whereas treatment with 200 μ M SB-431542, an Alk4/5/7 inhibitor, had no effect on EGFP expression (Figure 31d, h). Taken together with *alk1^{CA}* overexpression studies, these results demonstrate that the *bre:egfp* transgene is indeed specifically responsive to pSmad1/5/9, and not pSmad2/3.

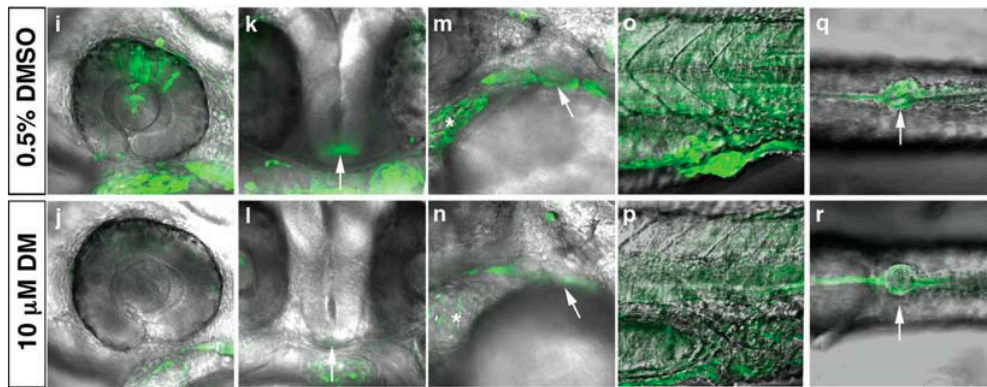
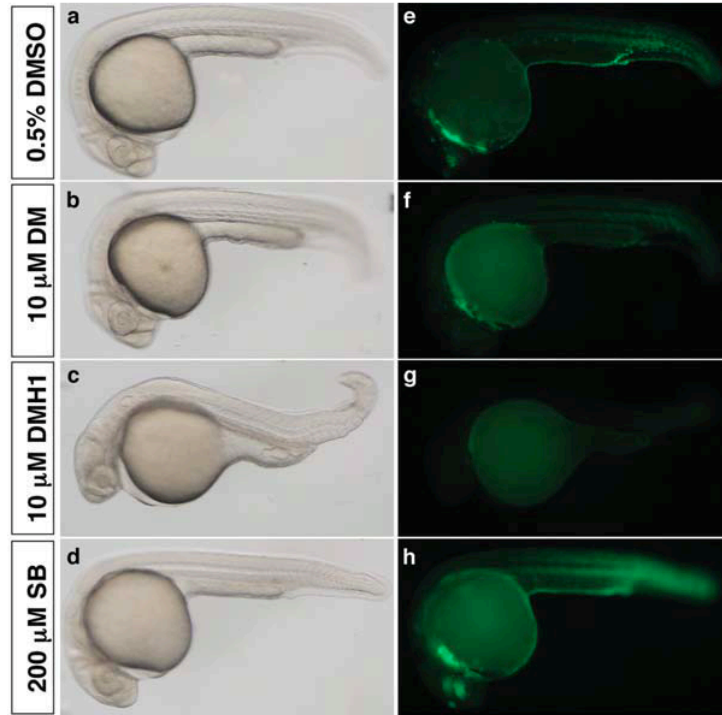


Figure 31: Expression of the *bre:egfp* transgene is globally downregulated by small molecule inhibition of BMP type I receptor-mediated Smad phosphorylation.

Embryos were treated with either 0.5% DMSO (a, e, i, k, m, o, q); 10 μ M dorsomorphin (DM) (b, f, j, l, n, p, r); 10 μ M DMH1 (c, g), or 200 μ M SB-431542 (SB) (d, h) between 10 and 24 hpf and imaged shortly after washout. In all images, green indicates *bre*-driven EGFP expression. Brightfield (a–d) and fluorescent (e–h) images, lateral view, anterior left, 80x magnification. i–r: 2D projections of confocal Z-series showing EGFP and transmission overlays, 400x magnification. Expression domains shown include (i, j) retina; (k, l) hypothalamus (arrow); (m, n) heart (asterisk) and pharyngeal arches (arrow); (o, p) somites; and (q, r) cloaca (arrow). i, j, m–p: Lateral view, anterior left. k, l: Frontal view, left is right. q, r: Ventral view, anterior left.

4.2.5 *bre:egfp* transgene expression is decreased by knockdown of *smad1* or *smad5*

To further analyze the dependence of *bre*-driven EGFP on *smad1* and *smad5*, I knocked down expression of each of these genes in zebrafish embryos using translation blocking morpholino-modified antisense oligonucleotides (morpholinos). Injection of 4 ng *smad5* morpholino severely dorsalized embryos [C4 phenotype [314]], precluding later analysis (Figure 32). Injection of 2 ng *smad5* morpholino resulted in slight tail truncations but had little effect on EGFP expression in most domains at 1 dpf, with substantial decreases observed only in the somites and moderate to minimal decreases in dorsal retina and cloaca (Figure 32 and Table 1). These results demonstrate that *bre*-driven EGFP expression in somites, retina, and cloaca is most sensitive to *smad5* levels. However, since knockdown in these experiments is incomplete, I cannot make strong conclusions regarding the role of *smad5* in other *bre*-driven EGFP expression domains.

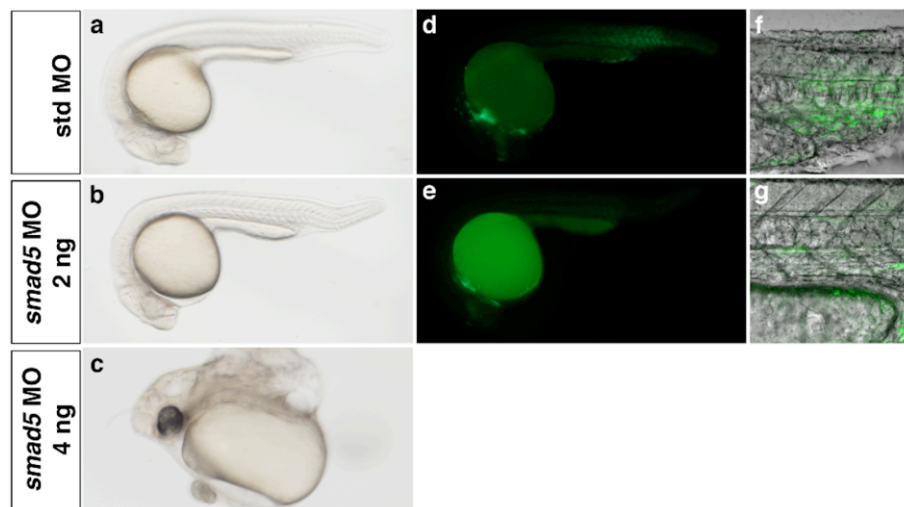


Figure 32: *smad5* knockdown down-regulates *bre:egfp* transgene expression primarily in somites.

Embryos were injected with 2 ng standard control morpholino (a, d, f), 2 ng *smad5* morpholino (b, e, g), or 4 ng *smad5* morpholino (c) at the one- to two-cell stage and imaged at 1 dpf. In all images, green indicates *bre*-driven EGFP expression. Brightfield (a, b, c) and fluorescent (d, e) images, lateral view, anterior left, 80× magnification. f,

g: 2D projections of confocal Z-series showing somites, EGFP, and transmission overlays, 400× magnification. Lateral views, anterior left.

In contrast to the limited effect of *smad5* knockdown on organ-specific *bre*-driven EGFP expression, *smad1* knockdown dampened EGFP expression in many domains (Figure 33 and Table 1). Injection of 2 ng *smad1* morpholino resulted in moderate to substantial decreases in transgene expression in the dorsal retina (Figure 33e, f) and hypothalamus (Figure 33h, i) at 1 dpf, and the stomodeum (Figure 33k, l) and pectoral fin (Figure 33n, o) at 2 dpf. These affected domains correlated well with the presence of *smad1* transcripts (Figure 33g, j, m, p). EGFP expression in *smad1* morphants was also substantially decreased in the cloaca at 1 dpf, and somites and median finfold at 2 dpf (Table 1). However, these expression domains did not correlate well with *smad1* mRNA expression, likely due at least in part to EGFP perdurance (Figure 29). Additional domains showing minimal decreases in EGFP fluorescence included the heart, pharyngeal arches, pineal gland, and somites at 1 dpf; and the pharyngeal arches at 2 dpf (Table 1). The inability of *smad1* knockdown to completely abrogate EGFP expression in any domain suggests either incomplete knockdown or a partial redundancy with *smad5*, which is nearly ubiquitously expressed, and/or *smad9*, which is expressed in the majority of EGFP-positive domains [295]. While it is possible that combined *smad1/5* knockdown might severely decrease *bre*-driven EGFP expression in many domains, I could not test this possibility because severe developmental defects precluded analysis (data not shown).

Expression domains	Dorsomorphin, 10 μ M, 1 dpf (%)	Smad5 MO, 2 ng, 1 dpf (%)	Smad1 MO, 2 ng, 1 dpf (%)	Smad1 MO, 2 ng, 2 dpf (%)
Cloaca	++ (26)	+/- (81)	++ (63)	NA
Heart	+ (76)	- (96)	+/- (86)	- (99)
Hypothalamus	++ (20)	- (101)	+ (74)	NA
Median finfold	NA	NA	NA	++ (62)
Pectoral fin	NA	NA	NA	++ (64)
Pharyngeal arches	+/- (82)	- (96)	+/- (76)	+/- (83)
Pineal gland	+/- (81)	- (95)	+/- (86)	NA
Retina	++ (52)	+ (75)	++ (47)	NA
Somites/tailbud	+/- (82)	++ (60)	+/- (82)	++ (58)
Spinal cord neurons	NA	NA	NA	- (111)
Stomodeum	NA	NA	NA	++ (42)
Trigeminal ganglia	NA	NA	NA	- (99)

Table 1: Sensitivity of bre:egfp expression to manipulation of Smad1/5 activity and expression^a

^aEGFP expression in individual embryos was subjectively scored by two independent observers as strong (3), moderate (2), weak (1), or not expressed (0), and scores averaged within control (0.5% DMSO for comparison to 10 mM dorsomorphin; 2 ng standard control morpholino for comparison to 2 ng smad1 and smad5 morpholinos) and experimental groups. Average scores for experimental groups are expressed as percent of control. Sensitivity to treatment was gauged as substantial (++, < 65% of control), moderate (+, 65–80% of control), minimal (+/-, 80–90% of control), or unaffected (-, > 90% of control). n 1/4 24 per group for dorsomorphin treatment; 17 per group for smad5 morpholino at 1 dpf; 27 per group for smad1 morpholino at 1 dpf; and 24 per group for smad1 MO at 2 dpf. Results are qualitatively reflective of 3–5 additional independent experiments. NA, not assessed.

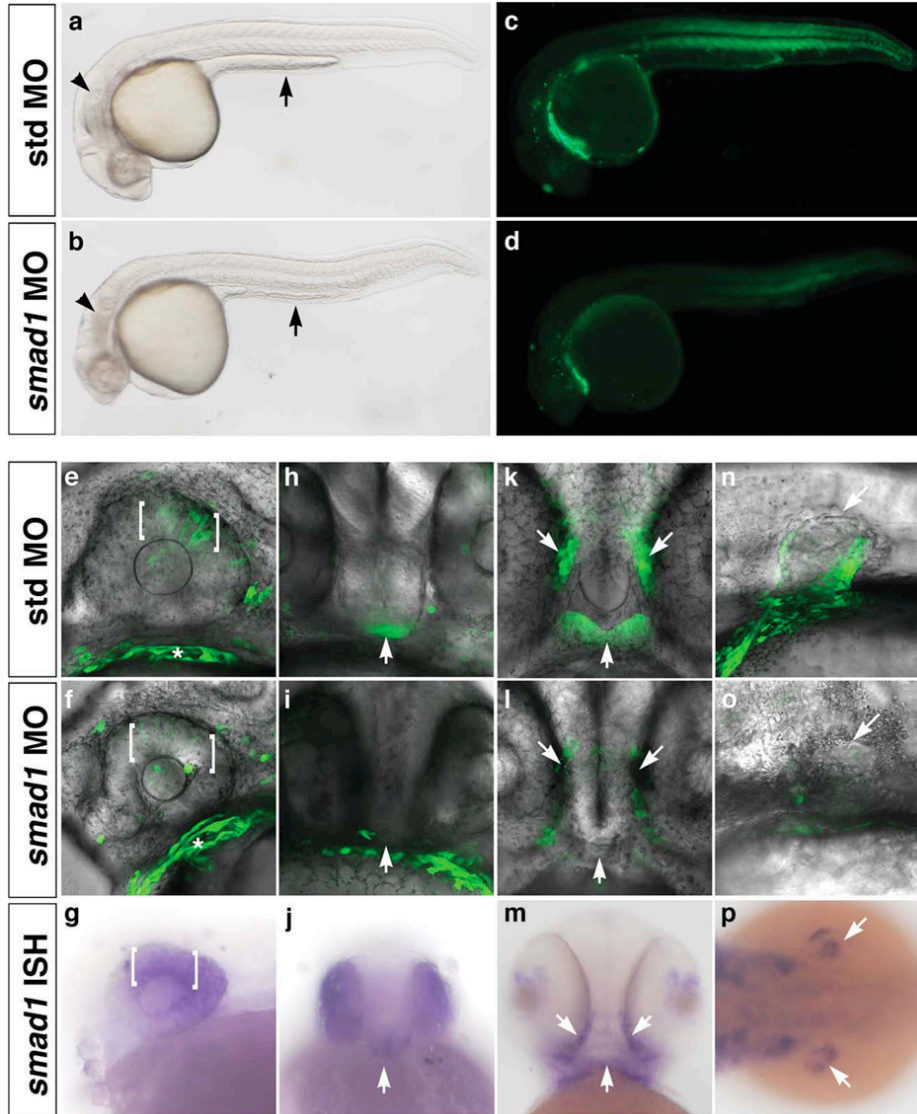


Figure 33: *smad1* knockdown downregulates *bre:egfp* transgene expression in *smad1*-expressing domains.

Embryos were injected with 2 ng standard control morpholino (a, c, e, h, k, n) or 2 ng *smad1* morpholino (b, d, f, i, l, o) at the one- to two-cell stage. In all images, green indicates *bre*-driven EGFP expression. Brightfield (a, b) and fluorescent (c, d) images, 1 dpf, lateral view, anterior left, 80_ magnification. Note defects in yolk extension (arrow) in *smad1* morphant (b) versus control embryo (a). e, f, h, i, k, l, n, o: 2D projections of confocal Z-series showing EGFP and transmission overlays, 400x magnification. g, j, m, p: Expression of *smad1* mRNA assayed by in situ hybridization. Expression domains shown include (e–g) dorsal retina (brackets), 1 dpf; (h–j) hypothalamus (arrow), 1 dpf; (k–m) stomodeum (arrows), 2 dpf; and (n–p) pectoral fin (arrows), 2dpf. e–g, n, o: Lateral view, anterior left. h–j: Frontal view, left is right. k–m: Ventral view, anterior up. p: Dorsal view, anterior left.

4.3 DISCUSSION

I have generated a stable transgenic zebrafish line, *Tg(bre:egfp)*, which reports pSmad1/5-mediated transcriptional activation in vivo. Support for this assertion includes a correlation between EGFP expression domains and published requirements for BMP signaling in development of these same cells or tissues; demonstrated sensitivity to modulation of BMP type I receptor activity; and demonstrated correlation with *smad1* expression and sensitivity to *smad1* knockdown. Because BMP signaling is negatively regulated at multiple levels – for example, dephosphorylation of receptors and Smads, I-Smad interference with type I receptor/Smad binding or R-Smad/Smad4 binding, and Smad binding to co-repressors – expression patterns of BMP receptors and Smads cannot accurately predict sites of BMP-mediated transcriptional activity [289]. My *Tg(bre:egfp)* line overcomes this limitation inherent in the analysis of simple expression patterns by directly reporting pSmad1/5-mediated transcriptional activity, and can therefore be used as a tool to define cells that respond to BMP signals over the course of development. It should be noted that phosphorylated BMP R-Smad/Smad4 complexes can regulate gene expression independently of canonical *Bre* sites, either by binding directly to unrelated *cis* elements [286] or by interacting with non-Smad transcription factors to mediate gene expression through their cognate *cis* elements [287, 288]. However, the mouse *Id1*-derived BRE used to generate my transgenic reporter line is pSmad1/5-responsive in vitro and in vivo in many different cell types [194, 250, 285, 290, 291] and is postulated to require no additional transcription factor binding partners for activity [290]. Therefore, while EGFP expression in my *Tg(bre:egfp)* line may not reflect endogenous binding and activation of “canonical” *Bre* sites, it

should report the presence of all nuclear phosphorylated BMP R-Smad/Smad4 complexes, regardless of which *cis*-acting element is being activated within each domain in vivo.

Transgene expression in *Tg(bre:egfp)* embryos is observed primarily within domains with reported requirements for BMP signaling. For example, EGFP is expressed in the dorsal retina, the specification of which requires GDF6a (BMP-13)-mediated Smad1/5 phosphorylation within retinal cells [264]. And EGFP is expressed in the forming mouth opening or stomodeum, likely reflecting a requirement for BMP signaling in lip development, as has been previously demonstrated in mice [261]. However, the role of BMP signaling in other EGFP-positive domains is less clear. For example, to our knowledge, a requirement for BMP-induced Smad1/5 activity in pineal gland development or function has not been reported, although this structure is known to express the Smad1/5-responsive gene, *idl* [304], as well as *bmp2a* [295]. Similarly, while I observe strong EGFP expression in putative osteogenic mesenchymal cells in the median finfold, I could find no reports of a requirement for BMP signaling specifically within these cells. Thus, I have defined two previously unidentified domains in which BMP signaling is active during zebrafish embryonic development. Given that *Tg(bre:egfp)^{pt509}* and *Tg(bre:egfp)^{pt510}* showed identical EGFP expression patterns, and that EGFP expression in nearly all domains was decreased by dorsomorphin treatment or *smad1* or *smad5* morpholino injection and eliminated (at 1 dpf) by DMH1 treatment, it is highly unlikely that expression domains reflect insertional artifacts or expression via cryptic enhancers within our *bre:egfp* construct. The only domain that I cannot say with certainty is not artifactual is the 2 dpf spinal cord neurons, which was not affected by *smad1* morpholino but not assayed in drug or *smad5* morpholino experiments because of dorsalized phenotypes.

While *bre*-driven EGFP expression was observed in many anticipated domains in my transgenic line, some structures were unexpectedly negative, despite convincing evidence in the literature for a role for BMP signaling in specification and/or function. For example, while *smad5* is clearly required for gastrulation [247, 315] and pSmad1/5/9 is detectable ventrally in shield stage embryos, *bre*-driven EGFP expression was undetectable in this domain. Also, while the BMP type I receptor, Alk1, is expressed exclusively in particular arteries in zebrafish embryos and loss of function results in enlarged vessels and arteriovenous malformations [182], I could not detect EGFP expression in *alk1*-positive vessels (data not shown). Finally, BMP signaling during somitogenesis promotes pronephric cell fates and inhibits blood and vascular differentiation [316], but I could not detect EGFP expression in the posterior lateral or intermediate mesoderm or their derivatives (data not shown). These examples highlight the limitations of this transgenic reporter approach. The lack of detection of EGFP in the ventral region of shield stage embryos is likely due to the fact that temporal transgene expression patterns do not precisely reflect endogenous BMP activity due to delayed EGFP fluorescence (Fig. 27). In domains in which the effectors of BMP signaling are less clear, the reasons for the lack of EGFP expression could be manifold. Because the BRE used to drive transgene expression may not efficiently report pSmad9/Smad4-mediated gene expression [250], it is possible that Smad9 is the major effector in unexpectedly negative domains. Alternatively, these cells may engage non-traditional Smad pathways downstream of receptor activation. For example, TGF- β binding to a non-canonical receptor complex containing both Smad1/5-specific and Smad2/3-specific type I receptors can generate mixed pSmad1/pSmad2 complexes [278]; BMP9, acting through Alk1, can activate Smad2 phosphorylation [283]; and ligand-induced R-Smad activation can enhance microRNA processing in a Smad4-independent, post-

transcriptional manner [147]. None of these pathways results in BRE activation. Another possible explanation for the lack of EGFP expression in established BMP activity domains is that Smad-independent pathways might relay signals downstream of BMP type I receptors. For example, in endothelial cells, Alk1 may signal at least in part through MAP kinases [146, 197]. Finally, as BMP signaling can both activate and repress transcription, it is possible that co-repressors present within these unexpectedly negative domains prevent pSmad1/5-mediated *bre:egfp* transactivation. For example, a pSmad1/5-responsive element derived from the *Xenopus laevis Vent2* promoter can mediate heterologous gene activation or repression, depending on the presence of trans-acting co-activators or co-repressors [317]. However, other reports suggest that pSmad-mediated transcriptional repression occurs in a non-BRE-dependent manner [318, 319], which could not account for the lack of *bre*-driven EGFP expression in anticipated domains.

In summary, I have generated and validated a transgenic zebrafish line that reports pSmad1/5-mediated transcriptional activation. Using genetic approaches, this BMP reporter line can be used to define ligand, receptor, and Smad requirements within individual BMP signaling domains, as we demonstrated using *smad1* morpholinos. Furthermore, these fish can be used to screen for small molecule modulators of BMP signaling, as I demonstrated using dorsomorphin and DMH1, or to screen for genetic modulators of BMP signaling. Besides the obvious advantages of screening for BMP inhibitors in an intact animal model, the *Tg(bre:egfp)* line affords the possibility of uncovering novel drugs with particular BMP ligand or BMP receptor specificity – based on effects within select expression domains – in a single, high content assay. These drugs could prove useful in targeting specific disorders of BMP signaling.

5.0 SUMMARY AND FUTURE DIRECTIONS

The work presented in this thesis lends considerable insight into how Alk1 functions in normal arterial development and why pathway dysregulation causes AVMs in cases of HHT. Previous work in the lab had shown that Alk1 was critical in prevention of AVMs, *alk1* was dependent on flow, and loss of flow phenocopied *alk1* mutants in endothelial cell number increase and dysregulation of target genes [181, 182]. Here, I expanded upon these findings and the current knowledge in the field in several meaningful ways: I identified Bmp10 as the in vivo ligand for Alk1 in zebrafish vascular development; I showed that the requirement for flow in Alk1 signaling stems from circulation of cardiac-derived Bmp10; and I defined detection of pSmad1/5/9 by immunofluorescence as a readout for Alk1 activity in vivo. Altogether, I constructed a novel blood flow-responsive signaling pathway, involving Bmp10, Alk1, and pSmads1/5/9, and demonstrated its involvement in the regulation of flow-responsive genes, arterial quiescence, and prevention of deleterious AVMs (Figure 34). Furthermore, I have generated and described a zebrafish pSmad1/5/9-responsive transgenic reporter, *Tg(bre:egfp)*. Examination of *Tg(bre:egfp)* has spawned interesting questions as to the role of pSmads1/5/9 downstream of Alk1 in the endothelium. Moreover, this transgenic line provides the scientific community a novel means to study dynamic BMP signaling in vivo, identify inhibitors/activators of BMP signaling cascades, and describe previously unidentified roles for BMP signaling during development and pathogenesis.

The work in this thesis significantly enhances our understanding of Alk1 signaling but also provides many avenues for future research. The mechanisms that initiate and maintain *bmp10* and *alk1* expression in the heart and endothelium, respectively, remain to be determined. What triggers Bmp10 release into circulation and how do alternatively processed forms affect Alk1 activity? What governs the requirement for Bmp9 versus Bmp10 in different vascular beds and what does this mean for HHT? In addition, although I have demonstrated pSmads1/5/9 to be activated downstream of Alk1, whether this signal is necessary and sufficient for vascular development and AVM prevention requires further examination.

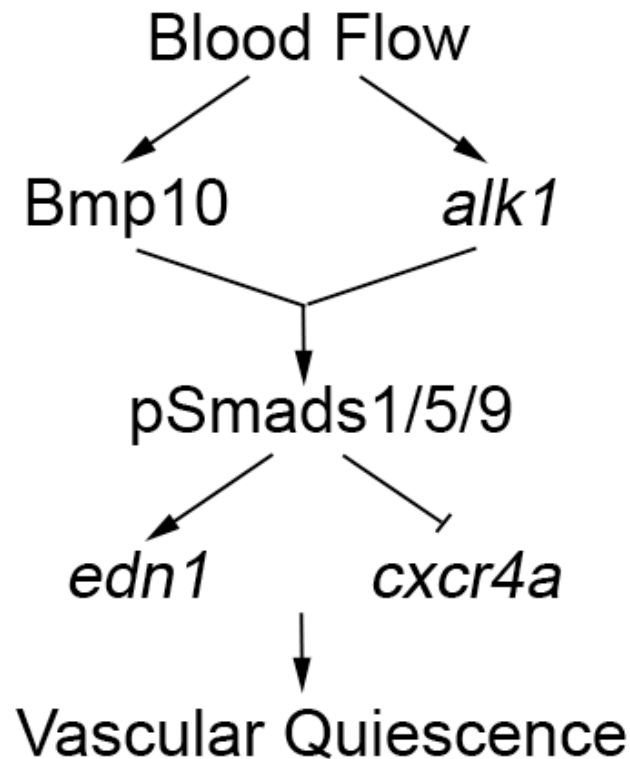


Figure 34: Proposed pathway for Bmp10 and Alk1.

Blood flow is necessary for *alk1* expression within the endothelium and also for carrying endocardial-derived Bmp10 to the Alk1 receptor. Bmp10 and Alk1 are both necessary for activating Smads1/5/9 and for the upregulation

of vasoconstrictive *edn1* and downregulation of the pro-migratory chemokine receptor *cxcr4a*. Altogether this pathway functions to promote vascular quiescence upon the onset of blood flow.

5.1 BMP10 COORDINATES WITH ALK1 TO MEDIATE VASCULAR QUIESCENCE

This work is the first to demonstrate that Bmp10 is the only physiologically relevant ligand for Alk1 during zebrafish embryonic development. *bmp10* knockdown phenocopies *alk1* mutants in AVM formation, endothelial cell number, and pSmad1/5/9 loss of expression. Conversely, *bmp9* knockdown had no effect on *alk1*-positive vessels suggesting that Bmp9 is not required for Alk1 signaling during early zebrafish embryonic development. In support of my data, Bmp9 is not detectable in mouse plasma until E12.5 [320] while *Alk1*^{-/-} embryos die by E10.5. This may suggest that similar to in zebrafish, Bmp10 may be the only necessary in vivo ligand for Alk1 during early mouse development. I do not discount a role for Bmp9 in Alk1 signaling entirely. Indeed, many have shown Bmp9 capable of inducing Alk1. Similarly, I found rhBMP9 could restore Alk1 activity in the absence of flow, similar to rhBMP10, demonstrating that indeed Bmp9 is clearly a necessary in vivo ligand for Alk1, which may function, in different spatiotemporal milieus.

I show that the source of Bmp10 during embryogenesis is the heart. Expression within the heart is not unique to *bmp10* as *Bmp2* and *Bmp4* have both been described as present within this domain. *Bmp2* and *Bmp4* both show reduced atrial expression in mouse *cobblestone* mutants, which have defective cilia, implicating mechanical force in their induction [321]. In contrast, although first detectable within the heart at 24 hpf, upon onset of circulation, neither *bmp10* nor its paralog, *bmp10-like*, are dependent on flow in either expression level or

localization to the heart. The expression domains of *bmp10* and *bmp10-like* are fascinating in that they mimic expression of *Tg(bre:egfp)* in which we detect endocardial expression at 1 day (similar to *bmp10*) and myocardial expression at 2 days (similar to *bmp10-like*). Whether this similarity in *Tg(bre:egfp)* expression indicates an involvement of alternative BMPs, or Bmp10/Bmp10-like themselves, in activation and maintenance of *bmp10* and *bmp10-like* expression levels, through pSmads1/5/9, remains to be seen.

Although not required for expression, heart contraction may stimulate release of Bmp10 ligand into the bloodstream. In mice and humans, other sources for Bmp9 and Bmp10 are the liver and lungs, respectively [320, 322]. It will be interesting to see how Bmp9 and Bmp10 protein enter circulation from their respective sources of production. Additional work will also need to be done to understand how Bmp10-like enters circulation from the myocardium and whether localization differences in *bmp10* and *bmp10-like* imply functional differences between the two proteins outside of vascular development.

Once within circulation, do Bmp10/Bmp10-like circulate in an active or inactive form? In newborn mice, 60% of Bmp9 circulates in an active cleaved form while 40% circulates in an inactive uncleaved form [320]. Inactive circulating ligand could serve several purposes. First, uncleaved peptide may bestow structural stability, allowing ligand to circulate longer under harsh flow conditions. Alternatively, the prodomain may confer an additional level of regulation, becoming released only in areas that possess the appropriate proprotein convertases needed for processing [152]. Circulation of Bmp9/Bmp10 attached to their respective prodomains may also underscore a requirement for Type III receptor, endoglin, in ligand processing which I will describe below.

In certain contexts, the prodomain can provide necessary contacts between ligand and ECM [150]. In this regard, endoglin may serve as a necessary scaffold for binding the prodomains of the “inactive” circulating ligand. Although Bmp9 and Bmp10 may function redundantly in certain spatiotemporal milieus, it is interesting to note that the prodomain-bound form of Bmp9 can still activate Alk1 because of competitive displacement by Type II receptor [150], while Bmp10 requires prodomain release for full activity. Necessity for Endoglin may therefore stem from its ability to remove the prodomain of Bmp10 within vascular beds exposed to high levels of inactive Bmp10. If this is the case, then vascular beds exposed to Bmp9 would be less reliant on Endoglin expression. In humans, BMP10 is expressed exclusively in the right atrium feeding pulmonary circulation [322]. Therefore, the lung vasculature may be more dependent on BMP10 and thus more dependent on Endoglin. Indeed, the pulmonary vasculature is most affected in HHT1 patients, who harbor mutations in Endoglin [137].

5.2 ALK1 INITIATION AND MAINTENANCE

Recent results in the lab suggest that *alk1* may in fact be a target of its own activity with diminished *alk1* in *alk1* mutants and *bmp10* morphants (E. Rochon, J. Donovan). Furthermore, expression of *alk1* is dynamic, with temporary cessation of flow triggering transient drops in *alk1* expression (M. Schubert, J. Donovan). Coupled with my findings that Bmp10/Alk1 provides a link between flow and flow-responsive genes, these data suggest that persistent Bmp10/Alk1 is required for *alk1* maintenance in response to flow. It remains to be determined however, what first initiates *alk1* expression. We have shown that *alk1* is unchanged with knockdown of flow-responsive transcription factor, *klf2a*, however we cannot rule out the possibility that there is functional compensation by zebrafish *klf2b*, an alternative Klf transcription factor, or another laminar shear-responsive pathway. In support of our findings

however, in cultured immortalized mouse endothelial cells, *Alk1* expression is not responsive to shear stress [323]. It is plausible that *alk1* expression may be induced by an oscillatory shear program and then rely on Bmp10/Alk1 signaling for maintenance in the face of laminar shear. Recently, pSmads1/5/9 were shown to be induced in endothelial cells in vivo and in vitro in response to oscillatory shear stress [324], suggesting perhaps, that their activity may preface *alk1* expression, but then become sustained by Alk1 in response to laminar shear.

We can also not rule out potential dependency on another Type I receptor for *alk1* expression. In human aortic ECs (HAECs), *ALK1* expression is stimulated by high density lipoprotein (HDL) induced ALK2/BMPRII/SMAD1 signaling [325], and in BAECs, *ALK1* is regulated by both BMP2 and BMP4, suggesting roles for alternative Type I receptors in *ALK1* induction [326]. BMP2 and BMP4 have also been shown to be induced in endothelial cells in response to oscillatory shear stress [327] and *bmp4* is expressed in the zebrafish heart prior to 24 hpf [328]. All of this evidence suggests the possibility of another program in which an alternative BMP/receptor complex primes the endothelium for laminar shear by initiating *Alk1* expression. We have not examined *alk1*-positive arteries for expression of other Type I receptors or pSmad2/3 activity. However, quantification of my pSmad1/5/9 data suggests some residual expression, even in *alk1* mutants, suggesting that indeed, another receptor cannot be discounted.

5.3 THE ROLE OF SMADS IN ALK1 SIGNALING

In this thesis, I demonstrate that pSmad1/5/9 is present in *alk1*-positive arteries and is dependent on *bmp10*, *alk1*, and Alk1 activity. This finding is significant given the discrepancy in the literature showing Alk1 dependence on pSmads1/5/9 to be variable based on cellular context [for

examples, see [146, 196, 197]]. I also show that proposed Alk1 signal mediator, MAPK (dpERK1/2), expression is independent of *alk1* and therefore, not responsible for AVM development in *alk1* mutants. Although pSmad1/5/9 expression is dependent on *alk1* expression and Alk1 kinase activity in *alk1*-positive arteries, whether this signal is necessary and sufficient and the mode of action for these Smad proteins remains to be uncovered.

pSmads1/5/9 is diminished in *alk1* mutants and *bmp10* morphants. Furthermore, inhibition of Alk1 kinase activity abolishes pSmad1/5/9 detection, but surprisingly, produces AVMs with little penetrance and expressivity. Given these data, a major question remaining to be answered is whether Smad activation is necessary and sufficient downstream of Alk1 in AVM prevention. Decrease in endothelial cell number and morphology in *alk1*-arteries in *smad* morphants would argue against a role for Smad1 and Smad5 however this may be attributed to earlier developmental defects and poor circulation caused by impairment of heart beat. As an alternative means of addressing Smad-involvement we have begun generating fluorescently-tagged *smad1^{CA}*, *smad5^{CA}*, and *smad9^{CA}* constructs driven under the control of an endothelial specific promoter. Constitutively active Smads are generated by substituting aspartic acid residues (DVD) in place of serine (SVS) at the carboxyl-terminus thereby preventing autoinhibition [329]. In theory, if pSmads1/5/9 are sufficient downstream of Alk1, then constitutively active forms of these proteins will rescue endothelial cell number and AVMs in *alk1* mutants. Although we have successfully generated the constitutively active Smad middle entry clones [pME, gateway cloning], fluorescent tags render constructs inactive (fail to ventralize embryos). Future work will need to be aimed at exploring alternative construct options.

As a complementary approach, endothelial driven *smad4^{DN}* should phenocopy *alk1^{-/-}* embryos. There are limitations to this approach however, as pSmad1/5 controlled processing of microRNAs is reportedly Smad4 independent [147] and rSmads2/3 and MAPKs may also function through Smad4 [330]. With this in mind, although it may serve as an important tool in beginning to understand Smads in vascular function, absence of phenotype may simply indicate a non-transcriptional role for pSmads1/5/9 and therefore, not dismiss them as necessary signaling components for Alk1. Alternatively, the formation of AVMs will not fully rule out the possibility for alternative signaling pathways intersecting with Smad4 controlled processes.

Although results clearly indicate Smad1/5/9 is phosphorylated downstream of Alk1, we do not detect pSmad1/5/9 mediated *Tg(bre:egfp)* expression in *alk1*-positive arteries. These data suggest that pSmads1/5/9 may act in non-canonical fashion in this system. pSmads function as heterotrimers with two r-Smads and Smad4 [149]. In dorsoventral patterning however, BMP heterodimers can bind heteromeric Type I complexes allowing for formation of mixed TGF- β /BMP Smad complexes which bind sequences without a traditional BRE [331] and in HPAECs, BMP9 can induce Smad2 phosphorylation through Alk1 [283]. Although we have helped to show that Alk5 is dispensable to Alk1 signaling in mouse and zebrafish [187] we cannot fully discount the actions of another receptor, or the possibility that mixed Smad heterotrimers may form and activate non-canonical sites.

Lack of *Tg(BRE:EGFP)* may also be attributed to pSmads1/5/9 acting independently of transcription and rather controlling gene expression at the post-transcriptional level through the processing of micro-RNAs as they have been shown to do in pulmonary arterial smooth muscle cells (PASMC) [147]. Many microRNAs have been identified to be endothelial-specific, and they comprise a complex network balancing angiogenic states [332]. The embryonic lethality of

mouse *Dicer* mutants has been attributed to angiogenic defects and knockdown of *Dicer* in HUVECs reduces proliferation and cord formation in part through miR-221/222 targeting of c-Kit and other receptors [332-334]. micro-RNAs also serve as a critical hub between hemodynamics and angiogenesis. In zebrafish, mir-126 is activated downstream of Klf2a to promote VEGF signaling [335]. Since I have identified Bmp10/Alk1 as a novel blood flow-responsive signaling pathway, it remains possible that, like Klf2a, it may serve in part to activate pSmads1/5/9 and therefore target mi-RNAs to specific gene sets necessary in controlling vascular quiescence. If true, this would provide many additional questions including which microRNAs are necessary downstream of Alk1, how do they interact with Smads and control processing/target selection, and which genes do they regulate to control endothelial cell behavior? Dissecting the microRNA network may be critical to our understanding of Alk1 and vascular quiescence.

Non-transcriptional roles for BMPs also include stimulation of early cellular responses controlling cell polarity and migration independent of transcriptional pathways. Bmp-2 induces rapid activation of cortical protrusions via actin filament rearrangements in mouse myoblast C2C12 cells by activation of Cdc42 and PI3K [336]. Although in this example BMP2 induces migration, dynamic control of cytoskeletal dynamics independent of transcription by BMPs provides another plausible mechanism of action for Bmp10/Alk1/pSmads1/5/9 outside transcription. The ability to inhibit filopodial extensions would also help to explain why loss of Alk1 can trigger hypersprouting and increased tip cell phenotype at the expense of stalk cells in mouse retinal explants [199]

If instead we are limited by detection and pSmads1/5/9 are indeed activating traditional transcriptional profiles that favor quiescence, what then guides specific Smad-mediated

responses? During hematopoietic regeneration and ESC differentiation, Smad occupancy is guided by a set of master transcription factors, Oct4, Myod1, and PU.1[337, 338]. An intriguing possibility in the case of Alk1 is that Smads could be recruited by master transcription factors that mediate flow response, such as a Klf transcription factor. In this case, the external signal of flow would direct flow responsive transcription factors to open chromatin, thereby exposing Smad binding elements (SBE). Alternatively, Smads could bind directly to these master regulators, which could guide them in specific regulatory pathways.

Regardless of whether they are regulated at the transcriptional or post-transcriptional level, identification of gene sets regulated by Bmp10/Alk1/pSmads1/5/9 and necessary for arterial cell quiescence is of utmost interest. Here, I have shown that two genes, *cxcr4a* and *edn1*, previously known to be responsive to changes in flow, rely on Bmp10/Alk1/pSmads1/5/9 to mediate this flow response. We have shown however that neither mutations in *cxcr4a* or *edn1* can rescue AVMs in *alk1*^{-/-} mutants [181] implying many additional genes remain to be identified. Identification of additional targets downstream of Bmp10/Alk1/pSmads1/5/9 will provide potential targets for HHT treatment and enhance our understanding of Alk1 function in the endothelium.

5.4 ALK1 AND CANCER

The constructed pathway in this thesis may also aid our understanding of Alk1 signaling in pathological settings such as cancer. Tumors above 2-3 mm require the process of angiogenesis to meet their oxygen and nutrient requirement [339] The expression of *ALK1* is diminished in adult arteries, but is upregulated in tumor blood vessels of the prostate, skin, thyroid, kidney,

ovary, lung, pancreas, and kidney [178, 340]. Recent work has shown that application of a chimeric protein (Alk1-Fc), which serves as a sink for Alk1 ligands, can reduce tumor size and vascularization [178]. Co-treatment with Alk1 and VEGF (i.e. bevacizumab) antibodies can also limit angiogenesis and tumor growth in mouse and human cell culture models [340]. An enhanced understanding of Alk1 signaling may lead to more targeted therapies inhibiting Alk1-mediated vascularization of tumors.

5.5 SUMMARY

In summary, endothelial specific type I receptor, Alk1, binds circulating Bmp10 and signals through pSmads1/5/9 to promote vascular quiescence. This novel pathway serves as a critical response to blood flow and is ultimately responsible for preventing arteriovenous malformations. Knowledge gained during the course of my thesis work may ultimately lead to treatments for patients with HHT.

6.0 MATERIALS AND METHODS

6.1 ZEBRAFISH LINES AND MAINTENANCE

Adult zebrafish (*Danio rerio*) were maintained according to standard protocols (Westerfield, 1995). When appropriate, embryo medium was supplemented with 0.003% phenylthiourea (PTU) (Sigma, St. Louis, MO, USA) at 24 hours post-fertilization (hpf) to prevent melanin synthesis. Mutant line *alk1^{y6}* and the *alk1^{y6}* genotyping assay have been described [182]. Transgenic lines *Tg(fli1a:negfp)^{y7}*, *Tg(kdrl:gfp)^{la116}*, *Tg(gata1a:DsRed)^{sd2}*, and *Tg(fli1a.ep:mrfp-CAAX)^{pt505}* have been described [181, 182, 341, 342]. To drive wild type *alk1* in endothelial cells, we generated *ptol-fli1a.ep:alk1-myc* by Gateway cloning (Invitrogen, Carlsbad, CA, USA), recombining pDESTtol2pA2 [343] with p5E *fli1a.ep* [344], pME-*alk1*, and p3E-*MTpA* [343]. To drive ligand- and type II receptor-independent constitutively active *alk1* [182] in endothelial cells, we generated *ptol-fli1a.ebs:alk1^{CA}-mCherry*, recombining pDESTtol2pA2, p5E *fli1a.ebs* (*fli1a* Ets binding site, kind gift from N. Lawson, University of Massachusetts Medical School), pME *alk1^{CA}*, and p3E *mCherry-pA* [343]. These constructs were co-injected with *transposase* mRNA [293] into one-cell embryos to generate *Tg(fli1a.ep:alk1-myc)^{pt516}*, referred to as *Tg(fli1a:alk1-myc)*, and a series of P0 founders for *Tg(fli1a.ebs:alk1^{CA}-mCherry)*, referred to as *Tg(fli1a:alk1^{CA}-mCh)*. The constitutively active *alk1* transgene causes severe vascular defects and is embryonic lethal.

6.2 MORPHOLINO KNOCKDOWN

Splice blocking (SB) and translation blocking (TB) morpholino-modified antisense oligonucleotides (GeneTools, Philomath, OR, USA) were generated. Morpholino sequences are shown below (Table 2).

Target	Sequence (5'-3')
<i>alk1</i>	ATCGGTTTCACTCACCAACACACTC
<i>Bmp9^{SD}</i>	CTCTTTTGTGTA CTACCCTGAAC
<i>Bmp9^{TB}</i>	GGAGCAAATGTCCTACGCGCCACAT
<i>bmp10^{SD}</i>	AGGAAAATATGCAGTTACCTTCATT
<i>bmp10^{TB}</i>	AAAAGTGATTTCTGCTACCAGCCAT
<i>bmp10-like^{TB}</i>	GCAGCAGAGAATCAGCCATGACTGC
<i>smad1</i>	TAACAATTTAGCCACGCTCACCTGG
<i>smad5</i>	ACATGGAGGTCATAGTGCTGGGCTG
<i>smad9</i>	CATCGTGAGACGGGTTGATTTTAAA
<i>standard</i>	CCTCTTACCTCAGTTACAATTTATA
<i>tnnt2a</i>	CATGTTTGCTCTGATCTGACACGCA

Table 2: Morpholino sequences.

Morpholino sequences (5'-3') generated to target their respective targets for the experiments in these studies.

6.3 MORPHOLINO VALIDATION

For TB morpholinos, (*bmp9*, *bmp10*, *bmp10-like*) efficacy and specificity were evaluated by injecting into one-cell embryos CMV-driven EGFP DNA containing morpholino binding sites upstream of the initiator methionine, with or without cognate or non-cognate morpholino, and assessing EGFP expression at ~ 6 hpf.

6.4 IN SITU HYBRIDIZATION

Digoxigenin-labeled riboprobes (Roche, Indianapolis, IN, USA) for *cdh5*, *cxcr4a*, *edn1*, and *myl7* have been described previously [181, 345]. Zebrafish *bmp10* was amplified from cDNA using 5'-ACCACAGCTGAACTCCGACT-3' and 5'-TCCACACTTGGCCACTACCATT-3', and *bmp10-like* using primers 5'-CGCAATGAAGCACCCAGAGTA-3' and 5'-CCGTCCACTGTCTCTCATCA-3'. Both fragments were cloned into pCRII-TOPO (Invitrogen). Whole mount in situ hybridization was performed as described [182]. PCR-amplified fragments of *smad1* and *egfp* were inserted into pCRII-TOPO (Invitrogen) and plasmids used to generate digoxigenin-labeled antisense riboprobes (DIG RNA Labeling Kit, Roche).

6.5 IMMUNOHISTOCHEMISTRY AND IMMUNOSTAINING

Immunohistochemistry was performed using primary antibodies MF20 at 1:200 (sarcomeric myosin, Developmental Studies Hybridoma Bank, Iowa City, IA, USA) or 9E10 at 1:200 (myc, Covance, Princeton, NJ, USA), biotinylated horse anti-mouse IgG at 1:200, ABC reagent (Vector Laboratories, Burlingame, CA), and 3,3'-diaminobenzidine (Sigma, St. Louis, MO, USA). Embryos were photographed using an MVX-10 MacroView microscope and DP71 camera (Olympus America, Center Valley, PA, USA). For sections, embryos were embedded in JB4 (Polysciences, Warrington, PA, USA), sectioned at 8 μ m, and imaged using an Olympus BX51 microscope and DP71 camera. Images were compiled with Adobe Photoshop CS2 version 9.0.2 (Adobe Systems, San Jose, CA, USA).

For immunofluorescence, embryos were fixed in 4% paraformaldehyde in PBS overnight at 4°C, embedded in 4% NuSieve GTG agarose (Lonza, Rockland, ME, USA), and sectioned at 50 µm with a VT1000S vibratome (Leica Microsystems, Buffalo Grove, IL, USA). Rabbit anti-phospho-Smad1/5/9 (also known as anti-phospho-Smad1/5/8; 9511, Cell Signaling Technology, Beverly, MA, USA) was used at 1:100, mouse anti-dpERK1/2 (Cell Signaling Technology, Beverly, MA, USA) at 1:200, goat-anti-mouse Alexa Fluor 568 at 1:200, and goat-anti-rabbit Alexa Fluor 647 at 1:200. Sections were mounted with Vectashield HardSet mounting medium (Vector) and imaged with an Olympus Fluoview 1000 confocal microscope outfitted with a UPFLN 40x oil immersion objective, with scan speed 244 Hz. Two-dimensional projections were generated from Z-series (1 µm steps) using MetaMorph 7.7 (Molecular Devices, Sunnyvale, CA, USA). Images were pseudocolored and colocalization highlighted using MetaMorph's "boost colocalization" function.

6.6 MICROINJECTION OF rhBMP9 AND rhBMP10

Embryos were anesthetized in 160 mg/ml tricaine (Sigma) and embedded in 1% NuSieve GTG agarose in 30% Danieau/PTU. Two nl of phenol red/KCl buffer or Qtracker 655 non-targeted quantum dots (Invitrogen) with or without 10 µM rhBMP10 or rhBMP9 protein (R&D Systems, Minneapolis, MN, USA) were injected into the base of one caudal division of the internal carotid artery (CaDI) at 28 hpf. Embryos were either imaged live for cell counts (see below) or fixed at 36 hpf and assayed by immunofluorescence or in situ hybridization as described above.

6.7 LIVE CONFOCAL IMAGING

For live imaging, embryos were anesthetized in 160 mg/ml tricaine (Sigma) and inserted into 500 μm troughs in 2% SeaKem LE agarose (Lonza)/30%Danieau. Z-series (0.5 - 2 mm steps) were collected using a TCS SP5 multiphoton/confocal microscope (Leica Microsystems, Wetzlar, Germany) outfitted with an APO L 20x/1.00 water immersion objective, non-descanned detectors, and spectral detectors. EGFP was excited with a Mai Tai DeepSee Ti:Sapphire laser (Newport/Spectra Physics, Santa Clara, CA, USA) at 900 nm, whereas dsRed and mCherry were excited with a 561 nm diode. Scanning was performed either with a point scanner (400 Hz) with 4x frame averaging or resonant scanner (8000 Hz) with 16x line averaging. Projections were generated using MetaMorph and endothelial cell numbers counted as described (Corti et al., 2011).

6.8 C2C12 TRANSFECTION AND LUCIFERASE ASSAYS

On the day prior to transfection, C2C12 cells were seeded at 4×10^4 cells/well in 24-well plates. Cells were washed once with Optimum I (Invitrogen) and incubated in Optimum I for 2 hr. All wells were transfected with Lipofectamine (2 μl /well; Invitrogen) in complex with BRE-luciferase (400 ng/well) and pRL-TK (40 ng/well). In plasmid test wells, 400 ng/well of either pcDNA3-hALK1; pcDNA3-hALK1(R411Q), a kinase-dead mutant; pcDNA3-hALK3-HA, or pCS2-zALK1 were also added. After 4 hours, lipoplexes were removed and DMEM containing 10% FBS and antibiotic-antimycotic solution (Invitrogen) added for 24 hr. Cells were washed twice with serum-free DMEM+antibiotic and incubated for 21 hr, then treated for 21 hr with 0.1-3000 pg/ml rhBMP9 or rhBMP10 (R&D Systems, Abingdon, UK). Cells were then lysed and

assayed for Firefly and *Renilla* luciferase activities using the Dual-Glo® Luciferase Assay kit (Promega, Southampton, UK) according to the manufacturer's instructions. Firefly luciferase activities were normalized to the *Renilla* control. Data were normalized as percentage responses using GraphPad Prism (San Diego, CA, USA) and EC₅₀ values calculated. Plasmids were obtained as follows: BRE-luciferase, P. ten Dijke (LUMC, Leiden, Netherlands); pcDNA3-hALK1 and pcDNA3-hALK1(R411Q), R. Trembath (King's College London, London, UK); and pcDNA3-hALK3-HA, K. Miyazono (University of Tokyo, Tokyo, Japan).

6.9 GENERATION OF *Tg(bre:egfp)*

Multisite Gateway cloning (Invitrogen) was used to generate a *bre:egfp* construct. The BRE is a synthetic palindromic sequence derived from fusing distinct regions of the mouse *Id1* promoter [285]. The *Bre* was released from *BRE:luc* [285] by NheI digest; ends were filled in using Klenow; and the blunt product was ligated into the SnaBI site in the 5' entry clone, *p5E-basprom*, just upstream of a minimal adenovirus *e1b* promoter and carp *b-actin* start site [292, 344]. This clone was then recombined with *pME-egfp*, *p3E-pA*, and *pdesttol2pA2* from the Tol2 kit [343] via standard Multisite Gateway procedures (Invitrogen). Twenty-five pg of the resulting clone, *ptol2-bre:egfp*, was injected into one-cell stage embryos along with 25 pg *transposase* mRNA to effect transposon-mediated transgenesis [293]. Embryos were sorted for EGFP expression and raised to adulthood. Founders were identified by incrossing followed by outcrossing to *Tg(fli1ep:dsRedEx)^{um13}*, which expresses dsRed specifically in endothelial cells [344, 346]. Thirteen *Tg(bre:egfp)* founders were identified, and two F1 lines (pt509, pt510) were established from two independent founders. The BRE sequence is as follows: 5'-

CTAGCTCAGACCGTTAGACGCCAGGACGGGCTGTCAGGCTGGCGCCGCGGGCGCCAGC
CTGACAGCCCGTCCTGGCGTCTAACGGTCTGAGCTAG-3'

6.10 mRNA SYNTHESIS

pCS2+ constructs containing constitutively active zebrafish *alk1* and *alk5*, or *smad5* [182, 187] were used to synthesize capped sense mRNA using SP6 polymerase (mMessage mMachine, Ambion).

6.11 DRUG EXPOSURES

To inhibit type I receptor-mediated Smad phosphorylation, embryos were dechorionated and exposed to 0.5% DMSO (vehicle control), 10-30 μ M dorsomorphin (BMP type I receptor inhibitor; Calbiochem), 10 μ M DMH1 (BMP type I receptor inhibitor; gift of Dr. Charles Hong, Vanderbilt University), 200 μ M SB-431542 (TGF- β type I receptor inhibitor; Tocris), or 100 μ M LDN-193189 (BMP type I receptor inhibitor; gift of Dr. Charles Hong, Vanderbilt University) beginning at either 10 hpf for *Tg(bre:egfp)* experiments or 23 hpf for antibody/phenocopy experiments. Exposure to 10 μ M dorsomorphin or 5 μ M DMH1 beginning at the one-cell stage resulted in severe dorsalization [313], whereas 100 μ M SB-431542 resulted in cyclopia [187], demonstrating that these drugs work as expected in our hands.

BIBLIOGRAPHY

1. Adams, R.H. and K. Alitalo, *Molecular regulation of angiogenesis and lymphangiogenesis*. Nat Rev Mol Cell Biol, 2007. **8**(6): p. 464-78.
2. Victoria, L.B. and M.P. Conn, *Animal Models of Vascular Development and Endothelial Cell Biology*. Sourcebook of Models for Biomedical Research, 2008: p. 355-358.
3. Pardanaud, L., et al., *Vasculogenesis in the early quail blastodisc as studied with a monoclonal antibody recognizing endothelial cells*. Development, 1987. **100**(2): p. 339-49.
4. Rupp, P.A., A. Czirok, and C.D. Little, *Novel approaches for the study of vascular assembly and morphogenesis in avian embryos*. Trends Cardiovasc Med, 2003. **13**(7): p. 283-8.
5. Ribatti, D., et al., *The chick embryo chorioallantoic membrane as a model for in vivo research on angiogenesis*. Int J Dev Biol, 1996. **40**(6): p. 1189-97.
6. Downing, G.J. and J.F. Battey, Jr., *Technical assessment of the first 20 years of research using mouse embryonic stem cell lines*. Stem Cells, 2004. **22**(7): p. 1168-80.
7. Metzger, D. and P. Chambon, *Site- and time-specific gene targeting in the mouse*. Methods, 2001. **24**(1): p. 71-80.
8. Carmeliet, P., L. Moons, and D. Collen, *Mouse models of angiogenesis, arterial stenosis, atherosclerosis and hemostasis*. Cardiovasc Res, 1998. **39**(1): p. 8-33.
9. deMello, D.E., et al., *Early fetal development of lung vasculature*. Am J Respir Cell Mol Biol, 1997. **16**(5): p. 568-81.
10. Lucitti, J.L., et al., *Vascular remodeling of the mouse yolk sac requires hemodynamic force*. Development, 2007. **134**(18): p. 3317-26.
11. Keller, B.B., et al., *In vivo assessment of embryonic cardiovascular dimensions and function in day-10.5 to -14.5 mouse embryos*. Circ Res, 1996. **79**(2): p. 247-55.
12. Sawamiphak, S., M. Ritter, and A. Acker-Palmer, *Preparation of retinal explant cultures to study ex vivo tip endothelial cell responses*. Nat Protoc, 2010. **5**(10): p. 1659-65.
13. Hak, S., et al., *Intravital microscopy in window chambers: a unique tool to study tumor angiogenesis and delivery of nanoparticles*. Angiogenesis, 2010. **13**(2): p. 113-30.
14. Weinstein, B.M., et al., *Gridlock, a localized heritable vascular patterning defect in the zebrafish*. Nat Med, 1995. **1**(11): p. 1143-7.
15. Bill, B.R., et al., *A primer for morpholino use in zebrafish*. Zebrafish, 2009. **6**(1): p. 69-77.
16. Zu, Y., et al., *TALLEN-mediated precise genome modification by homologous recombination in zebrafish*. Nat Methods, 2013. **10**(4): p. 329-31.
17. Isogai, S., et al., *Angiogenic network formation in the developing vertebrate trunk*. Development, 2003. **130**(21): p. 5281-90.
18. Stainier, D.Y., et al., *Cloche, an early acting zebrafish gene, is required by both the endothelial and hematopoietic lineages*. Development, 1995. **121**(10): p. 3141-50.
19. Isogai, S., M. Horiguchi, and B.M. Weinstein, *The vascular anatomy of the developing zebrafish: an atlas of embryonic and early larval development*. Dev Biol, 2001. **230**(2): p. 278-301.
20. Risau, W. and I. Flamme, *Vasculogenesis*. Annu Rev Cell Dev Biol, 1995. **11**: p. 73-91.
21. Weinstein, B.M., *What guides early embryonic blood vessel formation?* Dev Dyn, 1999. **215**(1): p. 2-11.

22. Dejana, E., A. Taddei, and A.M. Randi, *Foxs and Ets in the transcriptional regulation of endothelial cell differentiation and angiogenesis*. *Biochim Biophys Acta*, 2007. **1775**(2): p. 298-312.
23. Sato, Y., *Role of ETS family transcription factors in vascular development and angiogenesis*. *Cell Struct Funct*, 2001. **26**(1): p. 19-24.
24. Bernat, J.A., et al., *Distant conserved sequences flanking endothelial-specific promoters contain tissue-specific DNase-hypersensitive sites and over-represented motifs*. *Hum Mol Genet*, 2006. **15**(13): p. 2098-105.
25. Ferdous, A., et al., *Nkx2-5 transactivates the Ets-related protein 71 gene and specifies an endothelial/endocardial fate in the developing embryo*. *Proc Natl Acad Sci U S A*, 2009. **106**(3): p. 814-9.
26. Pham, V.N., et al., *Combinatorial function of ETS transcription factors in the developing vasculature*. *Dev Biol*, 2007. **303**(2): p. 772-83.
27. Sumanas, S., et al., *Interplay among Etsrp/ER71, Scl, and Alk8 signaling controls endothelial and myeloid cell formation*. *Blood*, 2008. **111**(9): p. 4500-10.
28. Sumanas, S. and S. Lin, *Ets1-related protein is a key regulator of vasculogenesis in zebrafish*. *PLoS Biol*, 2006. **4**(1): p. e10.
29. Liu, F., et al., *Fli1 acts at the top of the transcriptional network driving blood and endothelial development*. *Curr Biol*, 2008. **18**(16): p. 1234-40.
30. Hollenhorst, P.C., et al., *Genome-wide analyses reveal properties of redundant and specific promoter occupancy within the ETS gene family*. *Genes Dev*, 2007. **21**(15): p. 1882-94.
31. Maroulakou, I.G. and D.B. Bowe, *Expression and function of Ets transcription factors in mammalian development: a regulatory network*. *Oncogene*, 2000. **19**(55): p. 6432-42.
32. Liao, W., et al., *The zebrafish gene cloche acts upstream of a flk-1 homologue to regulate endothelial cell differentiation*. *Development*, 1997. **124**(2): p. 381-9.
33. Nishikawa, S.I., et al., *Progressive lineage analysis by cell sorting and culture identifies FLK1+VE-cadherin+ cells at a diverging point of endothelial and hemopoietic lineages*. *Development*, 1998. **125**(9): p. 1747-57.
34. Cleaver, O. and P.A. Krieg, *VEGF mediates angioblast migration during development of the dorsal aorta in Xenopus*. *Development*, 1998. **125**(19): p. 3905-14.
35. Drake, C.J., et al., *VEGF regulates cell behavior during vasculogenesis*. *Dev Biol*, 2000. **224**(2): p. 178-88.
36. Shalaby, F., et al., *Failure of blood-island formation and vasculogenesis in Flk-1-deficient mice*. *Nature*, 1995. **376**(6535): p. 62-6.
37. Bazzoni, G. and E. Dejana, *Endothelial cell-to-cell junctions: molecular organization and role in vascular homeostasis*. *Physiol Rev*, 2004. **84**(3): p. 869-901.
38. Martin-Belmonte, F., et al., *PTEN-mediated apical segregation of phosphoinositides controls epithelial morphogenesis through Cdc42*. *Cell*, 2007. **128**(2): p. 383-97.
39. Strilic, B., et al., *The molecular basis of vascular lumen formation in the developing mouse aorta*. *Dev Cell*, 2009. **17**(4): p. 505-15.
40. Gerhardt, H., et al., *VEGF guides angiogenic sprouting utilizing endothelial tip cell filopodia*. *J Cell Biol*, 2003. **161**(6): p. 1163-77.
41. Siekmann, A.F. and N.D. Lawson, *Notch signalling limits angiogenic cell behaviour in developing zebrafish arteries*. *Nature*, 2007. **445**(7129): p. 781-4.

42. Jakobsson, L., et al., *Endothelial cells dynamically compete for the tip cell position during angiogenic sprouting*. Nat Cell Biol, 2010. **12**(10): p. 943-53.
43. Tammela, T., et al., *Blocking VEGFR-3 suppresses angiogenic sprouting and vascular network formation*. Nature, 2008. **454**(7204): p. 656-60.
44. Hellstrom, M., et al., *Dll4 signalling through Notch1 regulates formation of tip cells during angiogenesis*. Nature, 2007. **445**(7129): p. 776-80.
45. Nicoli, S., et al., *miR-221 is required for endothelial tip cell behaviors during vascular development*. Dev Cell. **22**(2): p. 418-29.
46. Krueger, J., et al., *Flt1 acts as a negative regulator of tip cell formation and branching morphogenesis in the zebrafish embryo*. Development. **138**(10): p. 2111-20.
47. Zygmunt, T., et al., *Semaphorin-PlexinD1 signaling limits angiogenic potential via the VEGF decoy receptor sFlt1*. Dev Cell. **21**(2): p. 301-14.
48. Adams, R.H., et al., *Roles of ephrinB ligands and EphB receptors in cardiovascular development: demarcation of arterial/venous domains, vascular morphogenesis, and sprouting angiogenesis*. Genes Dev, 1999. **13**(3): p. 295-306.
49. Klagsbrun, M., S. Takashima, and R. Mamluk, *The role of neuropilin in vascular and tumor biology*. Adv Exp Med Biol, 2002. **515**: p. 33-48.
50. Gitler, A.D., M.M. Lu, and J.A. Epstein, *PlexinD1 and semaphorin signaling are required in endothelial cells for cardiovascular development*. Dev Cell, 2004. **7**(1): p. 107-16.
51. Torres-Vazquez, J., et al., *Semaphorin-plexin signaling guides patterning of the developing vasculature*. Dev Cell, 2004. **7**(1): p. 117-23.
52. Bates, D., et al., *Neurovascular congruence results from a shared patterning mechanism that utilizes Semaphorin3A and Neuropilin-1*. Dev Biol, 2003. **255**(1): p. 77-98.
53. Koch, A.W., et al., *Robo4 maintains vessel integrity and inhibits angiogenesis by interacting with UNC5B*. Dev Cell, 2011. **20**(1): p. 33-46.
54. Park, K.W., et al., *Robo4 is a vascular-specific receptor that inhibits endothelial migration*. Dev Biol, 2003. **261**(1): p. 251-67.
55. Adams, R.H. and A. Eichmann, *Axon guidance molecules in vascular patterning*. Cold Spring Harb Perspect Biol, 2010. **2**(5): p. a001875.
56. Huminiecki, L., et al., *Magic roundabout is a new member of the roundabout receptor family that is endothelial specific and expressed at sites of active angiogenesis*. Genomics, 2002. **79**(4): p. 547-52.
57. Jones, C.A., et al., *Robo4 stabilizes the vascular network by inhibiting pathologic angiogenesis and endothelial hyperpermeability*. Nat Med, 2008. **14**(4): p. 448-53.
58. Bedell, V.M., et al., *roundabout4 is essential for angiogenesis in vivo*. Proc Natl Acad Sci U S A, 2005. **102**(18): p. 6373-8.
59. Kamei, M., et al., *Endothelial tubes assemble from intracellular vacuoles in vivo*. Nature, 2006. **442**(7101): p. 453-6.
60. Davis, G.E. and K.J. Bayless, *An integrin and Rho GTPase-dependent pinocytic vacuole mechanism controls capillary lumen formation in collagen and fibrin matrices*. Microcirculation, 2003. **10**(1): p. 27-44.
61. Wang, Y., et al., *Moesin1 and Ve-cadherin are required in endothelial cells during in vivo tubulogenesis*. Development, 2010. **137**(18): p. 3119-28.
62. Beck, L., Jr. and P.A. D'Amore, *Vascular development: cellular and molecular regulation*. FASEB J, 1997. **11**(5): p. 365-73.

63. Dumont, D.J., et al., *Dominant-negative and targeted null mutations in the endothelial receptor tyrosine kinase, tek, reveal a critical role in vasculogenesis of the embryo.* Genes Dev, 1994. **8**(16): p. 1897-909.
64. Leveen, P., et al., *Mice deficient for PDGF B show renal, cardiovascular, and hematological abnormalities.* Genes Dev, 1994. **8**(16): p. 1875-87.
65. Puri, M.C., et al., *The receptor tyrosine kinase TIE is required for integrity and survival of vascular endothelial cells.* EMBO J, 1995. **14**(23): p. 5884-91.
66. Suri, C., et al., *Requisite role of angiopoietin-1, a ligand for the TIE2 receptor, during embryonic angiogenesis.* Cell, 1996. **87**(7): p. 1171-80.
67. Potter, L.R., et al., *Natriuretic peptides: their structures, receptors, physiologic functions and therapeutic applications.* Handb Exp Pharmacol, 2009(191): p. 341-66.
68. Seva Pessoa, B., et al., *Key developments in renin-angiotensin-aldosterone system inhibition.* Nat Rev Nephrol, 2012. **9**(1): p. 26-36.
69. Gaengel, K., et al., *The sphingosine-1-phosphate receptor SIP1 restricts sprouting angiogenesis by regulating the interplay between VE-cadherin and VEGFR2.* Dev Cell. **23**(3): p. 587-99.
70. Hahn, C. and M.A. Schwartz, *Mechanotransduction in vascular physiology and atherogenesis.* Nat Rev Mol Cell Biol, 2009. **10**(1): p. 53-62.
71. Wang, Y., et al., *Aortic arch morphogenesis and flow modeling in the chick embryo.* Ann Biomed Eng, 2009. **37**(6): p. 1069-81.
72. Yashiro, K., H. Shiratori, and H. Hamada, *Haemodynamics determined by a genetic programme govern asymmetric development of the aortic arch.* Nature, 2007. **450**(7167): p. 285-8.
73. Ito, W.D., et al., *Angiogenesis but not collateral growth is associated with ischemia after femoral artery occlusion.* Am J Physiol, 1997. **273**(3 Pt 2): p. H1255-65.
74. Kim, K., et al., *Polycystin 1 is required for the structural integrity of blood vessels.* Proc Natl Acad Sci U S A, 2000. **97**(4): p. 1731-6.
75. Jones, T.J., et al., *Primary cilia regulates the directional migration and barrier integrity of endothelial cells through the modulation of hsp27 dependent actin cytoskeletal organization.* J Cell Physiol, 2012. **227**(1): p. 70-6.
76. Van der Heiden, K., et al., *Endothelial primary cilia in areas of disturbed flow are at the base of atherosclerosis.* Atherosclerosis, 2008. **196**(2): p. 542-50.
77. Van der Heiden, K., et al., *Monocilia on chicken embryonic endocardium in low shear stress areas.* Dev Dyn, 2006. **235**(1): p. 19-28.
78. Iomini, C., et al., *Primary cilia of human endothelial cells disassemble under laminar shear stress.* J Cell Biol, 2004. **164**(6): p. 811-7.
79. Fu, B.M. and J.M. Tarbell, *Mechano-sensing and transduction by endothelial surface glycocalyx: composition, structure, and function.* Wiley Interdiscip Rev Syst Biol Med, 2013. **5**(3): p. 381-90.
80. Pohl, U., et al., *EDRF-mediated shear-induced dilation opposes myogenic vasoconstriction in small rabbit arteries.* Am J Physiol, 1991. **261**(6 Pt 2): p. H2016-23.
81. Tzima, E., et al., *A mechanosensory complex that mediates the endothelial cell response to fluid shear stress.* Nature, 2005. **437**(7057): p. 426-31.
82. Tzima, E., et al., *Activation of Rac1 by shear stress in endothelial cells mediates both cytoskeletal reorganization and effects on gene expression.* EMBO J, 2002. **21**(24): p. 6791-800.

83. Dekker, R.J., et al., *Prolonged fluid shear stress induces a distinct set of endothelial cell genes, most specifically lung Kruppel-like factor (KLF2)*. Blood, 2002. **100**(5): p. 1689-98.
84. Parmar, K.M., et al., *Integration of flow-dependent endothelial phenotypes by Kruppel-like factor 2*. J Clin Invest, 2006. **116**(1): p. 49-58.
85. Dekker, R.J., et al., *Endothelial KLF2 links local arterial shear stress levels to the expression of vascular tone-regulating genes*. Am J Pathol, 2005. **167**(2): p. 609-18.
86. Sharefkin, J.B., et al., *Fluid flow decreases preproendothelin mRNA levels and suppresses endothelin-1 peptide release in cultured human endothelial cells*. J Vasc Surg, 1991. **14**(1): p. 1-9.
87. Nayak, L., Z. Lin, and M.K. Jain, "Go with the flow": how Kruppel-like factor 2 regulates the vasoprotective effects of shear stress. Antioxid Redox Signal, 2011. **15**(5): p. 1449-61.
88. Lee, J.S., et al., *Klf2 is an essential regulator of vascular hemodynamic forces in vivo*. Dev Cell, 2006. **11**(6): p. 845-57.
89. McCormick, S.M., et al., *DNA microarray reveals changes in gene expression of shear stressed human umbilical vein endothelial cells*. Proc Natl Acad Sci U S A, 2001. **98**(16): p. 8955-60.
90. Hamik, A., et al., *Kruppel-like factor 4 regulates endothelial inflammation*. J Biol Chem, 2007. **282**(18): p. 13769-79.
91. Gimbrone, M.A., Jr. and G. Garcia-Cardena, *Vascular endothelium, hemodynamics, and the pathobiology of atherosclerosis*. Cardiovasc Pathol, 2013. **22**(1): p. 9-15.
92. Passerini, A.G., et al., *Coexisting proinflammatory and antioxidative endothelial transcription profiles in a disturbed flow region of the adult porcine aorta*. Proc Natl Acad Sci U S A, 2004. **101**(8): p. 2482-7.
93. Hajra, L., et al., *The NF-kappa B signal transduction pathway in aortic endothelial cells is primed for activation in regions predisposed to atherosclerotic lesion formation*. Proc Natl Acad Sci U S A, 2000. **97**(16): p. 9052-7.
94. Boon, R.A., et al., *KLF2-induced actin shear fibers control both alignment to flow and JNK signaling in vascular endothelium*. Blood. **115**(12): p. 2533-42.
95. Fledderus, J.O., et al., *Prolonged shear stress and KLF2 suppress constitutive proinflammatory transcription through inhibition of ATF2*. Blood, 2007. **109**(10): p. 4249-57.
96. SenBanerjee, S., et al., *KLF2 Is a novel transcriptional regulator of endothelial proinflammatory activation*. J Exp Med, 2004. **199**(10): p. 1305-15.
97. Partridge, J., et al., *Laminar shear stress acts as a switch to regulate divergent functions of NF-kappaB in endothelial cells*. FASEB J, 2007. **21**(13): p. 3553-61.
98. Greene, A.K., *Vascular anomalies: current overview of the field*. Clin Plast Surg, 2011. **38**(1): p. 1-5.
99. Kitajewski, J., *Arteriovenous malformations in five dimensions*. Sci Transl Med. **4**(117): p. 117fs3.
100. Garzon, M.C., et al., *Vascular malformations: Part I*. J Am Acad Dermatol, 2007. **56**(3): p. 353-70; quiz 371-4.
101. Kohout, M.P., et al., *Arteriovenous malformations of the head and neck: natural history and management*. Plast Reconstr Surg, 1998. **102**(3): p. 643-54.

102. Pujari, M., et al., *Arteriovenous Malformation of Tongue: A Case Report and Review of Literature*. Journal of Indian Academy of Oral Medicine and Radiology, 2011. **23**(2): p. 139-142.
103. Lawson, N.D., et al., *Notch signaling is required for arterial-venous differentiation during embryonic vascular development*. Development, 2001. **128**(19): p. 3675-83.
104. Lawson, N.D., A.M. Vogel, and B.M. Weinstein, *sonic hedgehog and vascular endothelial growth factor act upstream of the Notch pathway during arterial endothelial differentiation*. Dev Cell, 2002. **3**(1): p. 127-36.
105. Villa, N., et al., *Vascular expression of Notch pathway receptors and ligands is restricted to arterial vessels*. Mech Dev, 2001. **108**(1-2): p. 161-4.
106. Lindner, V., et al., *Members of the Jagged/Notch gene families are expressed in injured arteries and regulate cell phenotype via alterations in cell matrix and cell-cell interaction*. Am J Pathol, 2001. **159**(3): p. 875-83.
107. Reaume, A.G., et al., *Expression analysis of a Notch homologue in the mouse embryo*. Dev Biol, 1992. **154**(2): p. 377-87.
108. Shutter, J.R., et al., *Dll4, a novel Notch ligand expressed in arterial endothelium*. Genes Dev, 2000. **14**(11): p. 1313-8.
109. Duarte, A., et al., *Dosage-sensitive requirement for mouse Dll4 in artery development*. Genes Dev, 2004. **18**(20): p. 2474-8.
110. Fischer, A., et al., *The Notch target genes Hey1 and Hey2 are required for embryonic vascular development*. Genes Dev, 2004. **18**(8): p. 901-11.
111. Kokubo, H., et al., *Targeted disruption of hesr2 results in atrioventricular valve anomalies that lead to heart dysfunction*. Circ Res, 2004. **95**(5): p. 540-7.
112. Stainier, D.Y., et al., *Mutations affecting the formation and function of the cardiovascular system in the zebrafish embryo*. Development, 1996. **123**: p. 285-92.
113. Zhong, T.P., et al., *Gridlock signalling pathway fashions the first embryonic artery*. Nature, 2001. **414**(6860): p. 216-20.
114. Pasquale, E.B., *Eph-ephrin bidirectional signaling in physiology and disease*. Cell, 2008. **133**(1): p. 38-52.
115. Pitulescu, M.E. and R.H. Adams, *Eph/ephrin molecules--a hub for signaling and endocytosis*. Genes Dev, 2010. **24**(22): p. 2480-92.
116. Gerety, S.S., et al., *Symmetrical mutant phenotypes of the receptor EphB4 and its specific transmembrane ligand ephrin-B2 in cardiovascular development*. Mol Cell, 1999. **4**(3): p. 403-14.
117. Wang, H.U., Z.F. Chen, and D.J. Anderson, *Molecular distinction and angiogenic interaction between embryonic arteries and veins revealed by ephrin-B2 and its receptor Eph-B4*. Cell, 1998. **93**(5): p. 741-53.
118. You, L.R., et al., *Suppression of Notch signalling by the COUP-TFII transcription factor regulates vein identity*. Nature, 2005. **435**(7038): p. 98-104.
119. Huppert, S.S., et al., *Embryonic lethality in mice homozygous for a processing-deficient allele of Notch1*. Nature, 2000. **405**(6789): p. 966-70.
120. Kawasaki, T., et al., *A requirement for neuropilin-1 in embryonic vessel formation*. Development, 1999. **126**(21): p. 4895-902.
121. Pereira, F.A., et al., *The orphan nuclear receptor COUP-TFII is required for angiogenesis and heart development*. Genes Dev, 1999. **13**(8): p. 1037-49.

122. Itoh, M., et al., *Mind bomb is a ubiquitin ligase that is essential for efficient activation of Notch signaling by Delta*. Dev Cell, 2003. **4**(1): p. 67-82.
123. Krebs, L.T., et al., *Haploinsufficient lethality and formation of arteriovenous malformations in Notch pathway mutants*. Genes Dev, 2004. **18**(20): p. 2469-73.
124. Carlson, T.R., et al., *Endothelial expression of constitutively active Notch4 elicits reversible arteriovenous malformations in adult mice*. Proc Natl Acad Sci U S A, 2005. **102**(28): p. 9884-9.
125. Murphy, P.A., et al., *Notch4 normalization reduces blood vessel size in arteriovenous malformations*. Sci Transl Med. **4**(117): p. 117ra8.
126. Cermenati, S., et al., *Sox18 and Sox7 play redundant roles in vascular development*. Blood, 2008. **111**(5): p. 2657-66.
127. Pendeville, H., et al., *Zebrafish Sox7 and Sox18 function together to control arterial-venous identity*. Dev Biol, 2008. **317**(2): p. 405-16.
128. Herpers, R., et al., *Redundant roles for sox7 and sox18 in arteriovenous specification in zebrafish*. Circ Res, 2008. **102**(1): p. 12-5.
129. James, K., et al., *Sox18 mutations in the ragged mouse alleles ragged-like and opossum*. Genesis, 2003. **36**(1): p. 1-6.
130. Pennisi, D., et al., *Mutations in Sox18 underlie cardiovascular and hair follicle defects in ragged mice*. Nat Genet, 2000. **24**(4): p. 434-7.
131. Downes, M., et al., *Vascular defects in a mouse model of hypotrichosis-lymphedema-telangiectasia syndrome indicate a role for SOX18 in blood vessel maturation*. Hum Mol Genet, 2009. **18**(15): p. 2839-50.
132. Irrthum, A., et al., *Mutations in the transcription factor gene SOX18 underlie recessive and dominant forms of hypotrichosis-lymphedema-telangiectasia*. Am J Hum Genet, 2003. **72**(6): p. 1470-8.
133. Eerola, I., et al., *Capillary malformation-arteriovenous malformation, a new clinical and genetic disorder caused by RASAI mutations*. Am J Hum Genet, 2003. **73**(6): p. 1240-9.
134. Savitsky, K., et al., *A single ataxia telangiectasia gene with a product similar to PI-3 kinase*. Science, 1995. **268**(5218): p. 1749-53.
135. Cabana, M.D., et al., *Consequences of the delayed diagnosis of ataxia-telangiectasia*. Pediatrics, 1998. **102**(1 Pt 1): p. 98-100.
136. McDonald, J., P. Bayrak-Toydemir, and R.E. Pyeritz, *Hereditary hemorrhagic telangiectasia: an overview of diagnosis, management, and pathogenesis*. Genet Med, 2011. **13**(7): p. 607-16.
137. Faughnan, M.E., J.T. Granton, and L.H. Young, *The pulmonary vascular complications of hereditary haemorrhagic telangiectasia*. Eur Respir J, 2009. **33**(5): p. 1186-94.
138. Cottin, V., et al., *Pulmonary vascular manifestations of hereditary hemorrhagic telangiectasia (rendu-osler disease)*. Respiration, 2007. **74**(4): p. 361-78.
139. Kjeldsen, A.D., et al., *Prevalence of pulmonary arteriovenous malformations (PAVMs) and occurrence of neurological symptoms in patients with hereditary haemorrhagic telangiectasia (HHT)*. J Intern Med, 2000. **248**(3): p. 255-62.
140. Shovlin, C.L. and M. Letarte, *Hereditary haemorrhagic telangiectasia and pulmonary arteriovenous malformations: issues in clinical management and review of pathogenic mechanisms*. Thorax, 1999. **54**(8): p. 714-29.
141. Ross, J. and R. Al-Shahi Salman, *Interventions for treating brain arteriovenous malformations in adults*. Cochrane Database Syst Rev, 2010(7): p. CD003436.

142. Faughnan, M.E., et al., *International guidelines for the diagnosis and management of hereditary haemorrhagic telangiectasia*. J Med Genet. **48**(2): p. 73-87.
143. Marchuk, D.A., et al., *Report on the workshop on Hereditary Hemorrhagic Telangiectasia, July 10-11, 1997*. Am J Med Genet, 1998. **76**(3): p. 269-73.
144. Massague, J., *TGF-beta signal transduction*. Annu Rev Biochem, 1998. **67**: p. 753-91.
145. Massague, J., J. Seoane, and D. Wotton, *Smad transcription factors*. Genes Dev, 2005. **19**(23): p. 2783-810.
146. David, L., et al., *Activin receptor-like kinase 1 inhibits human microvascular endothelial cell migration: potential roles for JNK and ERK*. J Cell Physiol, 2007. **213**(2): p. 484-9.
147. Davis, B.N., et al., *SMAD proteins control DROSHA-mediated microRNA maturation*. Nature, 2008. **454**(7200): p. 56-61.
148. Song, B., K.D. Estrada, and K.M. Lyons, *Smad signaling in skeletal development and regeneration*. Cytokine Growth Factor Rev, 2009. **20**(5-6): p. 379-88.
149. David, L., J.J. Feige, and S. Bailly, *Emerging role of bone morphogenetic proteins in angiogenesis*. Cytokine Growth Factor Rev, 2009. **20**(3): p. 203-12.
150. Sengle, G., et al., *Prodomains of transforming growth factor beta (TGFbeta) superfamily members specify different functions: extracellular matrix interactions and growth factor bioavailability*. J Biol Chem, 2011. **286**(7): p. 5087-99.
151. Sengle, G., et al., *A new model for growth factor activation: type II receptors compete with the prodomain for BMP-7*. J Mol Biol, 2008. **381**(4): p. 1025-39.
152. Cui, Y., et al., *The activity and signaling range of mature BMP-4 is regulated by sequential cleavage at two sites within the prodomain of the precursor*. Genes Dev, 2001. **15**(21): p. 2797-802.
153. Sengle, G., et al., *Targeting of bone morphogenetic protein growth factor complexes to fibrillin*. J Biol Chem, 2008. **283**(20): p. 13874-88.
154. Bobik, A., *Transforming growth factor-betas and vascular disorders*. Arterioscler Thromb Vasc Biol, 2006. **26**(8): p. 1712-20.
155. Groppe, J., et al., *Cooperative assembly of TGF-beta superfamily signaling complexes is mediated by two disparate mechanisms and distinct modes of receptor binding*. Mol Cell, 2008. **29**(2): p. 157-68.
156. Massague, J., *TGFbeta in Cancer*. Cell, 2008. **134**(2): p. 215-30.
157. Kretzschmar, M., et al., *The TGF-beta family mediator Smad1 is phosphorylated directly and activated functionally by the BMP receptor kinase*. Genes Dev, 1997. **11**(8): p. 984-95.
158. Kusanagi, K., et al., *Characterization of a bone morphogenetic protein-responsive Smad-binding element*. Mol Biol Cell, 2000. **11**(2): p. 555-65.
159. Blitz, I.L. and K.W. Cho, *Finding partners: how BMPs select their targets*. Dev Dyn, 2009. **238**(6): p. 1321-31.
160. Gao, S., J. Steffen, and A. Laughon, *Dpp-responsive silencers are bound by a trimeric Mad-Medea complex*. J Biol Chem, 2005. **280**(43): p. 36158-64.
161. Nakahiro, T., et al., *Identification of BMP-responsive elements in the mouse Id2 gene*. Biochem Biophys Res Commun, 2010. **399**(3): p. 416-21.
162. Attisano, L. and J.L. Wrana, *Smads as transcriptional co-modulators*. Curr Opin Cell Biol, 2000. **12**(2): p. 235-43.
163. Derynck, R., Y. Zhang, and X.H. Feng, *Smads: transcriptional activators of TGF-beta responses*. Cell, 1998. **95**(6): p. 737-40.

164. Hatada, I., et al., *Astrocyte-specific genes are generally demethylated in neural precursor cells prior to astrocytic differentiation*. PLoS One, 2008. **3**(9): p. e3189.
165. Shi, X., et al., *Smad1 interacts with homeobox DNA-binding proteins in bone morphogenetic protein signaling*. J Biol Chem, 1999. **274**(19): p. 13711-7.
166. Davis, B.N., et al., *Smad proteins bind a conserved RNA sequence to promote microRNA maturation by Drosha*. Mol Cell, 2010. **39**(3): p. 373-84.
167. McAllister, K.A., et al., *Endoglin, a TGF-beta binding protein of endothelial cells, is the gene for hereditary haemorrhagic telangiectasia type 1*. Nat Genet, 1994. **8**(4): p. 345-51.
168. Cheifetz, S., et al., *Endoglin is a component of the transforming growth factor-beta receptor system in human endothelial cells*. J Biol Chem, 1992. **267**(27): p. 19027-30.
169. Johnson, D.W., et al., *Mutations in the activin receptor-like kinase 1 gene in hereditary haemorrhagic telangiectasia type 2*. Nat Genet, 1996. **13**(2): p. 189-95.
170. Fujiwara, M., et al., *Implications of mutations of activin receptor-like kinase 1 gene (ALK1) in addition to bone morphogenetic protein receptor II gene (BMP2) in children with pulmonary arterial hypertension*. Circ J, 2008. **72**(1): p. 127-33.
171. Trembath, R.C., *Mutations in the TGF-beta type 1 receptor, ALK1, in combined primary pulmonary hypertension and hereditary haemorrhagic telangiectasia, implies pathway specificity*. J Heart Lung Transplant, 2001. **20**(2): p. 175.
172. Gallione, C.J., et al., *SMAD4 mutations found in unselected HHT patients*. J Med Genet, 2006. **43**(10): p. 793-7.
173. Bayrak-Toydemir, P., et al., *Genotype-phenotype correlation in hereditary hemorrhagic telangiectasia: mutations and manifestations*. Am J Med Genet A, 2006. **140**(5): p. 463-70.
174. Kjeldsen, A.D., et al., *Clinical symptoms according to genotype amongst patients with hereditary haemorrhagic telangiectasia*. J Intern Med, 2005. **258**(4): p. 349-55.
175. Letteboer, T.G., et al., *Genotype-phenotype relationship in hereditary haemorrhagic telangiectasia*. J Med Genet, 2006. **43**(4): p. 371-7.
176. Cole, S.G., et al., *A new locus for hereditary haemorrhagic telangiectasia (HHT3) maps to chromosome 5*. J Med Genet, 2005. **42**(7): p. 577-82.
177. Bayrak-Toydemir, P., et al., *A fourth locus for hereditary hemorrhagic telangiectasia maps to chromosome 7*. Am J Med Genet A, 2006. **140**(20): p. 2155-62.
178. Cunha, S.I., et al., *Genetic and pharmacological targeting of activin receptor-like kinase 1 impairs tumor growth and angiogenesis*. J Exp Med, 2003. **207**(1): p. 85-100.
179. Park, S.O., et al., *Real-time imaging of de novo arteriovenous malformation in a mouse model of hereditary hemorrhagic telangiectasia*. J Clin Invest, 2009. **119**(11): p. 3487-96.
180. Goumans, M.J., et al., *Balancing the activation state of the endothelium via two distinct TGF-beta type I receptors*. EMBO J, 2002. **21**(7): p. 1743-53.
181. Corti, P., et al., *Interaction between alk1 and blood flow in the development of arteriovenous malformations*. Development, 2010. **138**(8): p. 1573-82.
182. Roman, B.L., et al., *Disruption of acvrl1 increases endothelial cell number in zebrafish cranial vessels*. Development, 2002. **129**(12): p. 3009-19.
183. Oh, S.P., et al., *Activin receptor-like kinase 1 modulates transforming growth factor-beta 1 signaling in the regulation of angiogenesis*. Proc Natl Acad Sci U S A, 2000. **97**(6): p. 2626-31.

184. Bassing, C.H., et al., *A transforming growth factor beta type I receptor that signals to activate gene expression*. Science, 1994. **263**(5143): p. 87-9.
185. Dickson, M.C., et al., *Defective haematopoiesis and vasculogenesis in transforming growth factor-beta 1 knock out mice*. Development, 1995. **121**(6): p. 1845-54.
186. Oshima, M., H. Oshima, and M.M. Taketo, *TGF-beta receptor type II deficiency results in defects of yolk sac hematopoiesis and vasculogenesis*. Dev Biol, 1996. **179**(1): p. 297-302.
187. Park, S.O., et al., *ALK5- and TGFBR2-independent role of ALK1 in the pathogenesis of hereditary hemorrhagic telangiectasia type 2*. Blood, 2008. **111**(2): p. 633-42.
188. Mitchell, D., et al., *ALK1-Fc inhibits multiple mediators of angiogenesis and suppresses tumor growth*. Mol Cancer Ther, 2010. **9**(2): p. 379-88.
189. Brown, M.A., et al., *Crystal structure of BMP-9 and functional interactions with pro-region and receptors*. J Biol Chem, 2005. **280**(26): p. 25111-8.
190. Lux, A., L. Attisano, and D.A. Marchuk, *Assignment of transforming growth factor beta1 and beta3 and a third new ligand to the type I receptor ALK-1*. J Biol Chem, 1999. **274**(15): p. 9984-92.
191. Keller, S., et al., *Molecular recognition of BMP-2 and BMP receptor IA*. Nat Struct Mol Biol, 2004. **11**(5): p. 481-8.
192. Lin, S.J., et al., *The structural basis of TGF-beta, bone morphogenetic protein, and activin ligand binding*. Reproduction, 2006. **132**(2): p. 179-90.
193. Townson, S.A., et al., *Specificity and structure of a high affinity activin receptor-like kinase 1 (ALK1) signaling complex*. J Biol Chem, 2012. **287**(33): p. 27313-25.
194. David, L., et al., *Identification of BMP9 and BMP10 as functional activators of the orphan activin receptor-like kinase 1 (ALK1) in endothelial cells*. Blood, 2007. **109**(5): p. 1953-61.
195. Scharpfenecker, M., et al., *BMP-9 signals via ALK1 and inhibits bFGF-induced endothelial cell proliferation and VEGF-stimulated angiogenesis*. J Cell Sci, 2007. **120**(Pt 6): p. 964-72.
196. David, L., et al., *Bone morphogenetic protein-9 is a circulating vascular quiescence factor*. Circ Res, 2008. **102**(8): p. 914-22.
197. Jadrich, J.L., M.B. O'Connor, and E. Coucouvanis, *The TGF beta activated kinase TAK1 regulates vascular development in vivo*. Development, 2006. **133**(8): p. 1529-41.
198. Somekawa, S., et al., *Tmem100, an ALK1 receptor signaling-dependent gene essential for arterial endothelium differentiation and vascular morphogenesis*. Proc Natl Acad Sci U S A, 2012. **109**(30): p. 12064-9.
199. Larrivee, B., et al., *ALK1 signaling inhibits angiogenesis by cooperating with the Notch pathway*. Dev Cell, 2012. **22**(3): p. 489-500.
200. Srinivasan, S., et al., *A mouse model for hereditary hemorrhagic telangiectasia (HHT) type 2*. Hum Mol Genet, 2003. **12**(5): p. 473-82.
201. Urness, L.D., L.K. Sorensen, and D.Y. Li, *Arteriovenous malformations in mice lacking activin receptor-like kinase-1*. Nat Genet, 2000. **26**(3): p. 328-31.
202. Chen, W., et al., *Reduced Mural Cell Coverage and Impaired Vessel Integrity After Angiogenic Stimulation in the Alk1-deficient Brain*. Arterioscler Thromb Vasc Biol, 2013. **33**(2): p. 305-10.
203. Jerkic, M., et al., *Pulmonary hypertension in adult Alk1 heterozygous mice due to oxidative stress*. Cardiovasc Res, 2011. **92**(3): p. 375-84.

204. Huang, Z., et al., *Defective pulmonary vascular remodeling in Smad8 mutant mice*. Hum Mol Genet, 2009. **18**(15): p. 2791-801.
205. Proulx, K., A. Lu, and S. Sumanas, *Cranial vasculature in zebrafish forms by angioblast cluster-derived angiogenesis*. Dev Biol, 2010. **348**(1): p. 34-46.
206. Roman, B.L. and K. Pekkan, *Mechanotransduction in embryonic vascular development*. Biomech Model Mechanobiol, 2012. **11**(8): p. 1149-68.
207. Dekker, R.J., et al., *KLF2 provokes a gene expression pattern that establishes functional quiescent differentiation of the endothelium*. Blood, 2006. **107**(11): p. 4354-63.
208. Lan, Q., K.O. Mercurius, and P.F. Davies, *Stimulation of transcription factors NF kappa B and AP1 in endothelial cells subjected to shear stress*. Biochem Biophys Res Commun, 1994. **201**(2): p. 950-6.
209. Khachigian, L.M., et al., *Nuclear factor-kappa B interacts functionally with the platelet-derived growth factor B-chain shear-stress response element in vascular endothelial cells exposed to fluid shear stress*. J Clin Invest, 1995. **96**(2): p. 1169-75.
210. Bhullar, I.S., et al., *Fluid shear stress activation of IkappaB kinase is integrin-dependent*. J Biol Chem, 1998. **273**(46): p. 30544-9.
211. Hay, D.C., et al., *Activation of NF-kappaB nuclear transcription factor by flow in human endothelial cells*. Biochim Biophys Acta, 2003. **1642**(1-2): p. 33-44.
212. Wang, D.L., et al., *Cyclical strain increases endothelin-1 secretion and gene expression in human endothelial cells*. Biochem Biophys Res Commun, 1993. **195**(2): p. 1050-6.
213. Melchionna, R., et al., *Laminar shear stress inhibits CXCR4 expression on endothelial cells: functional consequences for atherogenesis*. FASEB J, 2005. **19**(6): p. 629-31.
214. Bussmann, J., S.A. Wolfe, and A.F. Siekmann, *Arterial-venous network formation during brain vascularization involves hemodynamic regulation of chemokine signaling*. Development, 2011. **138**(9): p. 1717-26.
215. Seki, T., J. Yun, and S.P. Oh, *Arterial endothelium-specific activin receptor-like kinase 1 expression suggests its role in arterialization and vascular remodeling*. Circ Res, 2003. **93**(7): p. 682-9.
216. Seki, T., et al., *Isolation of a regulatory region of activin receptor-like kinase 1 gene sufficient for arterial endothelium-specific expression*. Circ Res, 2004. **94**(8): p. e72-7.
217. Moya, I.M., et al., *Stalk cell phenotype depends on integration of Notch and Smad1/5 signaling cascades*. Dev Cell, 2012. **22**(3): p. 501-14.
218. Guttmacher, A.E., D.A. Marchuk, and R.I. White, Jr., *Hereditary hemorrhagic telangiectasia*. N Engl J Med, 1995. **333**(14): p. 918-24.
219. Xu, P., J. Liu, and R. Derynck, *Post-translational regulation of TGF-beta receptor and Smad signaling*. FEBS Lett, 2012. **586**(14): p. 1871-84.
220. ten Dijke, P., et al., *Characterization of type I receptors for transforming growth factor-beta and activin*. Science, 1994. **264**(5155): p. 101-4.
221. Goumans, M.J., et al., *Activin receptor-like kinase (ALK)1 is an antagonistic mediator of lateral TGFbeta/ALK5 signaling*. Mol Cell, 2003. **12**(4): p. 817-28.
222. Ricard, N., et al., *BMP9 and BMP10 are critical for postnatal retinal vascular remodeling*. Blood, 2012. **119**(25): p. 6162-71.
223. Chen, H., et al., *BMP10 is essential for maintaining cardiac growth during murine cardiogenesis*. Development, 2004. **131**(9): p. 2219-31.
224. Woods, I.G., et al., *The zebrafish gene map defines ancestral vertebrate chromosomes*. Genome Res, 2005. **15**(9): p. 1307-14.

225. Neuhaus, H., V. Rosen, and R.S. Thies, *Heart specific expression of mouse BMP-10 a novel member of the TGF-beta superfamily*. Mech Dev, 1999. **80**(2): p. 181-4.
226. Korzh, S., et al., *Requirement of vasculogenesis and blood circulation in late stages of liver growth in zebrafish*. BMC Dev Biol, 2008. **8**: p. 84.
227. Liu, J., et al., *A dual role for ErbB2 signaling in cardiac trabeculation*. Development, 2010. **137**(22): p. 3867-75.
228. Peshkovsky, C., R. Totong, and D. Yelon, *Dependence of cardiac trabeculation on neuregulin signaling and blood flow in zebrafish*. Dev Dyn, 2011. **240**(2): p. 446-56.
229. Park, J.E., et al., *BMP-9 induced endothelial cell tubule formation and inhibition of migration involves Smad1 driven endothelin-1 production*. PLoS One, 2012. **7**(1): p. e30075.
230. Star, G.P., M. Giovinazzo, and D. Langleben, *Bone morphogenic protein-9 stimulates endothelin-1 release from human pulmonary microvascular endothelial cells: a potential mechanism for elevated ET-1 levels in pulmonary arterial hypertension*. Microvasc Res, 2010. **80**(3): p. 349-54.
231. Young, K., et al., *BMP9 regulates endoglin-dependent chemokine responses in endothelial cells*. Blood, 2012. **120**(20): p. 4263-73.
232. Zhou, J., et al., *BMP Receptor-Integrin Interaction Mediates Responses of Vascular Endothelial Smad1/5 and Proliferation to Disturbed Flow*. J Thromb Haemost, 2012.
233. Seemann, P., et al., *Mutations in GDF5 reveal a key residue mediating BMP inhibition by NOGGIN*. PLoS Genet, 2009. **5**(11): p. e1000747.
234. Chen, C.Y., et al., *Analysis of early embryonic great-vessel microcirculation in zebrafish using high-speed confocal muPIV*. Biorheology, 2011. **48**(5): p. 305-21.
235. Orlova, V.V., et al., *Controlling angiogenesis by two unique TGF-beta type I receptor signaling pathways*. Histol Histopathol, 2011. **26**(9): p. 1219-30.
236. Mahmoud, M., et al., *Pathogenesis of arteriovenous malformations in the absence of endoglin*. Circ Res, 2010. **106**(8): p. 1425-33.
237. Chang, H., et al., *Smad5 knockout mice die at mid-gestation due to multiple embryonic and extraembryonic defects*. Development, 1999. **126**(8): p. 1631-42.
238. Umans, L., et al., *Inactivation of Smad5 in endothelial cells and smooth muscle cells demonstrates that Smad5 is required for cardiac homeostasis*. Am J Pathol, 2007. **170**(5): p. 1460-72.
239. Lechleider, R.J., et al., *Targeted mutagenesis of Smad1 reveals an essential role in chorioallantoic fusion*. Dev Biol, 2001. **240**(1): p. 157-67.
240. Lan, Y., et al., *Essential role of endothelial Smad4 in vascular remodeling and integrity*. Mol Cell Biol, 2007. **27**(21): p. 7683-92.
241. Boergemann, J.H., et al., *Dorsomorphin and LDN-193189 inhibit BMP-mediated Smad, p38 and Akt signalling in C2C12 cells*. Int J Biochem Cell Biol, 2010. **42**(11): p. 1802-7.
242. Hao, J., et al., *In vivo structure-activity relationship study of dorsomorphin analogues identifies selective VEGF and BMP inhibitors*. ACS Chem Biol, 2010. **5**(2): p. 245-53.
243. Vogt, J., R. Traynor, and G.P. Sapkota, *The specificities of small molecule inhibitors of the TGFs and BMP pathways*. Cell Signal, 2011. **23**(11): p. 1831-42.
244. Yu, P.B., et al., *BMP type I receptor inhibition reduces heterotopic [corrected] ossification*. Nat Med, 2008. **14**(12): p. 1363-9.
245. Collery, R.F. and B.A. Link, *Dynamic smad-mediated BMP signaling revealed through transgenic zebrafish*. Dev Dyn, 2011. **240**(3): p. 712-22.

246. McReynolds, L.J., et al., *Smad1 and Smad5 differentially regulate embryonic hematopoiesis*. Blood, 2007. **110**(12): p. 3881-90.
247. Hild, M., et al., *The smad5 mutation somitabun blocks Bmp2b signaling during early dorsoventral patterning of the zebrafish embryo*. Development, 1999. **126**(10): p. 2149-59.
248. Flanders, K.C., E.S. Kim, and A.B. Roberts, *Immunohistochemical expression of Smads 1-6 in the 15-day gestation mouse embryo: signaling by BMPs and TGF-betas*. Dev Dyn, 2001. **220**(2): p. 141-54.
249. Dick, A., A. Meier, and M. Hammerschmidt, *Smad1 and Smad5 have distinct roles during dorsoventral patterning of the zebrafish embryo*. Dev Dyn, 1999. **216**(3): p. 285-98.
250. Monteiro, R.M., et al., *Spatio-temporal activation of Smad1 and Smad5 in vivo: monitoring transcriptional activity of Smad proteins*. J Cell Sci, 2004. **117**(Pt 20): p. 4653-63.
251. Lele, Z., J. Bakkers, and M. Hammerschmidt, *Morpholino phenocopies of the swirl, snailhouse, somitabun, minifin, silberblick, and pipetail mutations*. Genesis, 2001. **30**(3): p. 190-4.
252. Laux, D.W., J.A. Febbo, and B.L. Roman, *Dynamic analysis of BMP-responsive smad activity in live zebrafish embryos*. Dev Dyn, 2011. **240**(3): p. 682-94.
253. Yang, X., et al., *Angiogenesis defects and mesenchymal apoptosis in mice lacking SMAD5*. Development, 1999. **126**(8): p. 1571-80.
254. Dosch, R., et al., *Bmp-4 acts as a morphogen in dorsoventral mesoderm patterning in Xenopus*. Development, 1997. **124**(12): p. 2325-34.
255. Nguyen, V.H., et al., *Ventral and lateral regions of the zebrafish gastrula, including the neural crest progenitors, are established by a bmp2b/swirl pathway of genes*. Dev Biol, 1998. **199**(1): p. 93-110.
256. Dick, A., et al., *Essential role of Bmp7 (snailhouse) and its prodomain in dorsoventral patterning of the zebrafish embryo*. Development, 2000. **127**(2): p. 343-54.
257. Beck, C.W., M. Whitman, and J.M. Slack, *The role of BMP signaling in outgrowth and patterning of the Xenopus tail bud*. Dev Biol, 2001. **238**(2): p. 303-14.
258. Bauer, H., et al., *The type I serine/threonine kinase receptor Alk8/Lost-a-fin is required for Bmp2b/7 signal transduction during dorsoventral patterning of the zebrafish embryo*. Development, 2001. **128**(6): p. 849-58.
259. Mintzer, K.A., et al., *lost-a-fin encodes a type I BMP receptor, Alk8, acting maternally and zygotically in dorsoventral pattern formation*. Development, 2001. **128**(6): p. 859-69.
260. Payne-Ferreira, T.L. and P.C. Yelick, *Alk8 is required for neural crest cell formation and development of pharyngeal arch cartilages*. Dev Dyn, 2003. **228**(4): p. 683-96.
261. Liu, W., et al., *Distinct functions for Bmp signaling in lip and palate fusion in mice*. Development, 2005. **132**(6): p. 1453-61.
262. Klaus, A., et al., *Distinct roles of Wnt/beta-catenin and Bmp signaling during early cardiogenesis*. Proc Natl Acad Sci U S A, 2007. **104**(47): p. 18531-6.
263. Marques, S.R. and D. Yelon, *Differential requirement for BMP signaling in atrial and ventricular lineages establishes cardiac chamber proportionality*. Dev Biol, 2009. **328**(2): p. 472-82.
264. French, C.R., et al., *Gdf6a is required for the initiation of dorsal-ventral retinal patterning and lens development*. Dev Biol, 2009. **333**(1): p. 37-47.

265. Berg, J.N., et al., *The activin receptor-like kinase 1 gene: genomic structure and mutations in hereditary hemorrhagic telangiectasia type 2*. Am. J. Hum. Genet., 1997. **61**(1): p. 60-7.
266. Lane, K.B., et al., *Heterozygous germline mutations in BMPR2, encoding a TGF-beta receptor, cause familial primary pulmonary hypertension*. Nat Genet, 2000. **26**(1): p. 81-4.
267. Deng, Z., et al., *Familial primary pulmonary hypertension (gene PPH1) is caused by mutations in the bone morphogenetic protein receptor-II gene*. Am J Hum Genet, 2000. **67**(3): p. 737-44.
268. Shore, E.M., et al., *A recurrent mutation in the BMP type I receptor ACVRI causes inherited and sporadic fibrodysplasia ossificans progressiva*. Nat Genet, 2006. **38**(5): p. 525-7.
269. Feng, X.H. and R. Derynck, *Specificity and versatility in tgf-beta signaling through Smads*. Annu Rev Cell Dev Biol, 2005. **21**: p. 659-93.
270. Hata, A., et al., *Mutations increasing autoinhibition inactivate tumour suppressors Smad2 and Smad4*. Nature, 1997. **388**(6637): p. 82-7.
271. Ross, S. and C.S. Hill, *How the Smads regulate transcription*. Int J Biochem Cell Biol, 2008. **40**(3): p. 383-408.
272. Chen, Y.G. and J. Massague, *Smad1 recognition and activation by the ALK1 group of transforming growth factor-beta family receptors*. J. Biol. Chem., 1999. **274**(6): p. 3672-7.
273. Lo, R.S., et al., *The L3 loop: a structural motif determining specific interactions between SMAD proteins and TGF-beta receptors*. Embo J, 1998. **17**(4): p. 996-1005.
274. Chen, Y.G., et al., *Determinants of specificity in TGF-beta signal transduction*. Genes Dev, 1998. **12**(14): p. 2144-52.
275. Persson, U., et al., *The L45 loop in type I receptors for TGF-beta family members is a critical determinant in specifying Smad isoform activation*. FEBS Lett, 1998. **434**(1-2): p. 83-7.
276. Feng, X.H. and R. Derynck, *A kinase subdomain of transforming growth factor-beta (TGF-beta) type I receptor determines the TGF-beta intracellular signaling specificity*. Embo J, 1997. **16**(13): p. 3912-23.
277. Liu, F., et al., *Assemblases and coupling proteins in thick filament assembly*. Cell Struct Funct, 1997. **22**(1): p. 155-62.
278. Daly, A.C., R.A. Randall, and C.S. Hill, *Transforming growth factor beta-induced Smad1/5 phosphorylation in epithelial cells is mediated by novel receptor complexes and is essential for anchorage-independent growth*. Mol Cell Biol, 2008. **28**(22): p. 6889-902.
279. Wrighton, K.H., et al., *Transforming Growth Factor {beta} Can Stimulate Smad1 Phosphorylation Independently of Bone Morphogenic Protein Receptors*. J Biol Chem, 2009. **284**(15): p. 9755-63.
280. Liu, I.M., et al., *TGFbeta-stimulated Smad1/5 phosphorylation requires the ALK5 L45 loop and mediates the pro-migratory TGFbeta switch*. Embo J, 2009. **28**(2): p. 88-98.
281. Pannu, J., et al., *Transforming growth factor-beta receptor type I-dependent fibrogenic gene program is mediated via activation of Smad1 and ERK1/2 pathways*. J Biol Chem, 2007. **282**(14): p. 10405-13.
282. Bharathy, S., et al., *Cancer-associated transforming growth factor beta type II receptor gene mutant causes activation of bone morphogenic protein-Smads and invasive phenotype*. Cancer Res, 2008. **68**(6): p. 1656-66.

283. Upton, P.D., et al., *Bone morphogenetic protein (BMP) and activin type II receptors balance BMP9 signals mediated by activin receptor-like kinase-1 in human pulmonary artery endothelial cells*. J Biol Chem, 2009. **284**(23): p. 15794-804.
284. Dennler, S., et al., *Direct binding of Smad3 and Smad4 to critical TGF beta-inducible elements in the promoter of human plasminogen activator inhibitor-type 1 gene*. Embo J, 1998. **17**(11): p. 3091-100.
285. Korchynskiy, O. and P. ten Dijke, *Identification and functional characterization of distinct critically important bone morphogenetic protein-specific response elements in the Id1 promoter*. J Biol Chem, 2002. **277**(7): p. 4883-91.
286. Mandel, E.M., et al., *The BMP pathway acts to directly regulate Tbx20 in the developing heart*. Development, 2010. **137**(11): p. 1919-29.
287. Wang, Q., et al., *Bone morphogenetic protein 2 activates Smad6 gene transcription through bone-specific transcription factor Runx2*. J Biol Chem, 2007. **282**(14): p. 10742-8.
288. Zhao, M., et al., *E3 ubiquitin ligase Smurf1 mediates core-binding factor alpha1/Runx2 degradation and plays a specific role in osteoblast differentiation*. J Biol Chem, 2003. **278**(30): p. 27939-44.
289. Itoh, S. and P. ten Dijke, *Negative regulation of TGF-beta receptor/Smad signal transduction*. Curr Opin Cell Biol, 2007. **19**(2): p. 176-84.
290. Blank, U., et al., *An in vivo reporter of BMP signaling in organogenesis reveals targets in the developing kidney*. BMC Dev Biol, 2008. **8**: p. 86.
291. Monteiro, R.M., et al., *Real time monitoring of BMP Smads transcriptional activity during mouse development*. Genesis, 2008. **46**(7): p. spcone.
292. Scheer, N. and J.A. Campos-Ortega, *Use of the Gal4-UAS technique for targeted gene expression in the zebrafish*. Mech Dev, 1999. **80**(2): p. 153-8.
293. Kawakami, K., et al., *A transposon-mediated gene trap approach identifies developmentally regulated genes in zebrafish*. Dev Cell, 2004. **7**(1): p. 133-44.
294. Urasaki, A., G. Morvan, and K. Kawakami, *Functional dissection of the Tol2 transposable element identified the minimal cis-sequence and a highly repetitive sequence in the subterminal region essential for transposition*. Genetics, 2006. **174**(2): p. 639-49.
295. Thisse, B. and C. Thisse, *Fast Release Clones: A high throughput expression analysis*. ZFIN direct data submission, 2004: p. <http://zin.org>.
296. Row, R.H. and D. Kimelman, *Bmp inhibition is necessary for post-gastrulation patterning and morphogenesis of the zebrafish tailbud*. Dev Biol, 2009. **329**(1): p. 55-63.
297. Muller, F., et al., *Characterization of zebrafish smad1, smad2 and smad5: the amino-terminus of smad1 and smad5 is required for specific function in the embryo*. Mech Dev, 1999. **88**(1): p. 73-88.
298. Faure, S., et al., *Endogenous patterns of BMP signaling during early chick development*. Dev Biol, 2002. **244**(1): p. 44-65.
299. Wang, J., et al., *Atrioventricular cushion transformation is mediated by ALK2 in the developing mouse heart*. Dev Biol, 2005. **286**(1): p. 299-310.
300. Choi, M., et al., *The bone morphogenetic protein antagonist noggin regulates mammalian cardiac morphogenesis*. Circ Res, 2007. **100**(2): p. 220-8.

301. Gaussin, V., et al., *Endocardial cushion and myocardial defects after cardiac myocyte-specific conditional deletion of the bone morphogenetic protein receptor ALK3*. Proc Natl Acad Sci U S A, 2002. **99**(5): p. 2878-83.
302. Santoro, M.M., G. Pesce, and D.Y. Stainier, *Characterization of vascular mural cells during zebrafish development*. Mech Dev, 2009. **126**(8-9): p. 638-49.
303. Hodge, L.K., et al., *Retrograde BMP signaling regulates trigeminal sensory neuron identities and the formation of precise face maps*. Neuron, 2007. **55**(4): p. 572-86.
304. Toyama, R., et al., *Transcriptome analysis of the zebrafish pineal gland*. Dev Dyn, 2009. **238**(7): p. 1813-26.
305. Kofler, B., et al., *Id-1 expression defines a subset of vimentin/S-100beta-positive, GFAP-negative astrocytes in the adult rat pineal gland*. Histochem J, 2002. **34**(3-4): p. 167-71.
306. Manning, L., et al., *Regional morphogenesis in the hypothalamus: a BMP-Tbx2 pathway coordinates fate and proliferation through Shh downregulation*. Dev Cell, 2006. **11**(6): p. 873-85.
307. Pyati, U.J., et al., *Sustained Bmp signaling is essential for cloaca development in zebrafish*. Development, 2006. **133**(11): p. 2275-84.
308. Liu, J. and D.Y. Stainier, *Tbx5 and Bmp Signaling Are Essential for Proepicardium Specification in Zebrafish*. Circ Res, 2010. **106**.
309. Smith, M., et al., *Trunk neural crest origin of caudal fin mesenchyme in the zebrafish Brachydanio rerio*. Proc Biol Sci, 1994. **256**(1346): p. 137-145.
310. Corish, P. and C. Tyler-Smith, *Attenuation of green fluorescent protein half-life in mammalian cells*. Protein Eng, 1999. **12**(12): p. 1035-40.
311. Jusuf, P.R. and W.A. Harris, *Ptfla is expressed transiently in all types of amacrine cells in the embryonic zebrafish retina*. Neural Dev, 2009. **4**: p. 34.
312. Verkhusha, V.V., et al., *High stability of Discosoma DsRed as compared to Aequorea EGFP*. Biochemistry, 2003. **42**(26): p. 7879-84.
313. Yu, P.B., et al., *Dorsomorphin inhibits BMP signals required for embryogenesis and iron metabolism*. Nat Chem Biol, 2008. **4**(1): p. 33-41.
314. Mullins, M.C., et al., *Genes establishing dorsoventral pattern formation in the zebrafish embryo: the ventral specifying genes*. Development, 1996. **123**: p. 81-93.
315. Kramer, C., et al., *Maternally supplied Smad5 is required for ventral specification in zebrafish embryos prior to zygotic Bmp signaling*. Dev Biol, 2002. **250**(2): p. 263-79.
316. Gupta, S., et al., *BMP signaling restricts hemato-vascular development from lateral mesoderm during somitogenesis*. Development, 2006. **133**(11): p. 2177-87.
317. Yao, L.C., et al., *Schnurri transcription factors from Drosophila and vertebrates can mediate Bmp signaling through a phylogenetically conserved mechanism*. Development, 2006. **133**(20): p. 4025-34.
318. Kang, J.S., et al., *Repression of Runx2 function by TGF-beta through recruitment of class II histone deacetylases by Smad3*. Embo J, 2005. **24**(14): p. 2543-55.
319. Liu, D., B.L. Black, and R. Derynck, *TGF-beta inhibits muscle differentiation through functional repression of myogenic transcription factors by Smad3*. Genes Dev, 2001. **15**(22): p. 2950-66.
320. Bidart, M., et al., *BMP9 is produced by hepatocytes and circulates mainly in an active mature form complexed to its prodomain*. Cell Mol Life Sci, 2012. **69**(2): p. 313-24.
321. Willaredt, M.A., et al., *Multiple essential roles for primary cilia in heart development*. Cilia, 2012. **1**(1): p. 23.

322. Kahr, P.C., et al., *Systematic analysis of gene expression differences between left and right atria in different mouse strains and in human atrial tissue*. PLoS One, 2011. **6**(10): p. e26389.
323. Seghers, L., et al., *Shear induced collateral artery growth modulated by endoglin but not by ALK1*. J Cell Mol Med, 2012. **16**(10): p. 2440-50.
324. Zhou, J., et al., *Force-specific activation of Smad1/5 regulates vascular endothelial cell cycle progression in response to disturbed flow*. Proc Natl Acad Sci U S A, 2012. **109**(20): p. 7770-5.
325. Yao, Y., et al., *High-density lipoproteins affect endothelial BMP-signaling by modulating expression of the activin-like kinase receptor 1 and 2*. Arterioscler Thromb Vasc Biol, 2008. **28**(12): p. 2266-74.
326. Yao, Y., et al., *Regulation of bone morphogenetic protein-4 by matrix GLA protein in vascular endothelial cells involves activin-like kinase receptor 1*. J Biol Chem, 2006. **281**(45): p. 33921-30.
327. Sorescu, G.P., et al., *Bone morphogenetic protein 4 produced in endothelial cells by oscillatory shear stress stimulates an inflammatory response*. J Biol Chem, 2003. **278**(33): p. 31128-35.
328. Chen, J.N., et al., *Left-right pattern of cardiac BMP4 may drive asymmetry of the heart in zebrafish*. Development, 1997. **124**(21): p. 4373-82.
329. Nojima, J., et al., *Dual roles of smad proteins in the conversion from myoblasts to osteoblastic cells by bone morphogenetic proteins*. J Biol Chem. **285**(20): p. 15577-86.
330. Philip, B., Z. Lu, and Y. Gao, *Regulation of GDF-8 signaling by the p38 MAPK*. Cell Signal, 2005. **17**(3): p. 365-75.
331. Little, S.C. and M.C. Mullins, *Bone morphogenetic protein heterodimers assemble heteromeric type I receptor complexes to pattern the dorsoventral axis*. Nat Cell Biol, 2009. **11**(5): p. 637-43.
332. Poliseno, L., et al., *MicroRNAs modulate the angiogenic properties of HUVECs*. Blood, 2006. **108**(9): p. 3068-71.
333. Bernstein, E., et al., *Dicer is essential for mouse development*. Nat Genet, 2003. **35**(3): p. 215-7.
334. Yang, W.J., et al., *Dicer is required for embryonic angiogenesis during mouse development*. J Biol Chem, 2005. **280**(10): p. 9330-5.
335. Nicoli, S., et al., *MicroRNA-mediated integration of haemodynamics and Vegf signalling during angiogenesis*. Nature, 2010. **464**(7292): p. 1196-200.
336. Gamell, C., et al., *BMP2 induction of actin cytoskeleton reorganization and cell migration requires PI3-kinase and Cdc42 activity*. J Cell Sci, 2008. **121**(Pt 23): p. 3960-70.
337. Mullen, A.C., et al., *Master transcription factors determine cell-type-specific responses to TGF-beta signaling*. Cell, 2011. **147**(3): p. 565-76.
338. Trompouki, E., et al., *Lineage regulators direct BMP and Wnt pathways to cell-specific programs during differentiation and regeneration*. Cell, 2011. **147**(3): p. 577-89.
339. Folkman, J., *Tumor angiogenesis: therapeutic implications*. N Engl J Med, 1971. **285**(21): p. 1182-6.
340. Hu-Lowe, D.D., et al., *Targeting activin receptor-like kinase 1 inhibits angiogenesis and tumorigenesis through a mechanism of action complementary to anti-VEGF therapies*. Cancer Res. **71**(4): p. 1362-73.

341. Choi, J., et al., *FoxH1 negatively modulates flk1 gene expression and vascular formation in zebrafish*. Dev Biol, 2007. **304**(2): p. 735-44.
342. Traver, D., et al., *Transplantation and in vivo imaging of multilineage engraftment in zebrafish bloodless mutants*. Nat Immunol, 2003. **4**(12): p. 1238-46.
343. Kwan, K.M., et al., *The Tol2kit: a multisite gateway-based construction kit for Tol2 transposon transgenesis constructs*. Dev Dyn, 2007. **236**(11): p. 3088-99.
344. Villefranc, J.A., J. Amigo, and N.D. Lawson, *Gateway compatible vectors for analysis of gene function in the zebrafish*. Dev Dyn, 2007. **236**(11): p. 3077-87.
345. Yelon, D., S.A. Horne, and D.Y. Stainier, *Restricted expression of cardiac myosin genes reveals regulated aspects of heart tube assembly in zebrafish*. Dev Biol, 1999. **214**(1): p. 23-37.
346. Covassin, L.D., et al., *A genetic screen for vascular mutants in zebrafish reveals dynamic roles for Vegf/Plcg1 signaling during artery development*. Dev Biol, 2009. **329**(2): p. 212-26.